CZECH TECHNICAL UNIVERSITY IN PRAGUE
Faculty of Nuclear Sciences and Physical Engineering

DOCTORAL THESIS

Chaos in the conditional dynamics of purification protocols

Ing. Stanislav Vymětal

Supervisor: Prof. Ing. Igor Jex, DrSc.

Prague, 2010

This thesis is the result of my own work, except where explicit reference is made to the work of others and has not been submitted for another qualification to this or any other university.

Ing. Stanislav Vymětal

Acknowledgements

I would like to thank to my supervisor prof. Ing. Igor Jex, DrSc., the head of the department of physics at the Faculty of Nuclear Sciences and Physical Engineering of the Czech Technical University in Prague, and to my close colleague Dr. Tamas Kiss, the senior researcher of the Department of Quantum Optics and Quantum Information within the Academy of Hungarian Sciences, for leadership and collaboration during my studies and scientific work. Also, I would like to thank to my colleagues from the working group of prof. Jex and Dr. Kiss, namely to Aurel Gábris Ph.D. and to Ing. Martin Štefaňák Ph.D..

I would like to thank to my closest and friends who supported and encouraged me. In parallel to post gradual studies I worked in IT/Telecom area. I would like to thank to the Faculty of Nuclear Sciences and Physical Engineering and to my employer Gemalto for the conditions to finish my studies.

Foreword

The presence of complex chaos in iterative applications of selective dynamics on quantum systems is a novel form of quantum chaos with true sensitivity to initial conditions. In this work, we will present techniques needed for study of selective dynamics for purification protocols. Such processes are important for quantum information and communication. The presented results are interesting for several reasons. We prove the existence of chaotic dynamics for generally robust purification protocols, even for the simplest one-qubit pure states. Also, we present actually unpublished results of chaotic dynamics in entanglement for purification of highly nontrivial two-qubit states. To achieve both analytical and numerical results, we apply the latest mathematical framework for the study of discrete dynamical systems generated by holomorphic maps, especially for rational functions of one complex variable.

Keywords: complex chaos, quantum chaos, purification protocol

PACS: 3.67.Lx, 05.45.Mt, 42.50.Lc, 89.70.-a

Contents

Chapter 1

Introduction

This thesis presents the results of studies of complex chaos in the dynamics of quantum purification protocols. To study the topic it was necessary to apply the knowledge of quantum physics, especially its branch of quantum information, together with recent results of complex dynamical systems. As a result it was possible to study analytically and numerically simulate the complicated dynamics of the purification protocols.

1.1 Motivation

The existence of entangled systems is at the heart of quantum mechanics as a direct consequence of the linearity principle of quantum theory for composed systems. The entangled system is a special type of correlated system. Such a system has been used for the famous EPR paradox [1], a thought experiment presented in 1935 by A. Einstein and his colleagues B. Podolsky and N. Rosen, which challenged the consistency of quantum theory by discussing possible measurements of observables for a two particle entangled system. The EPR paradox was a clear demonstration of the differences between quantum mechanics and classical intuition.

Later on, in the sixties, entangled systems were experimentally studied to confirm quantum mechanics predictions against alternative theories, like local hidden variable theories. In recent years, entangled systems raised in importance as a key element for several tasks of quantum information physics, a new branch of quantum mechanics which studies the possibilities of using quantum objects as a medium for the safe storing, transporting and effective processing of information. Highly entangled states have been crucial for the success of many processes of quantum cryptography and for the phenomena of quantum teleportation [2] with high interest for physical realization.

Entangled systems are usually not prepared in the ideal state, additional noise appears either from the source, producing the state or, from the communication channel distributing the system to remote parties. Therefore there has been a need to correct the presence of noise by physically relevant processes, so called purification protocols, investigated in last two decades together with the theory of entanglement measures [3]. Such a process has been first introduced by Bennett-Brassard [4] for the purification of two-qubit systems to maximally entangled Bell state $|\psi_{01}\rangle = \frac{1}{\sqrt{2}}(|01\rangle - |10\rangle)$. Later on, the Horodecki protocol [5] generalized the Bennet-Brassard protocol to purify generally D-level quantum systems and it was possible to easily setup the protocol to purify towards arbitrary pure entangled state. Both protocols are part of the class of so called nondeterministic protocols, using a large set of randomly chosen unitary transformations together with a depolarization channel. The physical realization of the protocols was experimentally difficult, therefore there was introduced the class of deterministic protocols, which uses a fixed set of unitary transformations and the depolarization channel is replaced by projections onto a subensemble of the states. In such a way, D. Deutsch et. al [6] and later on H. Bechmann-Pasquinucci et. al [7] introduced the analogues of the Bennet-Brassard protocol and finally G. Albert et. al [8] found the general deterministic protocol as an analogue of the Horodecki protocol. It has been proven in [8] that generic purification protocol achieves, for certain level of noise of the initial states, faster purification than the Horodecki protocol.

The general deterministic protocol [8] selects, in each step of the purification, only certain quantum states, based on the results of projection measurements on the subensemble of the states. In this sense, the protocol generates conditional dynamics on the initial ensemble of quantum states. In each step of the protocol, there exists the spillover of information about the states, meaning that on one side information about the system is extracted by projection measurements, on the other hand information about the selection is returned back to the system by conditional selection of the states (to purify in the next step of the protocol). Due to conditional selection of the states, the protocol becomes nonlinear and renormalization of the states is necessary after each step of the protocol.

The study of nonlinear dynamical systems has a long history [9] in physics and mathematics. One of the most spectacular results of this development is the analysis of chaos. Chaos, firstly introduced by H. Poincaré in 1880, during the study of the three-body mechanical system, was demonstrated by the discovery of nonperiodic orbits which neither escape forever nor approach any locally attracting state. In 1889 J. Hadamard proved that the three particle Hadamard's billiard dynamical system is unstable in the sense, that the evolution of the trajectories of all particles is exponentially sensitive to initial setting of the billiard. Hadamard proved that the billiard evolves with the positive Lyapunov exponent, meaning that for every two arbitrary close settings of the billiard, the distances of the trajectories of all particles diverge exponentially fast in time of the evolution. Exponential sensitivity of the system, to initial conditions, defines chaotic regime in the Poincaré sense.

Another problems, studied at the beginnings of chaos theory, were connected to long time dynamical processes studied under the name of ergodic theory and were motivated by processes in statistical physics. Later studies were linked to the study of the stability of differential equations for various physical process: many-body problems, astronomical problems and radio engineering by Birghoff, Kolmogorov and others.

The interest for the study of chaos intensified after the mid of 20-th century due to the observation of many nonlinear processes [10], for instance in sociology and represented for example by the logistics map (see the figure (1.1)). The studies exploded mainly after the construction of electronic computers, which enabled to visualize the results of long time runs of the process in real time. In 1961 E. Lorenz, dealing with weather prediction, realized a strong sensitivity of forecast calculations on the initial conditions. Lorentz's discovery, nowadays known as the butterfly effect, showed that even detailed atmospheric modeling can not give reliable long time predictions and therefore the weather predictions can be done only for few days ahead.

In modern literature [9; 11–14], a discrete chaotic dynamical system is defined by three properties (Devaney, 1960): the density of the set of periodic points, transitivity of the state space and sensitivity of the system to initial conditions (not necessarily exponential). Later it was proved, that for general dynamical system, the first two conditions imply the third condition, nevertheless the property of sensitivity of the system to initial conditions is still considered to be the essence of chaos [10; 13; 15].

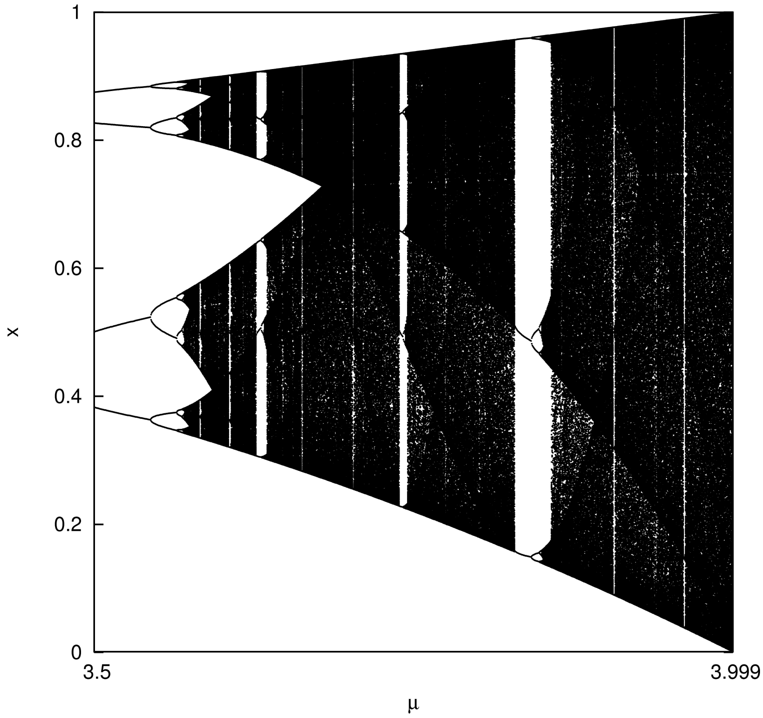

Figure 1.1: Logistics map [10], mathematically defined by the recurrent relation:

$$x_{n+1} = \mu x_n (1 - x_n)$$

was popularized in 1976 by the biologist Robert May, in part as a discrete-time demographic model. The discrete real valued variable x_n (between 0 and 1) represents the population at year n, x_0 represents the initial population. The parameter μ represents the rate of reproduction and starvation.
The figure represents the evolution of the system, with fixed initial $x_0 = 0.5$ and various values of μ, in 10^3 iterations after the initial 10^4 iterations. There exists various dynamical regimes, strongly depending on the setting of parameter μ. On the figure we observe the regime of bifurcations and period doubling i.e. oscillates in the even length cycle of the length: $2, 4, 8, \ldots$, which are the routes to chaos.

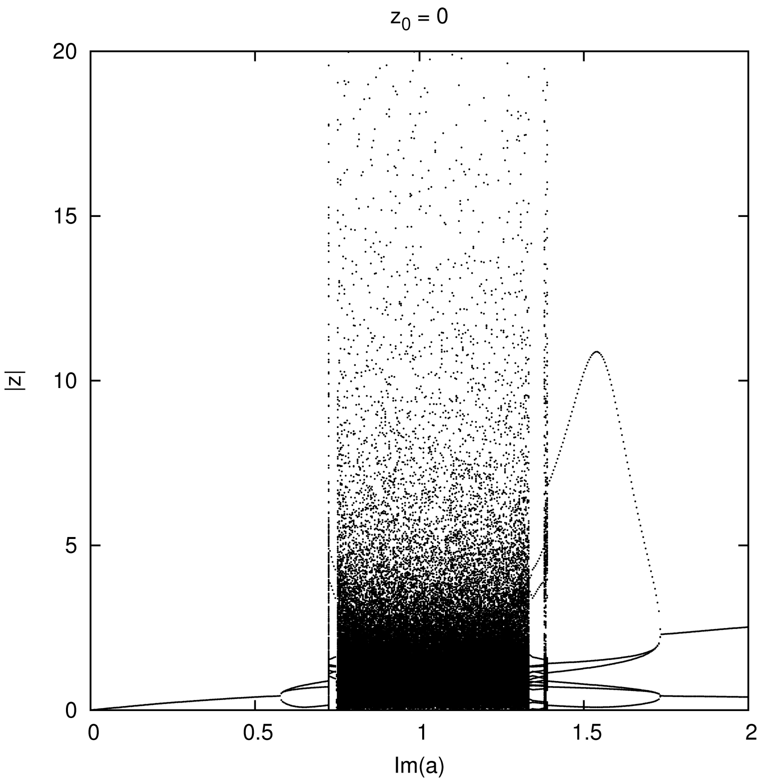

Figure 1.2: Purification of one-qubit pure states $|\psi\rangle = \mathcal{N}\left(z|0\rangle + |1\rangle\right)$, initially prepared for $z_0 = 0$ [I]. Purification protocols are specified by different additional unitary gates specified by the parameter a (for the plot the value of a is purely imaginary). The plot shows the evolution of $|z|$ in 10^3 purification steps after the initial 10^3 steps. We observe, that the evolution is similar to the Logistics map (1.1). We can identify the areas of strong sensitivity towards the value of parameter a (purely imaginary). We find bifurcations for $a = 0.580\imath$, $a = 0.728\imath$ and also regions of chaotic behavior (values of $a \in (0.752\imath, 1.332\imath)$).

Chaos for quantum systems was something difficult to understand for several reasons. Firstly, in quantum theory it is difficult to define trajectories in the phase space. Also, unitary evolution of quantum mechanical system guarantees constant distance between any two states of the system and prevents the existence of chaos in the classical sense. On the other hand, the correspondence principle demands, that a quantum mechanical system, in the semiclassical regime, behaves like the classical one and therefore the chaotic regime shall be observed for the quantum mechanical analogues of the classically chaotic systems. Since 1989 the study of the dynamics of these systems is known as quantum chaos [9; 16]. Quantum chaos has been proved for various systems, especially for the quantum billiard systems, like the evolution of electron states inside a collinear helium atom He^{++} [9]. Besides the study of quantum chaos for closed quantum systems, there are results for the dynamics of open quantum systems with nonunitary evolution, called true chaos. The nonlinear and nonunitary evolution was based on the conditional dynamics, mainly depending on the measurement results during the evolution. For example S. Habib [17] simulated a Duffing oscillator with the precondition of possible continuous measurements on the system and numerically calculated positive Liapunov exponent (exponential divergency of the trajectories in phase space) far from the classical limit.

The purification protocol [8] is an example of a truly quantum process, without any classical analogue, based on principle of superposition and with the nonunitary, selective evolution of the purified systems based on the projections in each step of the purification. For example, for certain settings of the purification, quantum systems may nonlinearly evolve like $\rho \mapsto U"\rho^2"U^\dagger$ i.e. firstly, the nonlinear part of the purification step "squares" and "renormalizes" the elements of the density matrices ("ρ^2") and secondly, it is applied an additional unitary gate U. Such a purification is similar to the nonlinear evolution of social system under the Logistic map: $x \mapsto \mu x\,(1-x)$. While the Logistic map induces the nonlinear, real parameter dynamics, the purification protocol represents complicated, nonlinear complex parameters dynamics in representation space. Naturally, one can ask the question if there exists the analogues with the classical systems and what are the tools for the study of the chaotic dynamics for the quantum process of purification [8].

Independent line of research, dating back to 20-th century, was provided by G. Julia and R. Fatou, who studied the stability of polynomial maps of one complex variable. Later on, the mathematicians Milnor, Beardon, Carlesson, Gamelin, Steinmetz, McMullen intensively studied iterative dynamical systems, generated by a holomorphic map in complex spaces and formulated strong theorems especially for polynomial and rational maps of one complex variable [11]. For a dynamical system, generated by such a map of the order two and higher, J. W. Milnor proved the existence of chaos on its Julia set [11]. Recent results for holomorphic dynamics, in complex spaces, are presented in the book of Morosawa et. al [13]. While the theory for one dimensional maps seems to be fully understood and classified, the theory for higher dimensional maps is subject to current research with many open problems, intensively studied by J. E. Fornæs [14].

The framework of complex rational maps is a natural tool for the study of purification protocols. While mathematically quite well understood there are just a handfull of physics examples where this theory is applicable. Purification protocols are a surprising and interesting examples (see the figure 1.2) by for not fully understood. Early 2005, our research group asked the following questions:

1. Is it possible to identify true chaotic regime for iterative dynamical system generated by the purification protocol [8] for the simplest case of single qubit?

2. Is it possible to identify chaotic regime for two-qubit pure states and also for two-qubit mixed states, especially for the property of entanglement?

3. Is there a way to classify possible regimes of the purification protocols?

In the thesis I provide the answers to these questions supported by analytical results and numerical simulations.

1.2 Content of the thesis

Thesis consists of the five chapters. The first chapter, *Introduction*, consists of the review of entanglement property for quantum systems. Then it continues with the brief overview of quantum computing and purification protocols. Reader learns about the history and progresses in the study of chaotic dynamical systems and especially about the quantum chaos with the overview of actual mathematical trends for iterative dynamical systems. Chapter also includes the thesis content review together with the mathematical symbols review.

The second chapter, *Basic concepts review*, consists of detailed presentation of purification protocols of the interest [8]. It contains of the review of the mathematical framework to study dynamical systems namely for rational maps in one complex variable, together with the analogues for study of holomorphic maps in higher dimensional complex spaces. Reader learns also about the Fano representation as the numerically efficient approach to study more dimensional quantum states dynamics.

The third chapter, *Results*, consists of the results for the study of chaotic dynamics for one-qubit pure states purifications, as already published in the papers [I; II] and in conference poster and the proceedings [III; IV]. There are also present yet unpublished results of the simulations of various Julia sets, representing sensitivity of the purifications to initial setting. And mainly, it will be presented yet unpublished results for the chaotic dynamics for two-qubit pure states and mixed states with the main target to prove chaos in the entanglement. Reader learns about the convenient representation of purification protocol dynamics, by rational function, and also about the usage of strong mathematical statements to achieve both analytic and efficient numerical results for highly physically interesting topic of the dynamics of purification protocols.

The fourth chapter, *Conclusion and outlook*, presents the survey of the thesis with the main conclusions. Also, reader finds here the outlook for the future research. The last chapter, *Appendixes*, includes an overview of used computer programs and numerical calculations stored in an attached data disc.

Chapter 2

Basic concepts review

Quantum mechanics diffused into the realm of information theory. Quite a number of concepts was adopted, but may acquired a different flavor. The ways we guarantee and process information has limitations which are not present in the classical case. Let us communicate some notions we need for own analysis. We do not give a consist review but merely list of concepts we need for an analysis.

2.1 Quantum information basics

As defined by D. Deutsch [18]: "*computation* is a process that produces *outputs* that depend in some desired way on given *inputs*" and a "*computing machine*" is a physical object whose notion can be regarded as the performance of *computation*." This definition is valid for classical electronic computation as well as for *quantum computation*, the novel branch of quantum physics, mathematics and informatics which uses the objects and the phenomena of quantum theory - especially the principle of superposition.

2.1.1 Bit, qubit and qudit

According to Deutsch [18] a *bit* is the smallest possible quantity of non-probabilistic information. A bit can take one of two values such "true" and "false" or "0" and "1". In classical computing a bit is the basic information unit. In quantum computing, the analogue of a bit is a *qubit*. A qubit is a physical object represented by a two level quantum system. The state of a qubit is represented by a ray in Hilbert space $\mathcal{H}(2)$. A *qudit* is the extension of qubit, it is realized by a D-level quantum system where $D \in \mathbb{N}$. Similarly to a qubit, a qudit state is represented by the ray in $\mathcal{H}(D)$.

2.1.2 Logical and quantum gates

According to Deutsch [18], in classical theory of computation a *logical gate* is a computing machine whose inputs and outputs consist of fixed number of bits and which performs fixed computation in fixed time. A *quantum gate* is defined in similar way. The only difference is that the states of the input and the output of quantum gate are not eigenstates of input and output observables and may be arbitrary mixtures of input or output quantum states.

For the construction of further studied purification protocols (chapter (3)) let us present here the most important reversible one-qubit gates of $\mathrm{SU}(2)$ and Hadamard and two-qubit gate of XOR, known for two qudits as GXOR gate.

$\mathrm{SU}(2)(\mathbb{C})$ **one-qubit gates** are the linear operators on the Hilbert space H(2), in matrix representation form a group of unitary transformations

$$U = \begin{pmatrix} \alpha & \beta \\ -\beta^* & \alpha^* \end{pmatrix}$$

where $\alpha, \beta \in \mathbb{C}$ with unit determinant $\mid \alpha \mid^2 + \mid \beta \mid^2 = 1$. Because of the equivalency of the beams in the Hilbert space, one can also define physical equivalency $\equiv$ of the $\{U\} \in \mathrm{SU}(2)(\mathbb{C})$ so that $U \equiv U.e^{\imath\psi}$, then matrix representation of U has 2 real variables $\phi, \psi \in \mathbb{R}$

$$U = \begin{pmatrix} \cos(\phi) & \sin(\phi)\, e^{\imath\psi} \\ -\sin(\phi)\, e^{-\imath\psi} & \cos(\phi) \end{pmatrix}. \tag{2.1}$$

Hadamard one-qubit gate H is a linear operator on the Hilbert space $\mathcal{H}(2)$ with the matrix representation

$$H = \frac{1}{\sqrt{2}} \begin{pmatrix} 1 & 1 \\ 1 & -1 \end{pmatrix}. \tag{2.2}$$

The H gate is a unitary operator and therefore reversible, it is also a hermitian operator. One physical realization of H gate, according to [19], can be the dual reil representation of a qubit. It is easy to verify that the H gate is identical to the discrete Fourier transformation [8] for the qubit

$$H|k\rangle \equiv \frac{1}{\sqrt{2}} \sum_{n=0}^{1} e^{\imath \frac{2\pi kn}{2}} |n\rangle$$

where $k \in \{0, 1\}$.

The XOR **and** GXOR **- two-qubit and two-qudit gates** According to [8], the quantum XOR *gate* is defined as a linear operator on the Hilbert space $\mathcal{H}_1(2) \otimes \mathcal{H}_2(2)$ by the relation

$$\mathrm{XOR}\,|i\rangle_1|j\rangle_2 = |i\rangle_1|i \oplus j\rangle_2 = |i\rangle_1|\,(i+j)\; mod\; 2\rangle_2 \tag{2.3}$$

where $i, j \in \{0, 1\}$ represent number state values for each qubit. The XOR gate is an unitary operator and therefore reversible, the XOR gate is also hermitian. Because of $i \oplus j = 0$ only if $i = j$, then $\mathrm{XOR}|i\rangle_1|j\rangle_2 = |i\rangle_1|0\rangle_2$ only if $i = j$.

The GXOR *gate* is a generalized XOR gate for D-qudit states, defined by the action

$$\mathrm{GXOR}\,|i\rangle_1|j\rangle_2 = |i\rangle_1|i \oplus j\rangle_2 = |i\rangle_1|\,(i+j)\; mod\; D\rangle_2$$

where $i, j \in \{0, 1, ..., D-1\}$. Such an operator is unitary but not hermitian for $D > 2$. According to [8], there exists the hermitian definition of the GXOR gate

$$\mathrm{GXOR}\,|i\rangle_1|j\rangle_2 = |i\rangle_1|i \ominus j\rangle_2 = |i\rangle_1|\,(i-j)\; mod\; D\rangle_2. \tag{2.4}$$

For $D = 2$ the GXOR is equivalent with the XOR. In general, GXOR is an unitary operator, it is hermitian and $i \ominus j = 0$ only if $i = j$. The physical realization of $GXOR$ gate, according to [8], can be realized by the nonlinear optical elements by the combination of Kerr interaction on the two modes of the radiation field, together with the phase shift on the second mode. The first mode represents one mode system $|i\rangle_1$, the second mode represents D mode system of the Fourier transformation of $|j\rangle_2$.

Application of GXOR **gate - generalized Bell states** An important application of $GXOR$ (2.4) is the creation of entangled two qudits systems. Let $|i\rangle_1|j\rangle_2$, $i, j \in \{0, ..., D-1\}$

is a number state basis of Hilbert space $\mathcal{H}_1(D) \otimes \mathcal{H}_2(D)$, then let me define

$$|\psi_{lm}\rangle = GXOR_{12}[F|l\rangle_1|m\rangle_2] \tag{2.5}$$

where F is the discrete Fourier transformation operator [8], defined by the action on the number basis states

$$F|k\rangle \equiv \frac{1}{\sqrt{D}} \sum_{n=0}^{D-1} e^{\imath \frac{2\pi kn}{D}} |n\rangle$$

where $k \in \{0, \ldots, D-1\}$. From equation (2.5) and for $D = 2$, one obtains the *Bell states*

$$\begin{aligned} |\psi_{00}\rangle &= \frac{1}{\sqrt{2}}(|00\rangle + |11\rangle), \ |\psi_{01}\rangle = \frac{1}{\sqrt{2}}(|01\rangle + |10\rangle), \\ |\psi_{10}\rangle &= \frac{1}{\sqrt{2}}(|00\rangle - |11\rangle), \ |\psi_{11}\rangle = \frac{1}{\sqrt{2}}(|01\rangle - |10\rangle). \end{aligned} \tag{2.6}$$

For $D > 2$ we obtain the *generalized Bell states*, this is one of the possible definitions. Because GXOR is unitary operator, then generalized Bell states are clearly orthonormal [20]. The number of the generalized Bell states is D^2, the same as dimension $\mathcal{H}_1(D) \otimes \mathcal{H}_2(D)$, so the generalized Bell states form a basis in the two qudits Hilbert space. In the next part we will present, that the Bell states are also maximally entangled states.

2.1.3 Entanglement and quantum states

Entanglement is one of the most important phenomenon for the theory of the quantum information and quantum computation. For the purpose of the thesis we will provide its definition for bipartite quantum state according to [3; 21]. Let suppose the bipartite quantum system with the density matrix ρ on product Hilbert space $\mathcal{H} = \mathcal{H}_1 \otimes \mathcal{H}_2$, we say that system is *separable* if ρ can be written as a convex (probabilistic) combination of product states $\rho_1^i \otimes \rho_2^i$ (where $\rho_{1,2}^i$ is the state of the first/second particle) i.e. when

$$\rho = \sum_{i=1}^{k} p_i \rho_1^i \otimes \rho_2^i, \ 0 \le p_i, \ \sum_{i=1}^{k} p_i = 1. \tag{2.7}$$

Such separable state does not have any quantum-mechanical correlation - *entanglement*. When the state ρ is not separable it is called called *inseparable* or *entangled*. At this point, let us mention a straightforward extension of the definition of separability (2.7) for M-particle system called *M-separability* [3]. Such a state ρ is defined on the M-particle Hilbert space $\mathcal{H} = \bigotimes_{i=1}^{M} \mathcal{H}_i$ as

$$\rho = \sum_{i=1}^{k} p_i \rho_1^i \otimes \ldots \otimes \rho_M^i, \;\; 0 \leq p_i, \;\; \sum_{i=1}^{k} p_i = 1. \tag{2.8}$$

Unfortunately, in contrast to the separable states the m-separable states may be also correlated [3]. Consequently, the dichotomy of the states onto entangled and M-separable is not generally unique. Therefore in chapter (3) we will study the dynamics of purification at most for bipartite systems (especially for two-qubit systems).

A very important problem is how to quantify entanglement of the bipartite state i.e. how to define a proper entanglement measure ([20]). Details of this topic are going beyond the content of the thesis and may be found in the literature [3]. At this point let us review only few basic properties.

Information content in the density matrix ρ is measured by its *entropy* $S(\rho)$, in quantum mechanics defined by von Neumann as a straightforward generalization of Boltzmann entropy in statistical mechanics

$$S(\rho) = -\operatorname{Tr}(\rho \ln \rho). \tag{2.9}$$

This quantity is zero for pure states and positive for mixed states (mixed state require more information than pure state to be fully specified) and so the von Neumann entropy (2.9) measures the deviation from pure state behavior. This quantity is also time independent where the dynamics of ρ is governed by unitary transformation.

Von Neumann index correlation I_C quantifies correlation of bipartite system [22]. Based on (2.9) it has the form

$$I_C = S_1 + S_2 - S \tag{2.10}$$

where $S_{1,2} = S\left(\mathrm{Tr}_{1,2}\,\rho\right)$ and the reduced density operators $\mathrm{Tr}_{1,2}\,\rho$, in respective matrix representation, have the elements

$$\begin{aligned} \left(\mathrm{Tr}_1\,\rho\right)_{\mu\nu} &= \sum_i \langle i\mu|\rho|i\nu\rangle \\ \left(\mathrm{Tr}_2\,\rho\right)_{ij} &= \sum_\mu \langle i\mu|\rho|j\mu\rangle. \end{aligned}$$

The kets $\{|i\rangle\}$, $\{|\mu\rangle\}$ define the respective orthonormal base of the state space of the first and the second particle. If we order the components of the system so that $S_2 \geq S_1$ then Araki-Lieb inequality implies $I_c \leq 2S_1$. The maximum possible value I_C will be $2S_1$. Consequently from (2.10) the maximum degree of correlation is obtained when $S_1 = S_2$ and $S = 0$ i.e. the total state is pure. One can conclude, that two particle system which is maximally correlated must be pure. It has been proven that the Bell states (2.5) are maximally correlated [21; 22].

Let us now calculate the value of I_C for two-qubit pure state, derived form will be used for calculations in section (3.6). Let us suppose pure state $|\psi\rangle$ of the form

$$|\psi\rangle = \alpha_{00}|00\rangle + \alpha_{01}|01\rangle + \alpha_{10}|10\rangle + \alpha_{11}|11\rangle.$$

For any pure state $|\psi\rangle$ Von Neuman index correlation (2.10) reduces onto

$$I_C = 2S_A = 2\left(-\lambda_1 \ln \lambda_1 - \lambda_2 \ln \lambda_2\right)$$

where $\lambda_{1,2}$ are the eigenvalues of the reduced density matrix

$$\mathrm{Tr}_A\,\rho = \begin{pmatrix} |\alpha_{00}|^2 + |\alpha_{10}|^2 & \alpha_{00}^*\alpha_{01} + \alpha_{10}^*\alpha_{11} \\ \alpha_{01}^*\alpha_{00} + \alpha_{11}^*\alpha_{10} & |\alpha_{01}|^2 + |\alpha_{11}|^2 \end{pmatrix}.$$

Then $\det\left(\mathrm{Tr}_A\,\rho - \lambda_{1,2}\mathbf{1}\right) = 0$ only if

$$\lambda_{1,2} = \frac{1 \pm \sqrt{1 - 4|\alpha_{01}\alpha_{10} - \alpha_{00}\alpha_{11}|^2}}{2}.$$

I_C may be studied as a function of real variable $u = |\alpha_{01}\alpha_{10} - \alpha_{00}\alpha_{11}|^2$ as

$$I_C\left(u\right) = -\left(1 + \sqrt{1-4u}\right) \ln\left(\frac{1+\sqrt{1-4u}}{2}\right) - \left(1 - \sqrt{1-4u}\right) \ln\left(\frac{1-\sqrt{1-4u}}{2}\right). \quad (2.11)$$

For $u = 1/4$ index correlation $I_C\left(u\right)$ reaches the maximum and $I_C\left(u\right) = 2\ln 2$. Clearly two-qubit Bell states (2.6) are maximally correlated.

Entanglement measures are classified according to the two approaches to quantify entanglement. The *operational approach* [3] says that system is more entangled if it allows for better performance of some task (impossible without entanglement), one such task can be, for instance, teleportation. The *abstract approach* [3] tries to introduce entanglement measures from certain properties which must be fulfilled. Theory of entanglement measures is still under study of the physicists and the mathematicians, but it has been proved in the paper [3] that the Bell states (2.5) are maximally entangled states, with respect to operational measure related to the teleportation process. For two particle pure states I_C (2.10) is the commonly used measure of entanglement.

Werner states are M-partite (D-qudit) states with density matrix $W^{\left[D^M\right]}(\lambda)$ on the Hilbert space $\mathcal{H} = \mathcal{H}\,(D)^{\otimes M}$. According to [23] Werner states are defined in the form

$$W^{[D^M]}(\lambda) = \lambda|\Psi\rangle\langle\Psi| + \frac{1-\lambda}{D^M}\mathcal{I}^{[D^M]},\ \ 0 \leq \lambda \leq 1 \tag{2.12}$$

where

$$|\Psi\rangle = \frac{1}{\sqrt{D}}\sum_{j=0}^{D-1}|j\dots j\rangle$$

and $\mathcal{I}^{[D^M]}$ is identity on the D^M dimensional Hilbert space $\mathcal{H}$. According to [23], Werner states are M-separable (2.8) only if

$$\lambda \leq \left(1 + D^{M-1}\right)^{-1}.$$

According to [8], every bipartite, entangled Werner states (2.12) (for $M = 2$ and $(1 + D)^{-1} < \lambda \leq 1$) can be effectively purified by the generic purification protocol [8] to the general Bell state $|\psi_{00}\rangle$ (2.5). Later in the thesis, in chapter (3), we will study the dynamics of purification for (and close to) the two-qubit Werner states $\rho_W(\lambda)$

$$\rho_W(\lambda) = W^{[2^2]}(\lambda) = \lambda|\psi_{00}\rangle\langle\psi_{00}| + \frac{1-\lambda}{4}\mathcal{I}^{[2^2]},\ \ 0 \leq \lambda \leq 1, \tag{2.13}$$

which are entangled for $1/3 < \lambda \leq 1$.

2.2 Purification protocols

2.2.1 Review of protocols

Purification protocols are used to increase the degree of entanglement on the ensemble of states. The protocol is realized by the application of physically relevant local operations and by the use of classical communication channel - so called *LOCC operations*. The scheme of general purification protocol is given on the figure (2.1).

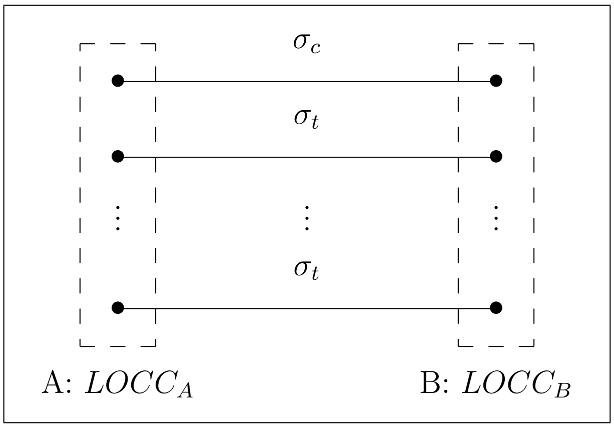

Figure 2.1: General purification protocol scheme

The protocol participants A(Alice) and B(Bob) mutually share the particles of the state according to the prescribed rule and they also divide the ensemble into control (c) and target (t) states. Each particle from control resp. target pair belongs to A and B. A and B perform on the particles local operations. In the end of the protocol step A and B perform measurement on the particles of target states and according to the results source pairs are held or discarded. If the source pairs are kept they become the source of target and control pairs for the next step of the protocol. For the communication of the results A and B use a classical communication channel. The outputs are purified systems. As already explained in chapter (1.1), there exist two classes of protocols according to the use of the chosen local operations: for random local unitaries we obtain so called *non-deterministic protocols*, or with the use of fixed local operations in each step of the protocol, so called *deterministic* *protocols*. Detailed review of the protocols may be found in [5].

In the paper of G. Albert et al., [8], there has been introduced a deterministic analogue of advanced non-deterministic Horodecki protocol, to purify general qudit states. In paper [8], it has been proven, that both of the protocols are efficient in purification of the Werner states (2.12) to the Bell's state $|\psi_{00}\rangle$ (2.5) and it was found by numerical simulations that generic deterministic protocol, for a certain level of initial noise is faster, meaning that it needs less purification steps to achieve desired fidelity with the state $|\psi_{00}\rangle$. In next paragraph we present the construction of purification protocol as defined in [8].

The generic deterministic protocol

The protocol, defined in [8], consists of iterative steps where each step is described by the action of nonlinear map T and unitary transformation U on the ensemble of the one control(c) and N target(t) M qudits systems

$$\begin{aligned} T:\ &\mathcal{B}(\mathcal{H})^{\otimes(N+1)} \mapsto \mathcal{B}(\mathcal{H})^{\otimes(N+1)},\ \mathcal{H} = \mathcal{H}(D)^{\otimes M} \\ T(\sigma_c, \sigma_{t_1}, \ldots, \sigma_{t_N}) &= \frac{A(\sigma_c \otimes \sigma_{t_1} \otimes \ldots \otimes \sigma_{t_N}) A^\dagger}{\mathrm{Tr}[A(\sigma_c \otimes \sigma_{t_1} \otimes \ldots \otimes \sigma_{t_N}) A^\dagger]}, \end{aligned}$$

where the operator A is defined as

$$A = (\mathcal{I}_{\mathbf{c}} \otimes P) \prod_{j=1}^{M} \prod_{i=1}^{N} \mathrm{GXOR}_{ct_i}^{j}$$

with control system identity $\mathcal{I}_c$ and projections onto target systems P

$$P = \prod_{k=1}^{N} P_{t_k},\ \ P_{t_k} = |\mathbf{p}_k\rangle_{t_k t_k}\langle \mathbf{p}_k|\,,\ \ |\mathbf{p}_k\rangle_{t_k} \in \{|0\ldots 0\rangle_{t_k}, \ldots, |D-1\ldots D-1\rangle_{t_k}\}\,.$$

The operator $\mathrm{GXOR}_{ct_i}^{j}$ represents GXOR gate (2.4) and acts on the j-th qudit of the control and i-th target system. In the number state basis the action has a form

$$\begin{aligned} &\mathrm{GXOR}_{ct_i}^{j}\, |\mathbf{k}\rangle_c |\mathbf{l}\rangle_{t_i} = |\mathbf{k}\rangle_c |\tilde{\mathbf{l}}^j\rangle_{t_i},\ \text{where}\ |\mathbf{k}\rangle_c = |k_1 \ldots k_n\rangle_c,\ \ |\mathbf{l}\rangle_{t_i} = |l_1 \ldots l_n\rangle_{t_i}, \\ &|\tilde{\mathbf{l}}^j\rangle_{t_i} = |l_1 \ldots (k_j - l_j)\, mod\, D \ldots l_n\rangle_{t_i}. \end{aligned}$$

Using the fact that both $GXOR_{ct_i}^{(j)}$ and P_{t_i} are Hermitian operators, one can derive the action of the protocol

$$
\begin{aligned}
T\left(\sigma_c, \sigma_{t_1}, \ldots, \sigma_{t_N}\right) &= \mathcal{N}\left(\mathcal{I}_c \otimes P\right) \prod_{j=1}^{M} \prod_{i=1}^{N} GXOR_{ct_i}^{(j)} \left(\sigma_c \otimes \sigma_{t_1} \otimes \ldots \otimes \sigma_{t_N}\right) \\
& \prod_{i=N}^{1} \prod_{j=M}^{1} GXOR_{ct_i}^{(j)} \left(\mathcal{I}_c \otimes P\right) = \left(\mathbf{1_c} \otimes \prod_{i=1}^{N} |\mathbf{p}_i\rangle_{t_i t_i}\langle \mathbf{p}_i|\right) \prod_{j=1}^{M} \prod_{i=1}^{N} GXOR_{ct_i}^{(j)} \\
& \left(\sum_{\mathbf{k},\mathbf{l}} (\sigma_c)_{\mathbf{kl}} |\mathbf{k}\rangle_{cc}\langle \mathbf{l}| \otimes \ldots \otimes \sum_{\mathbf{k}_N,\mathbf{l}_N} (\sigma_{t_N})_{\mathbf{k}_N \mathbf{l}_N} |\mathbf{k}_N\rangle_{t_N t_N}\langle \mathbf{l}_N|\right) \\
& \prod_{i=N}^{1} \prod_{j=M}^{1} GXOR_{ct_i}^{(j)} \left(\mathcal{I}_c \otimes \prod_{i=N}^{1} |\mathbf{p}_i\rangle_{t_i t_i}\langle \mathbf{p}_i|\right) = \\
&= \mathcal{N}\left(\sum_{\mathbf{k},\mathbf{l}} (\sigma_c)_{\mathbf{kl}} (\sigma_{t_1})_{\mathbf{k}\ominus\mathbf{p}_1, \mathbf{l}\ominus\mathbf{p}_1} \ldots (\sigma_{t_N})_{\mathbf{k}\ominus\mathbf{p}_N, \mathbf{l}\ominus\mathbf{p}_N} |\mathbf{k}\rangle_{cc}\langle \mathbf{l}|\right) \otimes P
\end{aligned}
$$

where $\mathbf{i} \ominus \mathbf{p} = (i_1 \ominus p_1, ..., i_M \ominus p_M)$ and the normalization $\mathcal{N}$ equals to

$$
\mathcal{N} = \left(\sum_{\mathbf{k}} (\sigma_c)_{\mathbf{kk}} (\sigma_{t_1})_{\mathbf{k}\ominus\mathbf{p}_1, \mathbf{k}\ominus\mathbf{p}_1} \ldots (\sigma_{t_N})_{\mathbf{k}\ominus\mathbf{p}_N, \mathbf{k}\ominus\mathbf{p}_N}\right)^{-1}.
$$

If the control and the target systems were initially prepared in the same state σ, the map T maps a control system σ_c onto the state

$$
\bar{\sigma}^c = \mathcal{N} \sum_{\mathbf{k},\mathbf{l}} (\sigma)_{\mathbf{k},\mathbf{l}} (\sigma)_{\mathbf{k}\ominus\mathbf{p}_1, \mathbf{l}\ominus\mathbf{p}_1} \ldots (\sigma)_{\mathbf{k}\ominus\mathbf{p}_N, \mathbf{l}\ominus\mathbf{p}_N} |\mathbf{k}\rangle_c \langle \mathbf{l}_c| \tag{2.14}
$$

Such a map is clearly nonlinear.

The action of the unitary transformation U is composed from the actions of local unitary transformations $\{U_i\}$

$$
U : \bar{\sigma}^c \mapsto \sigma_{cout} = U_1 \otimes \ldots \otimes U_M \bar{\sigma}^c U_M^\dagger \otimes \ldots \otimes U_1^\dagger. \tag{2.15}
$$

One iterative step F of the purification protocol is composed of the actions of T and U i.e.

$$
F \equiv F|_c : \sigma_c \mapsto \sigma_{cout} = (U \circ T|_c)\sigma_c. \tag{2.16}
$$

Let us close the description of the protocols with the study of the scheme describing the protocol setup and of the protocol efficiency, see the figures (2.2,2.3).

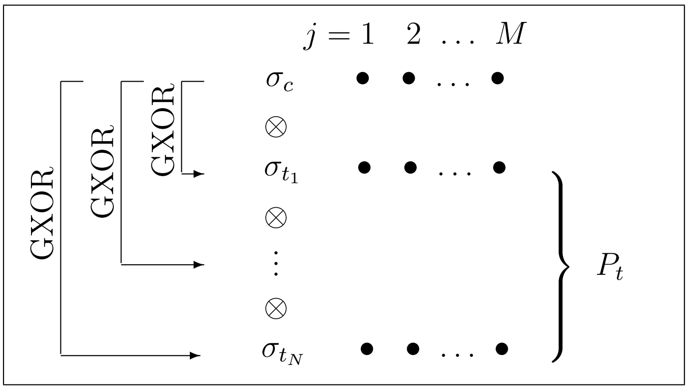

Figure 2.2: The scheme represents the action of a single step of the nonlinear map. Dots represent j qudits of the control σ_c or the i-th target σ^{t_i} system, where $i \in \{1, \ldots, N\}$, $j \in \{1, \ldots, M\}$. The GXOR gate (2.4) is applied on each of the qudit of control and i-th target system. Once the GXOR gate is applied, it is followed by the projection $P_t = |\mathbf{p}_1\rangle\langle\mathbf{p}_1| \otimes \ldots \otimes |\mathbf{p}_N\rangle\langle\mathbf{p}_N|$ on the target systems $\sigma_{t_1} \otimes \ldots \otimes \sigma_{t_N}$, dedicated for the purification of control state σ_c.

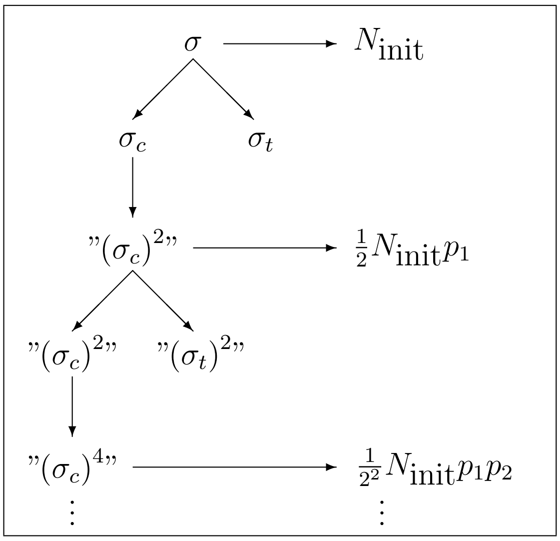

Figure 2.3: Scheme represent the calculation of the efficiency of the purification protocol with the number of target systems $N = 1$ and the target system projection $P_t = |\mathbf{0}\rangle\langle\mathbf{0}|$. Initially the ensemble of the N_{init} states σ is split into two equal parts of control σ_c and target σ_t states. The first step success with probability p_1 and consequently there are $\frac{1}{2}N_{\text{init}}p_1$ states which form the ensemble for the next iterative step. Protocol runs until the fidelity [8] of states reaches the expected level or the pool of the states is empty.

2.3 The Fano representation

This section presents a numerically simple representation of quantum states, similarly to [24]. Any n-qubit density matrix ρ can be written in the Fano form [25] as follows

$$\rho = \mathcal{N} \sum_{\alpha_1,\ldots,\alpha_n} c_{\alpha_1,\ldots,\alpha_n} \sigma_{\alpha_1} \otimes \ldots \otimes \sigma_{\alpha_n} \tag{2.17}$$

with normalization $\mathcal{N} = 2^{-n}$ and $\sigma_{\alpha_i} \in \{\mathcal{I}, \mathcal{X}, \mathcal{Y}, \mathcal{Z}\}$, $\mathcal{I}$ is identity on the Hilbert space $\mathcal{H}(2)$ and $\mathcal{X}$, $\mathcal{Y}$, $\mathcal{Z}$ are Pauli matrices. The matrices are represented as

$$\mathcal{I} \equiv \begin{pmatrix} 1 & 0 \\ 0 & 1 \end{pmatrix}, \ \mathcal{X} \equiv \begin{pmatrix} 0 & 1 \\ 1 & 0 \end{pmatrix}, \ \mathcal{Y} \equiv \begin{pmatrix} 0 & -\imath \\ \imath & 0 \end{pmatrix}, \ \mathcal{Z} \equiv \begin{pmatrix} 1 & 0 \\ 0 & -1 \end{pmatrix}.$$

Since the density operator ρ is Hermitian, all the parameters $c_{\alpha_1,\ldots,\alpha_n}$ are real. Moreover $\mathrm{Tr}(\rho) = 1$ implies $c_{\mathcal{I},\ldots,\mathcal{I}} = 1$, the other parameters are

$$c_{\alpha_1,\ldots,\alpha_n} = \mathrm{Tr}\left(\sigma_{\alpha_1} \otimes \ldots \otimes \sigma_{\alpha_n} . \rho\right).$$

Because of the fixed value of $c_{\mathcal{I},\ldots,\mathcal{I}} = 1$, each n-qubit quantum state may be represented by $4^n - 1$ real coefficients $\{c_{\alpha_1 \neq \mathcal{I},\ldots,\alpha_n \neq \mathcal{I}}\}$ which form the generalized Bloch vector $\mathbf{b}$. For the one-qubit case, the Bloch vectors $\mathbf{b}$ span the entire unit ball in $\mathbb{R}^3$, for two qubits the 15 elements of vector $\mathbf{b}$ are

$$\begin{aligned} \mathbf{b} \ = \ & (c_{\mathcal{IX}}, c_{\mathcal{IY}}, c_{\mathcal{IZ}}, c_{\mathcal{XI}}, c_{\mathcal{XX}}, c_{\mathcal{XY}}, c_{\mathcal{XZ}}, c_{\mathcal{YI}}, c_{\mathcal{YX}}, c_{\mathcal{YY}}, c_{\mathcal{YZ}}, \\ & c_{\mathcal{ZI}}, c_{\mathcal{ZX}}, c_{\mathcal{ZY}}, c_{\mathcal{ZZ}}). \end{aligned} \tag{2.18}$$

2.4 Framework for the treatment of chaos

This section is mainly focused on the summary of existing mathematical framework of the study of discrete dynamical systems generated by a rational function in one complex variable. We also provide with the basic definitions to study dynamics of the holomorphic maps in more complex variables. The presented definitions and theorems will be used to study the chaotic dynamics of the generic purification protocol. As a source of information it has been used the books of I. D. Chueshov [15], R. Temam [26] (general theory of finite and infinite dimensional dynamical systems) and J. W. Milnor [11; 12] (framework to study chaos in the dynamical system generated by one complex variable map) and S. Morosawa et. al [13] (framework to study chaos in dynamical system generated by one and two complex variable maps). In the work of J. E. Fornæs [14] one can find the review of the actual progress and open problems of multidimensional complex dynamical systems.

First, let me introduce the definitions of a dynamical system and a chaotic dynamical system

Definition 2.4.1 (Dynamical system - see [15; 26])**.** *Let X be a complete metric space X. A* dynamical system - DS - *is taken to mean the pair of objects $(\{S_t\}, X)$ where $\{S_t\}$ is a family of continuous maps of the space X into itself with the properties*

1. $\forall\ t, u \in T: \quad S_{t+u} = S_t \circ S_u$,

2. $S_0 = \mathcal{I}$ *is identity,*

*where T coincides with either a set $\mathbb{R}$ of real numbers (*continues reversible DS*) or a set $\mathbb{R}_+$ of nonnegative real numbers (*continues irreversible DS*) or a set $\mathbb{Z} = \{\ldots, -1, 0, 1 \ldots\}$ of all integers (*discrete reversible DS*) or a set $\mathbb{N}_0 = \{0, 1, 2 \ldots\}$ of all nonnegative integers (*discrete irreversible DS*). Therewith X is called a* state space *(or* phase space*), the family of operators $\{S_t\}$ is called an* evolutionary operator *(or* semigroup*), parameter $t \in T$ plays the role of time.*

In the thesis we will study discrete irreversible DS where $S_n \equiv f^{\circ n}$, $n \in \mathbb{N}_0$ means n-times apply of f, i.e., $f^{\circ n}(x) = f(\ldots f(x)\ldots)$ and $f : X \mapsto X$ is a holomorphic endomorphism. We denote such DS by the pair (f, X).

Definition 2.4.2 (Chaotic dynamical system by Devaney - see [13; 14])**.** *Let X be a complete metric space with a metric ρ. The dynamical system (f, X) is said to be* chaotic *if*

1. *the set of periodic points of f is dense in X.*
2. *the function f has a transitivity property, i.e., for any two open sets U and V of X, there is a k such that $f^{\circ k}(U) \cap V \neq \emptyset$.*
3. *the function f has sensitive dependence on initial conditions, i.e., there is a constant δ such that, for any $x \in X$ and any neighborhood N, there are $y \in N$ and n satisfying $\rho(f^{\circ n}(x), f^{\circ n}(y)) > \delta$.*

After Devaney gave this definition, it was proven that the first two conditions imply the third one [13]. Nevertheless, the third condition, sensitive dependence of chaotic dynamical system on initial conditions, is the essence of chaos.

Now, let us introduce the definition of a normal family of continuous maps. It will help us to introduce basic dichotomy of the initial states of dynamical system onto the Julia set and the Fatou set. Fatou set represents states with regular dynamics while nonempty Julia set represents irregular dynamics and for certain systems even chaos.

Definition 2.4.3 (A normal family of maps - see [11; 14])**.** *Let X, Y are complete metric spaces. A set $\mathcal{A}$ of continuous maps f_α from X to Y is a* normal family *if every infinite sequence of maps from $\mathcal{A}$ contains a subsequence which converges locally uniformly to a continuous map from X to Y.*

The existence of the locally uniformly convergent subsequence in the series of iterative evolution $\{f^n\}$ of the system implies regular dynamics. A typical example is represented by the oscillation between finite number of states like $f^{2i}(z) = 0$ and $f^{2i+1}(z) = 1$.

Definition 2.4.4 (The Fatou and the Julia set - see [11; 14])**.** *Let X be a complete metric space, let f be a continuous endomorphism of X, and let $f^{\circ n} : X \mapsto X$ be its n-fold iterate.*

Fixing some point $x_0 \in S$, we have the following basic dichotomy. If there exists some neighborhood U of x_0 so that the sequence of iterates $\{f^{\circ n}\}$ restricted to U forms a normal family, then we say that x_0 is a regular or normal point, or that x_0 belongs to the Fatou set *of f. Otherwise, if no such neighborhood exists, we say that x_0 belongs to the* Julia set *$J = J(f)$.*

If f is a holomorphic endomorphism of Riemann surface - either $\mathbb{C}$ or the *Riemann sphere* $\equiv \hat{\mathbb{C}} = \mathbb{C} \cup \{\infty\}$ [11; 13] (union of the complex plane with complex infinity) - then the Fatou and the Julia set definitions coincide with the definitions of Morosawa et. al [13].

2.4.1 Rational functions of one complex variable

Let us focus now on the theory of dynamical systems of rational functions in one complex variable. According to [11; 13], the *rational function* f means the holomorphic endomorphism of $\hat{\mathbb{C}}$ in the form of the quotient $f(z) = p(z)/q(z)$ of two polynomials, where the polynomials $p(z)$ and $q(z)$ have no common roots. The *degree* of f is then equal to the maximum of the degrees of p, q.

Definition 2.4.5 (*Rat* set - see [11; 13]). *We denote by Rat the set of all rational functions of degree not less than two.*

Particularly, there exists a theorem about the backward invariance of Julia and Fatou sets which is useful for the numerical calculation of Julia sets.

Theorem 2.4.6 (Invariance of the Julia set and the Fatou set - see [11; 13]). *Let $f \in Rat$. Then the Julia set and the Fatou set are completely* invariant

- $f(J(f)) \subset J(f)$, $f^{-1}(J(f)) = J(f)$,
- $f(F(f)) \subset F(f)$, $f^{-1}(F(f)) = F(f)$.

For $f \in$ *Rat* it is easy to calculate all the pre images of the state in the Julia and the Fatou sets. From a numerical point of view, the backward iteration on the Fatou and the Julia sets are numerically stable, however because of the non existence of a unique pre-image, the number of possible pre-images grows exponentially with the increase of backward iteration steps and the simulation becomes computationally demanding.

Also, there exists a theorem which points out an interesting topology of the Julia and Fatou sets.

Theorem 2.4.7 (Basic topology of the Julia and Fatou sets - see [11; 13])**.** *Let $f \in Rat$. Then either the Julia set $J(f)$ of f contains no interior points, or the Fatou set $F(f)$ is empty i.e. $J(f) = \hat{\mathbb{C}}$.*

Now, let us introduce a classification of the periodic points for dynamical system generated by one complex variable holomorphic function.

Definition 2.4.8 (Classification of periodic points - see [11; 13])**.** *Let $f : D \to \hat{\mathbb{C}}$ be a meromorphic function on D, and z_0 be a* periodic point *of f of period $l \in \mathbb{N}$ i.e. $f^{\circ l}(z_0) = z_0$ and $f^{\circ j}(z_0) \neq z_0$ $(1 \leq j \leq l-1)$. We define the* multiplier *λ at z_0 of f by*

$$\lambda = \left(f^{\circ l}\right)'(z_0) .$$

Here, when $z_0 = \infty$, we consider that $\left(f^{\circ l}\right)'(z_0)$ is the value of

$$\left(\frac{1}{f^{\circ l}(1/z)}\right)'$$

at 0.

- *When $|\lambda| > 1$, we call z_0 a* repelling *periodic point.*
- *When $|\lambda| < 1$, we call z_0 an* attracting *periodic point. In particular, if $\lambda = 0$, then we call z_0 a* supperatracting *periodic point.*
- *When $|\lambda| = 1$, we call z_0* indifferent *periodic point. When there exists a positive integer m such that $\lambda^m = 1$, we call z_0 a* rationally indifferent *periodic point, or* parabolic *periodic point. Otherwise, we call z_0 an* irrationally indifferent *periodic point.*

  We call $\left\{z_0, z_1 \equiv f(z_0), \ldots, z_{l-1} \equiv f^{\circ(l-1)}(z_0)\right\}$ a cycle *of z_0 with the* length *l. Especially, in case $l = 1$ i.e. $f(z_0) = z_0$ we call z_0 a* fixed point.

According to [9; 11], one can calculate the multiplier λ using the *chain rule*

$$\lambda = \left(f^{\circ N}\right)^{'}(z_0) = f^{'}(z_0).f^{'}(z_1)\dots f^{'}(z_{l-1}). \tag{2.19}$$

The calculation of the multiplier λ of the periodic point z_0 (i.e. of the cycle of z_0) is decomposed into the multiplication of stability multipliers of each point of the cycle. The chain rule is a numerically convenient method to evaluate the stability of the cycle. Also, let us introduce the definition of preperiodic point.

Definition 2.4.9 (Preperiodic point - see [11; 13])**.** *For a general holomorphic endomorphism f, we say α is* preperiodic *if α is not periodic but there is positive $m \in \mathbb{N}$ such that $f^{\circ m}(\alpha)$ is periodic.*

Next let us summarize theorems connecting the Julia set properties with the periodic and preperiodic points properties. This part is crucial to fully understand the structure of Julia sets and consequently the chaotic dynamics.

Theorem 2.4.10 (Points in the Julia set - see [11; 13])**.** *Let $f \in Rat$. Then, every repelling periodic point or parabolic periodic point of f belongs to the Julia set. Every (super)attracting periodic point belongs to the Fatou set.*

It is proved in [13] that every $f \in Rat$ has either repelling fixed point or parabolic periodic point. Direct consequences of this theorem are:

Theorem 2.4.11 (Condition for the nonempty Julia set - see [11; 13])**.** *For every $f \in Rat$ the Julia set $J(f)$ is not empty.*

Theorem 2.4.12 (First fundamental theorem for *Rat* - see [11; 13])**.** *For every $f \in Rat$, the Julia set $J(f)$ is the closure of the set of the repelling periodic points.*

Theorem 2.4.13 (Julia set coincides with $\mathbb{C}$ - see [11; 13])**.** *If all the critical points of a rational function f are preperiodic, then its Julia set $J(f)$ coincides with $\mathbb{C}$.*

As a consequence of the theorems (2.4.11,2.4.12) the dynamical system is chaotic on its Julia set.

Theorem 2.4.14 (Existence of the chaotic dynamical system on its Julia set - see [13])**.** *For every $f \in Rat$, the dynamical system $(f, J(f))$ is chaotic (according to definition (2.4.2)).*

There exists an interesting subset of the hyperbolic, rational functions with the property to be expanding on its Julia set. Then the dynamical system $(f, J(f))$ is chaotic similar to the sense of Poincaré.

Definition 2.4.15 (Hyperbolic function - see [13])**.** *A rational function f is called* hyperbolic *if there is no intersection of Julia set with the closure of the forward orbit of the critical points i.e. if $J(f) \cap \overline{C^{+}(f)} = \emptyset$, where $C^{+}(f) = \bigcup_{n=1}^{\infty} f^{\circ n}(C_f)$ is forward orbit of $C_f = \{z \in \mathbb{C} | f'(z) = 0\}$ critical points.*

Definition 2.4.16 (Expanding function - see [13])**.** *A rational function f is* expanding *on $J(f)$ if there are a Riemannian metric $\sigma(z)^2|dz|^2$ on some neighborhood of $J(f)$ and positive constants c and $\lambda > 1$ such that*

$$\sigma\left(f^{\circ n}(z)\right) | \left(f^{\circ n'}(z)\right) | \geq c\lambda^{n}\sigma(z)$$

for all n and $z \in J(f)$. This λ is called an expanding constant *of f on $J(f)$.*

Theorem 2.4.17 (Conditions for expanding function - see [13])**.** *For $f \in Rat$, the following three conditions are equivalent to each other.*

- *The function f is hyperbolic.*
- *All the critical points are in $F(f)$, each of whose orbit converges towards an attracting cycle.*
- *The function f is expanding on $J(f)$.*

Theorem 2.4.18 (Lebesgue measure of the Julia set - see [13])**.** *The two-dimensional Lebesgue measure of the Julia set of a hyperbolic rational function is* 0*.*

For hyperbolic rational function the Julia set may exhibit complicated topological structure (self similarities) and may become a fractal, like famous Mandelbrot set [13]. Shishikura proved [13], that the Hausdorff dimension [13] of the boundary of the Mandelbrot set is 2. In the thesis, we are not going to calculate the Hausdorff dimension of the Julia sets, nevertheless let us mention following interesting theorem.

Theorem 2.4.19 (Hausdorff dimension of the Julia set - see [13])**.** *For the Julia set $J(f)$ of a hyperbolic rational function f,* $0 < dim\,(J(f)) < 2$.

J. W. Milnor presented, in details, the properties for quadratic rational maps [12]. Here bellow let us present central theorem to distinguish connectivity or total disconnectivity of the Julia set.

Theorem 2.4.20 (Connected and disconnected Julia set - see [12])**.** *The Julia set J of a quadratic rational function f is either connected, or totally dis-connected and homeomorphic, with its dynamics, to the one-sided shift on two symbols. It is totally disconnected if and only if either*

- *both critical orbits converge to a common attracting fixed point, or*
- *both critical orbits converge to a common fixed point of multiplicity two but neither critical orbit actually lands on this point.*

Let us point out that the converge of the critical orbits to a common attracting fixed point may be well simulated by numerical calculation and consequently one can decide about the disconnect Julia set $J(f)$ also using numerical methods. By this, one also proves that f is hyperbolic i.e. expanding on $J(f)$ (2.4.15,2.4.17) - then the dynamical system $(f, J(f))$ is chaotic (2.4.14) similar to the sense of Poincaré.

2.4.2 Holomorphic maps of several variables

Let me present the mathematical framework to study the dynamics of holomorphic maps of several complex or real variables, as presented in [13]. We use the presented framework especially for the numerical simulations of dynamics for two-qubit protocols.

Definition 2.4.21 (Holomorphic function - see [13])**.** *A complex valued function f defined in an open set $U \subset \mathbb{C}^N$ is said to be holomorphic if the following two conditions are satisfied*

1. *f is continuous in U*
2. *for each k $(1 \leq k \leq N)$, the function $f(z_1, \ldots, z_k, \ldots, z_N)$ is holomorphic with respect to the single variable z_k.*

Definition 2.4.22 (Holomorphic map - see [13; 14])**.** *A map $\mathcal{F}$*

$$\mathcal{F} : U \ni (z_1, \ldots, z_M) \mapsto (w_1, \ldots, w_M) = (f_1(z_1), \ldots, f_M(z_M)) \in \mathbb{C}^M$$

defined by an M-tuple of holomorphic functions $f_1, \ldots, f_M$ on an open set $U \subset \mathbb{C}^M$, is said to be a holomorphic map*.*
The (M, N) matrix $\mathcal{F}'(z) = (\partial w_j / \partial z_k)$ is said to be the (complex) Jacobian matrix *of the holomorphic map $\mathcal{F}$. In general, a map (not necessarily holomorphic) $\mathcal{F}$ from $U \subset \mathbb{C}^N$ to $\mathbb{C}^M$ can be regarded as a map from $U \subset \mathbb{R}^{2N}$ to $\mathbb{R}^{2M}$ with respective real Jacobian matrix.*

For the holomorphic map there exist also the definitions of *fixed point* resp. *periodic point* (*cycle*) equal to the definitions for one complex variable function (2.4.8). Also, there exists the classification theorem for these points.

Definition 2.4.23 (Classification of periodic points - see [13; 14])**.** *Let $\mathcal{F}$ be a holomorphic map, let z_0 be a periodic point of period l, $\mathcal{F}^{\circ l}(z_0) = z_0$. We say that z_0 is an* attracting *resp.* repelling *periodic point if all the eigenvalues of the Jacobian matrix $\left(\mathcal{F}^{\circ l}\right)'(z_0)$ are less resp. greater than 1 in absolute value. We say that z_0 is a* saddle *periodic point if some, but not all of the eigenvalues of $\left(\mathcal{F}^{\circ l}\right)'(z_0)$ are in absolute value less than 1 and the other are in absolute value greater than 1.*

Similarly to one dimensional maps (2.4.8), an attracting resp. a repelling periodic point represents locally stable resp. unstable state of the system. A saddle point does not exists for one dimensional maps, it represents locally stable and unstable submanifolds near z_0 [14]. Classification of periodic points can be done using the extended *chain rule*: $\left(\mathcal{F}^{\circ l}\right)'(z_0) \equiv \mathcal{F}'(z_0) \ldots \mathcal{F}'(z_{l-1})$.

According to literature [13; 14], there is a significant difference when studying the dynamics of one and multi-dimensional maps. For example, rational function of degree two, in one complex variable, induces chaos on its Julia set (2.4.14), but this is not generally true for the two complex variable rational function [14]. For the study of the dynamics of multidimensional maps another dichotomy of the Julia set points on *nonwandering* and *wandering* domains [13; 14] has to be introduced. The point p in the nonwandering domain $\mathcal{M}$ satisfies similar condition compared to the second condition of chaos (2.4.2) - i.e. $p \in \mathcal{M}$ if given any neigborhood U of $p \in \mathcal{M}$, there is an integer $n \geq 1$ so that $\mathcal{F}^{\circ n}(U) \cap U \neq \emptyset$. The points in wandering domain contradict it. Further details of the theory are beyond the scope of the thesis and reader can find more details in the existing literature [13; 14]. Note that the theory is still under the intensive research.

2.4.3 Liapunov characteristic exponents

Liapunov exponents are important characteristics of dynamical systems. According to Lichtenberg and Lieberman [10], Liapunov exponents of a given trajectory characterize the mean exponential rate of divergence of trajectories surrounding it. Characterization of the stochasticity of a phase state trajectory in terms of the divergence of nearby trajectories was introduced by Hénon and Heiles in 1964. The study continues and in 1980, Benettin et al. provided a full description and computational algorithm for Liapunov exponents.

Here bellow will be provided the definition of Liapunov exponents for a discrete dynamical system, derived from the definition for a continuous dynamical system [10]. We will use this definition in an application. Let us suppose the dynamical system on an n-dimensional metric space, with the orthonormal basis $\{e_i\}_{i=1}^{n}$, generated by the map $\mathcal{F}$. Let us study the trajectory $\mathbf{x}(n) = \mathcal{F}^{\circ n}(\mathbf{x}_0)$, where $\mathbf{x}_0$ is the initial state. Then the *mean exponential rate of divergency* of two initially close trajectories $\mathbf{x}_0$, $\mathbf{x}_0 + \Delta\mathbf{x}_0$, with the deviation $\Delta\mathbf{x}_0 = \|\Delta\mathbf{x}_0\|\mathbf{w}$ in the direction $\mathbf{w}$, is defined as

$$\sigma(x_0, w) = \lim_{n\to\infty} \left(\lim_{\|\Delta\mathbf{x}_0\|\to 0} \left(\frac{1}{n} \ln \frac{d(\mathbf{x}_0, n)}{\|\Delta\mathbf{x}_0\|} \right) \right) \tag{2.20}$$

where $d(\mathbf{x}_0, n)$ is the distance of the evolved, initially closed, points after the n-steps of the map

$$d(\mathbf{x}_0, n) = \|\mathcal{F}^n(\mathbf{x}_0 + \Delta\mathbf{x}_0) - \mathcal{F}^n(\mathbf{x}_0)\|.$$

We also define the i-th *Liapunov characteristic exponent* as the mean exponential rate of divergency in the direction of the i-th vector of the orthonormal basis

$$\sigma_i\left(\mathbf{x}_0\right) = \sigma\left(\mathbf{x}_0, e_i\right). \tag{2.21}$$

These can be ordered by magnitude

$$\sigma_1\left(\mathbf{x}_0\right) \geq \sigma_2\left(\mathbf{x}_0\right) \geq \ldots \geq \sigma_n\left(\mathbf{x}_0\right).$$

In 1968 it was proven, by Oseledec, that the Liapunov characteristic exponents are independent of the choice of metric for the phase space.

In chapter (3), we provide with the analytical calculation of the positive Liapunov exponent for the chaotic dynamical systems (in Poincareé sense) on the analytically known Julia set of the circle $K(0,1)$. For the chaotic dynamical systems on the analytically unknown Julia sets, we will not provide with the numerical calculations of the Liapunov exponent, even if the numerical method exists [10]. To numerically calculate the Liapunov exponent one faces the issue to find a "sufficiently good" points of the Julia set from the perspective of long run iterations using finite precision of computation. Secondly one needs to eliminate the numerical errors during the long run iterations by calculation with a huge amount of digits, this impacts the performance of the computation.

Chapter 3

Results

The main interest of the thesis is to study, both analytically and numerically, the dynamics of a generic purification protocol and the existence of chaos for one and two-qubit systems. This chapter contains the original results of the study. First of all we analyze the properties of the protocol to preserve purity and separability of the outputs. Then we start to study the dynamics for one-qubit states the existence of chaos will be proven. After that we will continue with the analysis of the dynamics for two-qubit pure separable states. Then we turn our interest to the dynamics for general two-qubit pure states and we prove a strong sensitivity of the protocol to converge either to the completely separable of maximally entangled attractors. Finally we will study the two-qubit mixed states. We will learn that for two-qubit mixed states also a third attractor appears, which represents completely mixed state. These results are consistent with our expectations, based only on random numerical sampling of the problem, and prove a novel form of quantum chaos.

3.1 Generic purification protocol properties

Before we analyze the dynamics of the generic purification protocol, let us point out the general properties of the protocol acting on the ensemble of pure and separable states. We will prove that in each step of the protocol (2.16) a pure state is mapped onto a pure state and a separable state onto a separable state. These properties will be useful for later studies of the protocol dynamics.

3.1.1 Action on a pure state

One can ask the question, what is the action of the nonlinear map (2.14) on M-qudits pure state? Any M-qudits pure state $|\psi\rangle$ can be represented, in number state basis, in the form

$$|\psi\rangle = \sum_{\mathbf{k}} \alpha_{\mathbf{k}} |\mathbf{k}\rangle,$$

where $\mathbf{k} = (k_1, \ldots, k_M)$, $k_i \in \{0, \ldots, D-1\}$. Pure state is also represented by the density matrix σ, in the form

$$\sigma = |\psi\rangle\langle\psi| = \sum_{\mathbf{k},\mathbf{l}} (\sigma)_{\mathbf{k},\mathbf{l}} |\mathbf{k}\rangle\langle\mathbf{l}|, \;\; (\sigma)_{\mathbf{k},\mathbf{l}} = \alpha_{\mathbf{k}} \alpha^*_{\mathbf{l}}.$$

Consequently, the nonlinear map (2.14) maps the density matrix σ_c of the pure state onto the density matrix of the pure state

$$\bar{\sigma}_c = \mathcal{N} \sum_{\mathbf{k},\mathbf{l}} \alpha_{\mathbf{k}} \alpha^*_{\mathbf{l}} \alpha_{\mathbf{k}\ominus\mathbf{p}_1} \alpha^*_{\mathbf{l}\ominus\mathbf{p}_1} \ldots \alpha_{\mathbf{k}\ominus\mathbf{p}_N} \alpha^*_{\mathbf{l}\ominus\mathbf{p}_N} |\mathbf{k}\rangle_{cc}\langle\mathbf{l}| = |\bar{\psi}\rangle_{cc}\langle\bar{\psi}|$$

where

$$\mathcal{N} = \left(\sum_{\mathbf{k}} |\alpha_{\mathbf{k}}|^2 |\alpha_{\mathbf{k}\ominus\mathbf{p}_1}|^2 \ldots |\alpha_{\mathbf{k}\ominus\mathbf{p}_N}|^2 \right)^{-1}$$

and

$$|\bar{\psi}\rangle_c = \sum_{\mathbf{k}} \beta_{\mathbf{k}} |\mathbf{k}\rangle_c, \;\; \beta_{\mathbf{k}} = \sqrt{\mathcal{N}} \alpha_{\mathbf{k}} \alpha_{\mathbf{k}\ominus\mathbf{p}_1} \ldots \alpha_{\mathbf{k}\ominus\mathbf{p}_N}. \tag{3.1}$$

The nonlinear map (2.14) behaves like a filter for the pure state $|\mathbf{k}\rangle_c$ if $\beta_{\mathbf{k}} = 0$. Because the unitary map (2.15) maps a pure state onto a pure state, the whole purification protocol (2.16) maps a pure state onto a pure state or one step of the protocol behaves like a filter.

3.1.2 Action on separable state

Similarly, one can ask the question, what is the action of the nonlinear map (2.14) on the M-separable (2.8) state? Such a M-qudits state can be represented by the density matrix σ, in the form

$$\sigma = \sum_{i=1}^{k} p_i \sigma^i_1 \otimes \ldots \otimes \sigma^i_M, \;\; \sigma^i_j = \sum_{k_j,l_j=0}^{D-1} \left(\sigma^i_j\right)_{k_j,l_j} |k_j\rangle\langle l_j|,$$

where the density matrix $\sigma^{i,j}$ represents the j-th particle, which belongs to the ensemble for the weight p_i and the sum of the weights for all the possible ensembles is 1 i.e. $\sum_i^k w_i = 1$. Then the coefficient of the density matrix σ is in the form

$$(\sigma)_{\mathbf{k},\mathbf{l}} = \sum_{i=1}^{k} p_i \left(\sigma_1^i\right)_{k_1,l_1} \dots \left(\sigma_M^i\right)_{k_M,l_M},$$

where $\mathbf{k} = (k_1, \dots, k_M)$, $\mathbf{l} = (l_1, \dots, l_M)$, $k_i, l_i \in \{0, \dots, D-1\}$.

The action of the nonlinear map (2.14) maps the density matrix of the separable state onto a density matrix which again represents the separable state

$$\begin{aligned}
\bar{\sigma}^c &= \mathcal{N} \sum_{\mathbf{k},\mathbf{l}} \left[\sum_{i_0} p_{i_0} \left(\sigma_1^{i_0}\right)_{k_1,l_1} \dots \left(\sigma_M^{i_0}\right)_{k_M,l_M} \right] \cdot \\
&\quad \cdot \left[\sum_{i_1} p_{i_1} \left(\sigma_1^{i_1}\right)_{k_1\ominus(\mathbf{p}_1)_1, l_1\ominus(\mathbf{p}_1)_1} \dots \left(\sigma_M^{i_1}\right)_{k_M\ominus(\mathbf{p}_1)_M, l_M\ominus(\mathbf{p}_1)_M} \right] \dots \\
&\quad \dots \left[\sum_{i_N} p_{i_N} \left(\sigma_1^{i_N}\right)_{k_1\ominus(\mathbf{p}_N)_1, l_1\ominus(\mathbf{p}_N)_1} \dots \left(\sigma_M^{i_N}\right)_{k_M\ominus(\mathbf{p}_N)_M, l_M\ominus(\mathbf{p}_N)_M} \right] |\mathbf{k}\rangle_{cc}\langle\mathbf{l}| = \\
&= \mathcal{N} \sum_{\mathbf{k},\mathbf{l}} \left[\sum_{i_0,\dots,i_N} p_{i_0} p_{i_1} \dots p_{i_N} \left[\left(\sigma_1^{i_0}\right)_{k_1,l_1} \dots \left(\sigma_1^{i_N}\right)_{k_1\ominus(\mathbf{p}_N)_1, l_1\ominus(\mathbf{p}_N)_1} \right] \dots \right. \\
&\quad \left. \dots \left[\left(\sigma_M^{i_0}\right)_{k_M,l_M} \dots \left(\sigma_M^{i_N}\right)_{k_M\ominus(\mathbf{p}_N)_M, l_M\ominus(\mathbf{p}_N)_M} \right] \right] |\mathbf{k}\rangle_{cc}\langle\mathbf{l}| = \\
&= \sum_{i_0,\dots,i_N} p_i \dots p_{i_N} \bar{\sigma}^{(i_0,\dots,i_N),1} \otimes \dots \otimes \bar{\sigma}^{(i_0,\dots,i_N),M}
\end{aligned}$$

where

$$\bar{\sigma}^{(i_0,\dots,i_N),j} = \mathcal{N}_i \sum_{k_j,l_j} \left(\sigma_j^{i_0}\right)_{k_j,l_j} \left(\sigma_j^{i_1}\right)_{k_j\ominus(\mathbf{p}_1)_j, l_j\ominus(\mathbf{p}_1)_j} \dots \left(\sigma_j^{i_N}\right)_{k_j\ominus(\mathbf{p}_N)_j, l_j\ominus(\mathbf{p}_N)_j} |k_j\rangle\langle l_j| \tag{3.2}$$

with

$$\mathcal{N}_j = \left(\sum_{k_j} \left(\sigma_j^{i_0}\right)_{k_j,k_j} \left(\sigma_j^{i_1}\right)_{k_j\ominus(\mathbf{p}_1)_j, k_j\ominus(\mathbf{p}_1)_j} \dots \left(\sigma_j^{i_N}\right)_{k_j\ominus(\mathbf{p}_N)_i, k_j\ominus(\mathbf{p}_N)_i} \right)^{-1} \geq 0.$$

Let us prove that $\bar{\sigma}^{(i,\dots,i_N),j}$ represents a hermitian operator with unit trace i.e. a density matrix

$$\begin{aligned}
\left(\bar{\sigma}^{(i_0,\ldots,i_N),j}\right)_{k_j,l_j} &= \mathcal{N}_i\left(\sigma_j^{i_0}\right)_{k_j,l_j}\left(\sigma_j^{i_1}\right)_{k_j\ominus(\mathbf{p}_1)_j,l_j\ominus(\mathbf{p}_1)_j}\cdots\left(\sigma_j^{i_N}\right)_{k_j\ominus(\mathbf{p}_N)_j,l_j\ominus(\mathbf{p}_N)_j} = \\
&= \mathcal{N}_j\left(\sigma_j^{i_0}\right)^*_{l_j,k_j}\left(\sigma_j^{i_1}\right)^*_{l_j\ominus(\mathbf{p}_1)_j,k_j\ominus(\mathbf{p}_1)_j}\cdots\left(\sigma_j^{i_N}\right)^*_{l_j\ominus(\mathbf{p}_N)_j,k_j\ominus(\mathbf{p}_N)_j} = \\
&= \left(\bar{\sigma}^{(i_0,\ldots,i_N),j}\right)^*_{l_j,k_j} = \left(\bar{\sigma}^{(i_0,\ldots,i_N),j^\dagger}\right)_{k_j,l_j}, \\
\left(\bar{\sigma}^{(i_0,\ldots,i_N),j}\right)_{k_j,k_j} &\geq 0, \\
\mathrm{Tr}\left(\bar{\sigma}^{(i_0,\ldots,i_N),j}\right) &= 1 \text{ or the subsystem is filtered out by the purification.}
\end{aligned}$$

Finally, if none of the subsystems is filtered out, then

$$\begin{aligned}
\mathrm{Tr}\left(\bar{\sigma}_c\right) &= \sum_{i_0,\ldots,i_N} p_{i_0}p_{i_1}\ldots p_{i_N}\,\mathrm{Tr}\left(\bar{\sigma}^{(i_0,\ldots,i_N),1}\otimes\ldots\otimes\bar{\sigma}^{(i_0,\ldots,i_N),M}\right) = \\
&= \sum_{i_0,\ldots,i_N} p_{i_0}.p_{i_1}\ldots p_{i_N}.1 = \prod_{m=0}^{N}\sum_{i_m} p_{i_m} = \prod_{m=0}^{N} 1 = 1.
\end{aligned}$$

The nonlinear map (2.14) behaves like a filter for the separable state σ_c in the case $\bar{\sigma}_c^{(\alpha_0,\ldots,\alpha_N),i} = \mathbf{0}$ for some $i \in \hat{M}$. As already mentioned for the pure states, the unitary map (2.15) maps a pure state onto a pure state. Therefore, the whole purification protocol (2.16) maps a separable state onto a separable state or the protocol behaves like a filter.

3.1.3 Summary

Let us summarize now the main statements, valid for every generic purification protocol (2.16):

i. generic purification protocol maps a pure state onto a pure state,

ii. generic purification protocol maps a separable state onto a separable state

These statements are valid for every purification protocol under study, meaning for the purification of the general qudit systems, using arbitrary number N of the target systems per control one and for every setting of the target system projections P_{t_i}. Also the generic purification protocol may behave like a filter for certain states. If this happens, then the purification procedure stops, because none of the possible target states pass the selective projection in the purification step.

3.2 Representation by rational maps

To represent the dynamics of any physical system by rational map in complex or in real variables has advantages for analytic studies as well as for numerical calculations. For such a map there exist efficient algorithms to find its roots i.e. one can calculate its periodic points. Also, the rational functions are holomorphic, so one can easily calculate their Jacobians and evaluate the stability of periodic points. By this one can study the dynamics. In particular, chaotic dynamics generated by rational function in one complex variable can be analytically treated and numerically studied using extensive mathematical framework (2.4). This has been the motivation to find an effective representation of purification protocols by rational functions.

Also the representation shall be minimal in terms of needed variables. Taking into account only the properties of purified states, n qudits pure state $|\psi\rangle$ is represented only by $nD-1$ complex parameters, because of normalization and rays equivalence of pure states in the Hilbert space. Therefore one-qubit pure state dynamics can be represented by one complex variable. Similarly, each n qudits density matrix σ, the Hermitian operator with unite trace, is represented by only $(nD)^2-1$ real parameters. For two-qubit states it means there are fifteen real, independent, parameters.

We focus now on finding of the explicit transformation for one-qubit pure states and for two-qubit pure and general mixed states. Later on, we will apply found results for the analysis of purification dynamics.

3.2.1 One-qubit pure states

As introduced in the papers [I], [27] a one-qubit pure state

$$|\psi(\boldsymbol{\alpha})\rangle = \alpha_0|0\rangle + \alpha_1|1\rangle,$$

is represented in the number state basis by two complex numbers $\alpha_{0,1}$. Using the transformation

$$z = \frac{\alpha_0}{\alpha_1} \in \hat{\mathbb{C}} \tag{3.3}$$

we can write $|\psi\rangle$ as

$$|\psi(z)\rangle = \mathcal{N}(z)\,(z|0\rangle + |1\rangle)\,,$$

where $\mathcal{N}(z) = \left(1+|z|^2\right)^{-1/2}$ is the normalization. In this notation, $z=\infty$ represents the state $|0\rangle$ and $z=0$ represents the state $|1\rangle$. This is a unique representation of $|\psi(\boldsymbol{\alpha})\rangle \equiv |\psi(z)\rangle$.

The nonlinear part of the purification step (2.14), with the parameters $M=1$ and $D=2$, maps a pure state $|\psi(\boldsymbol{\alpha})\rangle$ onto a pure state $|\psi(\bar{\boldsymbol{\alpha}})\rangle = \bar{\alpha}_0|0\rangle + \bar{\alpha}_1|1\rangle$ and according to the relation (3.1)

$$\begin{aligned}\bar{\alpha}_0 &= \sqrt{\mathcal{N}}\alpha_0\alpha_{0\ominus p_1}\ldots\alpha_{0\ominus p_N}\\ \bar{\alpha}_1 &= \sqrt{\mathcal{N}}\alpha_1\alpha_{1\ominus p_1}\ldots\alpha_{1\ominus p_N}\end{aligned}$$

where the projection onto the i-th target qubit is $P_{t_i} = |p_i\rangle\langle p_i|$ with $p_i \in \{0,1\}$. Consequently, using the transformation (3.3), we receive

$$\frac{\alpha_{0\ominus p_i}}{\alpha_{1\ominus p_i}} = \begin{cases} z, & p_i = 0\\ z^{-1}, & p_i = 1\end{cases}$$

and one can see, that the nonlinear part of purification is represented by the map $\mathcal{T}$ from $\hat{\mathbb{C}}$ to $\hat{\mathbb{C}}$

$$\mathcal{T}:\ \ z \longrightarrow \bar{z} = \frac{\bar{\alpha}_0}{\bar{\alpha}_1} = \frac{\alpha_0\alpha_{0\ominus p_1}\ldots\alpha_{0\ominus p_N}}{\alpha_1\alpha_{1\ominus p_1}\ldots\alpha_{1\ominus p_N}} = z^q,\ \ q\in\mathbb{Z}. \tag{3.4}$$

The complete purification consists in addition by the action of the additional unitary gate

$$U = \begin{pmatrix} u_{00} & u_{01}\\ u_{10} & u_{11}\end{pmatrix}.$$

which maps the pure state $|\psi(\bar{z})\rangle$ onto pure state $|\psi(z^{out})\rangle$, and may be represented by the map $\mathcal{U}$ from $\hat{\mathbb{C}}$ to $\hat{\mathbb{C}}$

$$\mathcal{U}:\ \ \bar{z} \longrightarrow z^{out} = \frac{u_{00}\bar{z} + u_{01}}{u_{10}\bar{z} + u_{11}}.$$

Consequently, a complete purification of the one-qubit pure state may be represented by the rational (or polynomial) map $\mathcal{F}$ from $\hat{\mathbb{C}}$ to $\hat{\mathbb{C}}$

$$\mathcal{F} = \mathcal{U}\circ\mathcal{T}:\ \ z \longrightarrow \frac{u_{00}z^q + u_{01}}{u_{10}z^q + u_{11}},\ \ q\in\mathbb{Z}. \tag{3.5}$$

3.2.2 Two-qubit states - pure and mixed

There is significant difference in the study of the dynamics for one and two-qubit states. Let's suppose the two-qubit pure state, in number state basis, it is represented by the state

$$|\psi(\boldsymbol{\alpha})\rangle = \alpha_{00}|00\rangle + \alpha_{01}|01\rangle + \alpha_{10}|10\rangle + \alpha_{11}|11\rangle.$$

Because of the equivalency of beams in Hilbert space $\mathcal{H}(2) \otimes \mathcal{H}(2)$ and the unite norm, only three of the coefficients α_{00}, α_{01}, α_{10}, α_{11} are independent. If one represents the pure state $|\psi\rangle$ by three independent complex variables $z_i = \alpha_i/\alpha_{11}$ where $i \in \{00, 01, 10\}$, similarly to the one-qubit map approach (3.3), difficulties with singularities in z_i arise. Namely, for every state $|\psi\rangle \in \operatorname{span}\{|00\rangle, |01\rangle, |10\rangle\}$ we have at least one $z_i = \infty$. If two of the $z_i = \infty$ the representation becomes ambiguous. With this representation one can study the closed sub-dynamics, which leaves β coordinate strictly nonzero during the purification process. One can prove, similarly to one-qubit case, that the protocol is represented by a rational map. The existing mathematical framework allows us to study in depth the sub-dynamics in one complex variable, I focus on the study of such a case.

The numerically effective approach, to study two and multi-qubit states protocols, is offered by the Fano representation (2.17). In the Fano representation each mixed state density matrix σ is represented by a Bloch vector $\mathbf{b}$ with $4^n - 1$ real coordinates. Consequently, one can realize that the action of the protocol step (2.16) is described by the map $\mathcal{F}$, which consists of the rational (or polynomial) functions $\mathcal{F}_i$ of the Bloch vector coordinates

$$\mathcal{F}_i: \ \mathbf{b}_i \mapsto \mathcal{N} g_i(\mathbf{b}_1, \ldots, \mathbf{b}_{4^n-1}) \tag{3.6}$$

with the normalization

$$\mathcal{N} = \frac{1}{h(\mathbf{b}_1, \ldots, \mathbf{b}_{4^n-1})}$$

where $\{g_i\}$, h are polynomial functions of degree at most $N+1$. Consequently, for two-qubit state the Bloch vector (2.18) has 15 real coordinates $c_{IX}, \ldots, c_{ZZ}$.

3.3 Purification to be analyzed

Since now we focus on study of the purification protocols (2.16) for one and two-qubit states and with the fixed projections $\mathbf{P}_{t_i} = |\mathbf{p}\rangle_{t_i t_i}\langle\mathbf{p}|$ for all the target systems $i \in \hat{N}$. This choice of the nonlinear part of the map simplifies the analysis and still allows to prove interesting chaotic regimes of the protocol. For such a case the action of the nonlinear part of the protocol (2.14) maps σ_c onto $\bar{\sigma}_c$

$$\bar{\sigma}_c = \mathcal{N} \sum_{\mathbf{k},\mathbf{l}} \sigma_{\mathbf{k},\mathbf{l}} \left(\sigma_{\mathbf{k}\ominus\mathbf{p},\mathbf{l}\ominus\mathbf{p}}\right)^N |\mathbf{k}\rangle_{cc}\langle\mathbf{l}|. \tag{3.7}$$

Firstly, we will analyze the simplest case of the one-qubit pure state protocol using the additional unitary gates $U \in \mathrm{SU}(2)$ (2.1), which form a one parametric set of the purifications. This allows us to study the sensitivity of the protocol not only to the continues setting of the initial state, but also to the continues internal setting of the protocol. Then we will study the purifications of one-qubit pure states using additional unitary of the Hadamard gate (2.2). The extension of this protocol, for multi-qubit systems, using one target system per control one, i.e. for $N = 1$, was identified by Albert et al. [8] as the efficient purification for the Werner states (2.12) to the general Bell state $|\psi_{00}\rangle$ (2.5). Then we focus our interest on the study of two-qubit pure, separable, states purifications. We will summarize the scenarios of the composed, one-qubit pure states subdynamics. Finally we focus our interest for the general two-qubit pure and mixed states. We focus on the protocol using additional Hadamarad gate, for the several reasons: for the importance of the protocol to the purification (as already mentioned), for the sufficient simplicity of the protocol (additional unitary gate is used as fixed, without the parametrization) and for the existence of the nontrivial subdynamic (we will be able to prove the existence of chaos).

For further analysis, we will represent the one-qubit pure state purifications by the rational maps, using the expression (3.5). Then, using the theorems of section (2.4) we find the Julia sets and we prove chaos on the Julia sets. Numerical calculations prove sensitivity in the structure of the Julia sets. We will observe the complicated structure of the Julia set itself as well as the ability to change its topology from connected onto disconnected (and vice versa) if we change the setting of the additional unitary gate. As another proof of the sensitivity of the dynamics we calculate the positive, maximal Liapunov characteristic exponent (2.21). Finally we prove the sensitivity of the purification to achieve the irregular motion for one of the critical points.

For the two-qubit separable states purification we re-use the rational maps representation of one-qubit pure state purifications. We will prove that the two-qubit separable states dynamics is decomposed onto two one-qubit pure state dynamics.

Then we turn our attention to the dynamics of the purifications for two-qubit nonseparable pure states, especially for the perturbed Bell states

$$|\psi(r)\rangle = \mathcal{N}(r)\left(r|00\rangle + |11\rangle\right), \ \mathcal{N}(r) = \left(1+|r|^2\right)^{-1/2}, \ r \in \hat{\mathbb{C}}.$$

We will prove, both analytically and numerically the existence of chaotic sub-dynamics, generated by rational function in $\hat{\mathbb{C}}$. We will numerically calculate its Julia set and consequently we observe strong sensitivity of the protocol to the setting of the initial state. Using the Fano representation (3.6) we will effectively simulate the complete purification for various initial states. We will prove that the initial state may converge to maximally entangled Bell state (2.6) $|\psi(1)\rangle = |\psi_{00}\rangle$ or to the cycle of completely separable pure states.

We will also analyze the dynamics of the purifications for the two-qubit mixed states, especially for the class of perturbed Werner like states (2.13)

$$\rho(\lambda, r) = \lambda|\psi(r)\rangle\langle\psi(r)| + \frac{1-\lambda}{4}\mathcal{I}, \ 0 \le \lambda \le 1, \ \lambda \in \hat{\mathbb{C}}$$

as the extension of two pure states dynamics. By numerical simulations using the Fano representation (3.6) we will prove, according to our expectation, also the sensitivity of the purification to converge to the third option - the cycle of completely separable mixed states.

3.4 Dynamics of one-qubit pure states purifications

Let us start now the detailed study of the dynamics of the purification protocols. First of all let us focus on the study of one-qubit pure state purifications without the additional unitary gate. Applying the definitions and the theorems of the section (2.4), we will prove the existence of the chaos in Poiancareé sense, we will also prove this by direct calculation of the Liapunov characteristic exponent. From now, when we will speak about a (super)attracting resp. a repelling resp. an indifferent fixed/periodic point or cycle, it will always be in coincidence with the definition (2.4.8), if not stated otherwise.

3.4.1 Purification without additional unitary gate

The nonlinear part of the protocol (3.7) maps a pure state

$$|\psi(\boldsymbol{\alpha})\rangle = \alpha_0|0\rangle + \alpha_1|1\rangle$$

onto a pure state $|\psi(\bar{\boldsymbol{\alpha}})\rangle$. According to the relation (3.1) , the output depends on the number of target states N and target state projection $P_{t_i} = |p\rangle\langle p|$, $p \in \{0,1\}$:

$$\begin{aligned} p = 0: \;\; \boldsymbol{\alpha} \mapsto \bar{\boldsymbol{\alpha}} &= \sqrt{\mathcal{N}}\left(\alpha_0^{N+1}, \alpha_1^{N+1}\right), \\ p = 1: \;\; \boldsymbol{\alpha} \mapsto \bar{\boldsymbol{\alpha}} &= \sqrt{\mathcal{N}}\left(\alpha_0\alpha_1^{N}, \alpha_1\alpha_0^{N}\right). \end{aligned} \tag{3.8}$$

One observes, that for the projection $P_{t_i} = |1\rangle\langle 1|$ protocol filters out every state $|0\rangle$ or $|1\rangle$.

Using the transformation (3.3) and according to (3.4), one express the nonlinear part of the purification resp. purification itself (in case of no additional unitary) by the map $\mathcal{F}_{p,N}$:

$$\mathcal{F}_{p=0,N}(z) = z^{N+1}, \tag{3.9}$$

$$\mathcal{F}_{p=1,N}(z) = z^{1-N}, z \neq \{0,\infty\}. \tag{3.10}$$

Purification with the projections $P_{t_i} = |0\rangle\langle 0|$

is represented by the function (3.9)

$$\mathcal{F}_{0,N}(z) = z^{N+1}$$

having $N+1$ fixed points

$$z \in \left\{0,\ \infty,\ e^{2\imath k\pi/N}\right\},\ k \in \{0,1,\ldots,(N-1)\}.$$

From those only $z \in \{0,\ \infty\}$ are supperattracting one, the remaining fixed points are repelling. Also, the map has cycles of n-th order

$$z^{n(N+1)} = z \text{ i.e. } z = \left\{e^{2\imath k\pi/(nN+n-1)}\right\},\ k \in \{0,1,\ldots,(nN+n-2)\}$$

all the cycles are repelling.

According to the definition (2.4.4) the Julia set $J\left(\mathcal{F}_{0,N}\right)$ is the unit circle $K(0,1) \in \hat{\mathbb{C}}$. The states inside resp. outside the Julia set converge to the states $|1\rangle$ resp. $|0\rangle$. According to theorem (2.4.14) the dynamical system is chaotic on the Julia set. The map $\mathcal{F}_{0,N}(z)$ has the two critical points $z \in \{0,\infty\}$ - see the definition (2.4.15), these are also superattracting fixed points. Then, according to definition (2.4.15), the map is hyperbolic and from theorem (2.4.17) the map is expanding on the Julia set $K(0,1)$. One can demonstrate the property of expanding map by calculating the mean exponential rate of divergency σ (2.20) between the two points of Julia sets. For the Julia set $K(0,1)$, the rate σ is also the maximal Liapunov characteristic exponent (2.21)

$$\sigma = \lim_{n\to\infty}\left(\lim_{\Delta_z(0)\to 0}\left(\frac{1}{n}\ln\frac{\Delta_z(n)}{\Delta_z(0)}\right)\right)$$

where the distance $\Delta_z(k)$ of initial points $z_0,\ z_1$ after k steps of the protocol is defined as

$$\begin{aligned}\Delta_z(k) \quad &= 1 - \left|\left\langle\psi\left({\mathcal{F}_{0,N}}^{\circ k}(z_1)\right)\middle|\psi\left({\mathcal{F}_{0,N}}^{\circ k}(z_0)\right)\right\rangle\right|^2 = \\ &= 1 - \left|\left\langle\psi\left({z_1}^{(N+1)^k}\right)\middle|\psi\left({z_0}^{(N+1)^k}\right)\right\rangle\right|^2.\end{aligned}$$

Without loss of generality one can choose $z_0 = 1,\ z_1 = \exp(i\varphi)$ and then calculate $\Delta_z(k)$ as

$$\begin{aligned}\Delta_z(0) &= \sin^2\left(\frac{\varphi}{2}\right), \\ \Delta_z(n) &= \sin^2\left(\frac{(N+1)^n\varphi}{2}\right).\end{aligned}$$

Using the symmetry of circle of Julia set $K(0,1)$ and applying the theorem about the limit of composed function (c.f.) and two times applying L'Hospital theorem (L'.H.), one can calculate a Liapunov index σ as

$$\begin{aligned}
\sigma &= \lim_{n\to\infty}\left(\lim_{\varphi\to 0}\left(\frac{1}{n}\ln\frac{\sin^2\left(\frac{(N+1)^n\varphi}{2}\right)}{\sin^2\left(\frac{\varphi}{2}\right)}\right)\right) = \{\text{ c.f.}\} = \\
&= \lim_{n\to\infty}\left(\frac{1}{n}\ln\lim_{\varphi\to 0}\left(\frac{\sin^2\left(\frac{(N+1)^n\varphi}{2}\right)}{\sin^2\left(\frac{\varphi}{2}\right)}\right)\right) = \{\text{ L'.H.}\} = \\
&= \lim_{n\to\infty}\left(\frac{1}{n}\ln\lim_{\varphi\to 0}\left(\frac{\sin\left((N+1)^n\varphi\right)}{\sin(\varphi)}(N+1)^n\right)\right) = \{\text{ L'.H.}\} = \\
&= \lim_{n\to\infty}\left(\frac{1}{n}\ln\lim_{\varphi\to 0}\left(\frac{\cos\left((N+1)^n\varphi\right)}{\cos(\varphi)}(N+1)^{2n}\right)\right) = \\
&= \lim_{n\to\infty}\left(\frac{2n}{n}\ln(N+1)\right) = 2\ln(N+1) > 0.
\end{aligned}$$

The positivity of the Liapunov index $\sigma = 2\ln(N+1)$ implies an exponential divergency of the trajectories inside the Julia set $K(0,1)$ and proves there the existence of chaos in Poincaré sense.

Purification with the projections $P_{t_i} = |1\rangle\langle 1|$

is represented by the function (3.10)

$$\mathcal{F}_{1,N}(z) = z^{1-N},\;\; z \neq \{0,\infty\},$$

for $z \in \{0,\infty\}$ purification stops (protocol filters out the states $|0\rangle$, $|1\rangle$). For $z \neq \{0,\infty\}$ there exist several regimes:

- for the purification with $N = 1$, using one target system, the protocol behaves like the constant map

  $$\mathcal{F}_{1,1}(z) = 1,\;\; z \neq \{0,\infty\},$$

  which leads to the trivial dynamics: $|\psi\rangle \mapsto \frac{1}{\sqrt{2}}(|0\rangle + |1\rangle)$, $|\psi\rangle \neq \{|0\rangle,\; |1\rangle\}$.

- for the purification with $N = 2$, using two target systems, we observe regular dynamics

  $${\mathcal{F}_{1,2}}^{\circ 2k}(z) = z \text{ and } {\mathcal{F}_{1,2}}^{\circ(2k+1)}(z) = z^{-1}$$

After the second step the map behaves like the identity ${\mathcal{F}_{1,2}}^{\circ 2}(z) = z$, then for each $z \in \hat{\mathbb{C}} \setminus \{0, \infty\}$ there exists a neighborhood U of z such that the sequence of the iterates $\{{\mathcal{F}_{1,2}}^{\circ n}\}$, restricted to U, contains the subsequence $\left\{{\mathcal{F}_{1,2}}^{\circ 2k}\right\}$ which converges locally uniformly on U. Consequently $\{{\mathcal{F}_{1,2}}^{\circ n}\}$ forms a normal family for each $z \in \hat{\mathbb{C}} \setminus \{0, \infty\}$, see the definition (2.4.3), then the Fatou set of the map is all $\hat{\mathbb{C}}$ and there is no chaotic regime for the map $\mathcal{F}_{1,2}$. The two fixed points $\{\pm 1\}$, representing the states $\frac{1}{\sqrt{2}}(|0\rangle \pm |1\rangle)$, are indifferent.

- finally for $N \geq 3$ the purification is represented by the rational function of degree at least two

$$\mathcal{F}_{1,N}(z) = \frac{1}{\mathcal{F}_{0,N-2}(z)}.$$

One can see that the Julia set of the map $\mathcal{F}_{1,N}$ is again unit circle $K(0,1)$ and that the point out of Julia set approaches the value 0 or ∞ (for even or odd number of purification steps), meaning that the purification approaches to the filtering out of all the states. The map $\mathcal{F}_{1,N}(z)$ has no critical point, then the map is hyperbolic and expanding on the Julia set $K(0,1)$. For this Julia set we can also calculate the maximal Liapunov characteristic exponent $\sigma = 2\ln(N-1) > 0$ (2.21) and to confirm there the existence of chaos in Poincaré sense.

3.4.2 Purification using $SU(2)$ gates

Now we will analyze the dynamics of one-qubit pure state purification protocol with the additional, nontrivial, unitary transformation $U \in \mathrm{SU}(2)$ (2.1). We expect to observe complicated structures of the Julia set together with its possibility to loose the connectivity and to become totally disconnected. Fine structure of the Julia set, i.e. the area of the existence of chaotic dynamics, induces the existence of interesting dynamical regimes with the strong sensitivity either to the initial state (close to the Julia set), but also the sensitivity to the initial setting of the protocol itself (additional unitary, number of target systems, projection to the target system). We will analyze numerically the Julia set structure by exploiting two approaches, the first using the property of Julia set being close to the backward iterations and the second using the property of Julia set being the closure of the repelling cycles.

Using the transformation (3.3), the action of the complete protocol step (2.16) can be represented, depending on the projection parameter p and the additional unitary $U \in \mathrm{SU}(2)$ (2.1), by the rational or polynomial map (3.5) $\mathcal{F}_{a,p,N}$ onto $\hat{\mathbb{C}}$

$$\begin{aligned} \mathcal{F}_{a,p=0,N}(z) &= \frac{z^{N+1}+a}{1-a^* z^{N+1}}, \\ \mathcal{F}_{a,p=1,N}(z) &= \frac{1+a\ z^{N-1}}{z^{N-1}-a^*}, \end{aligned} \tag{3.11}$$

where $a = \tan\phi e^{\imath\psi}$ and $*$ means complex conjugation. For the case $a = 0$ we receive the purification without use of the additional unitary gate. This case was already studied in section (3.4.1), so we will be interested only for the purifications with $a \neq 0$. Consequently the Jacobian $\mathcal{F}^{'}_{a,p,N}(z)$ is equal to:

$$\begin{aligned} \mathcal{F}^{'}_{a,p=0,N}(z) &= \frac{(N+1)\, z^N\, (1+|a|^2)}{(a^* z^{N+1}-1)^2}, \\ \mathcal{F}^{'}_{a,p=1,N}(z) &= \frac{(1-N)\, z^{N-2}\, (1+|a|^2)}{(z^{N-1}-a^*)^2}\ . \end{aligned} \tag{3.12}$$

According to the absolute value of the Jacobian, evaluated for the given fixed point, one can classify all the fixed points of the map according to the definition (2.4.8).

Let us start now the detailed study of the nontrivial dynamics of these purification protocols. We will study two main sets of the protocols according to the setting of the target system projections P_{t_i}.

Purification with the projections $P_{t_i} = |0\rangle\langle 0|$

is represented by the rational map $\mathcal{F}_{a,0,N}(z)$ (3.11) of the order at least two in $\hat{\mathbb{C}}$. Then, in agreement with (2.4.14), the Julia set for the map is not empty and the map can be chaotic. According to the theorems (2.4.6,2.4.10) the Julia set can be numerically calculated as a backward orbit of repelling periodic point z_0 of the map. A list of the numerically calculated repelling periodic points, for the maps $\mathcal{F}_{a,0,1}$ (with various values of the parameter a but using only the one target system per control one) follows:

- $a = 1$: $z_0 = -1.83928676$,
- $a = 1 + 0.2\imath$: $z_0 = 0.51120002 - 0.57287547\imath$,
- $a = 0.8$: $z_0 = -2.08139042$,
- $a = 0.66$: $z_0 = 0.41426801 + 0.50503470\imath$,
- $a = 0.5$: $z_0 = 0.41558860 + 0.42484830\imath$.

For every map $\mathcal{F}_{a,0,1}$, each point z of the Julia set has 2 pre-images $z_{1,2}^{-1}$:

$$z_{1,2}^{-1} = \pm\sqrt{\frac{z-a}{1+za^*}} \tag{3.13}$$

meaning that the Julia set $J(\mathcal{F}_{a,0,1})$ is centrally symmetric under the point 0. Also, because the map $\mathcal{F}_{a,0,1}$ is a rational map of degree two, there exists chaos on $J(\mathcal{F}_{a,0,1})$ sets (2.4.14). On figures (3.1-3.4), one can observe strong self similarity of the Julia set structure and its complicated (fractal) structure. The Julia set can loose its local connectivity and may become totaly disconnected, see the plots in figure (3.4). If it happens, $\mathcal{F}_{a,0,1}$ may be hyperbolic i.e. expanding on $J(\mathcal{F}_{a,0,1})$ (2.4.17). A sufficient condition for such a dynamics is the convergence of critical orbits of the only critical points $z_{c_1} = 0$, $z_{c_2} = \infty$ (common for every $\mathcal{F}_{a,0,1}$) to a common attracting fixed point (2.4.20) - this is the case for the presented disconnected Julia sets (3.4), proved numerically. For special setting of the purification, as represented by $\mathcal{F}_{1,0,1}$, we can analytically prove that $\mathcal{F}_{1,0,1}$ is hyperbolic i.e. expanding on $J(\mathcal{F}_{a,0,1})$ (2.4.17). One can check, that the critical point $z_{2c} = \infty$ is part of the superattracting cycle $C = (-1, \infty)$ and the critical point $z_{c_1} = 0$ follows the orbit $0 \mapsto 1 \mapsto \infty$ which leads to the cycle C. By this we proved that $\mathcal{F}_{1,0,1}$ is hyperbolic (2.4.15) and therefore expanding on $J(\mathcal{F}_{1,0,1})$ (2.4.16).

Another way how to calculate the part of the Julia set is to simulate the speed of converge of the initial states z_0 to the superattracting cycle, so the Julia set represents the closure of the repelling cycles (2.4.10,2.4.12). Numerical results are present on figures (3.5,3.6). Calculations has been done for the map $\mathcal{F}_{1,0,1}$ with the superattracting cycle $C = (-1, \infty)$ $\left(|\frac{\partial}{\partial z}\mathcal{F}_{1,0,1}^{\circ 2}(z)|_{z=-1} = 0 \text{ resp. } |\frac{\partial}{\partial z}\left(1/\mathcal{F}_{1,0,1}^{\circ 2}(1/z)\right)|_{z=0} = 0\right)$ (2.4.8).

From the perspective of existence of irregular motion, it is also interesting to study the evolution of the critical points (2.4.15), especially if they converge to the attracting cycle. Let us focus now on the numerical studies of the length of the attracting cycle which may appear in the evolution of the critical point $z_{c_1} = 0$ for various maps $\mathcal{F}_{a,0,1}$. This simulations reveal strong sensitivity of the protocol properties on the parameter a. One can identify the set of protocols where the evolution leads to irregular motion. The yellow areas in figure (3.7) correspond to the irregular motion. We note that there exists also fine structures corresponding to the convergency to the superattracting cycle including second critical point $z_{c_2} = \infty$, see black color areas - these maps $\mathcal{F}_{a,0,1}$ are hyperbolic and therefore expanding on their Julia sets (2.4.17). White color areas represent the existence of the other attracting cycle during the evolution of z_0. Figures (3.8) then represent the self similarity in the patterns of the length of the limiting attractive cycle.

Plots (3.7, 3.8) allow us to identify those protocols which evolve $z_{c_1} = 0$ in a irregular fashion. Existence of both regular and irregular evolutions of z_{c_1} for various purifications is demonstrated on figure (1.2). Qualitatively the plot (1.2) is very similar to the plot enhance it is natural to expect chaotic behavior in the quantum domain (1.1).

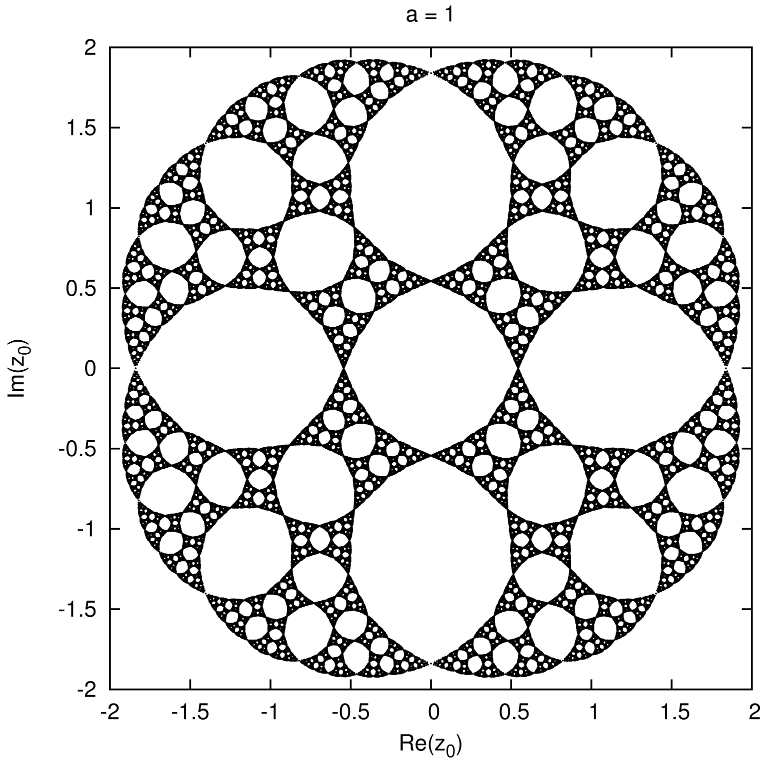

Figure 3.1: Julia set calculated for 21 backward steps (3.13) - dynamical systems is chaotic here (2.4.14) and $\mathcal{F}_{1,0,1}$ is expanding here (2.4.16).

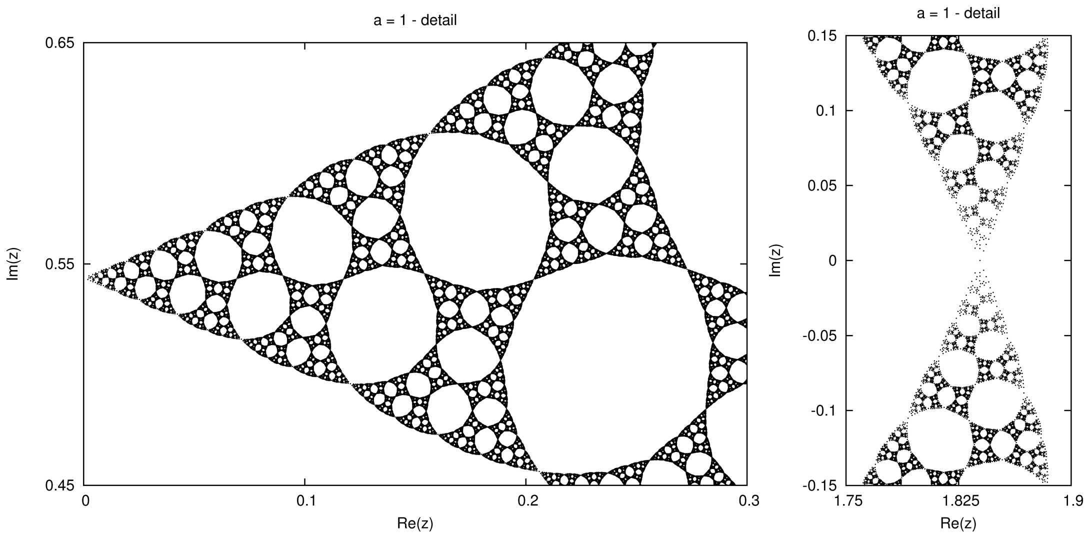

Figure 3.2: Details of the Julia set for the parameter $a = 1$, calculated for 25 backward steps.

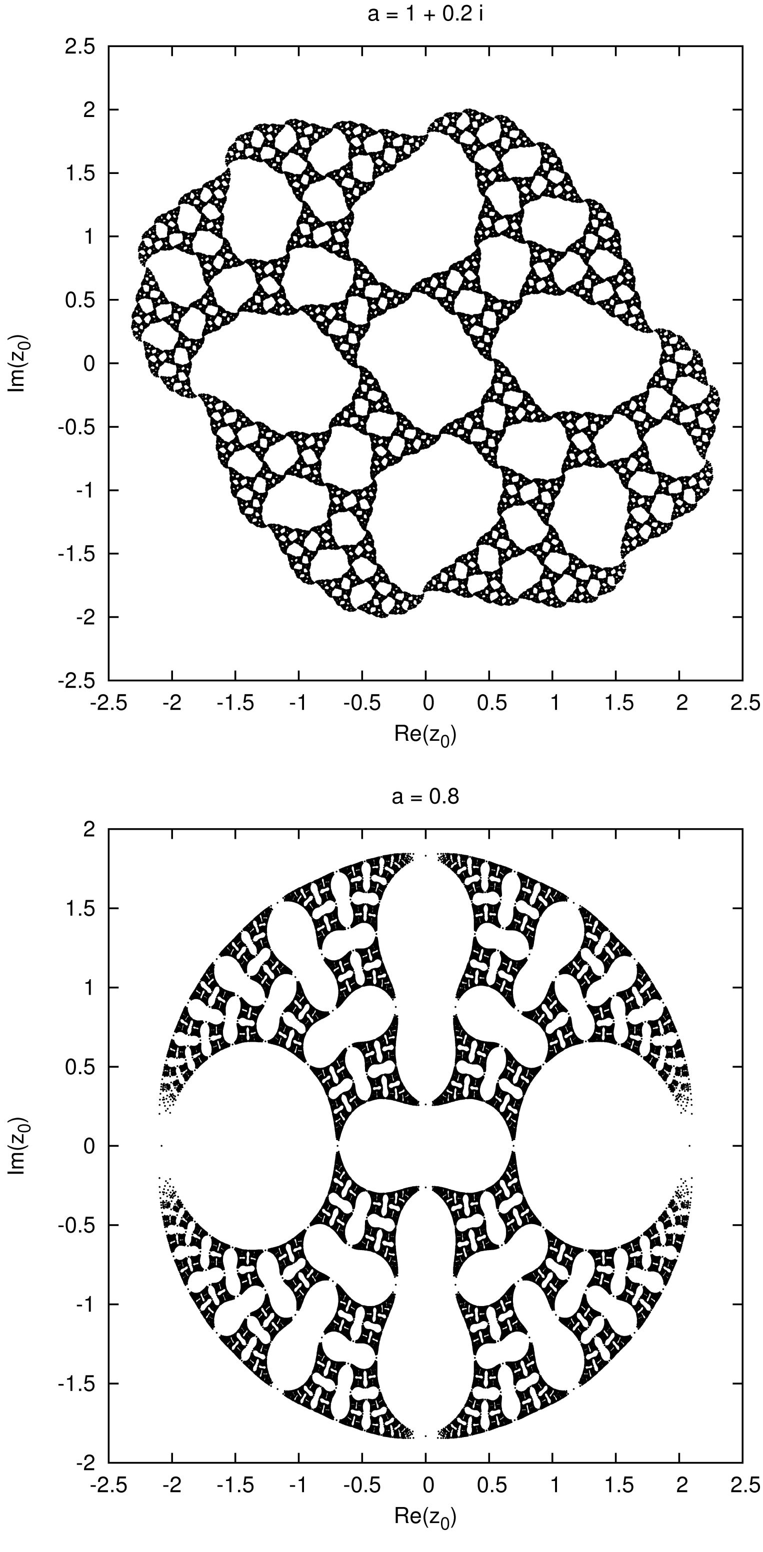

Figure 3.3: Julia sets calculated for 21 backward steps (3.13) - dynamical systems are chaotic here (2.4.14).

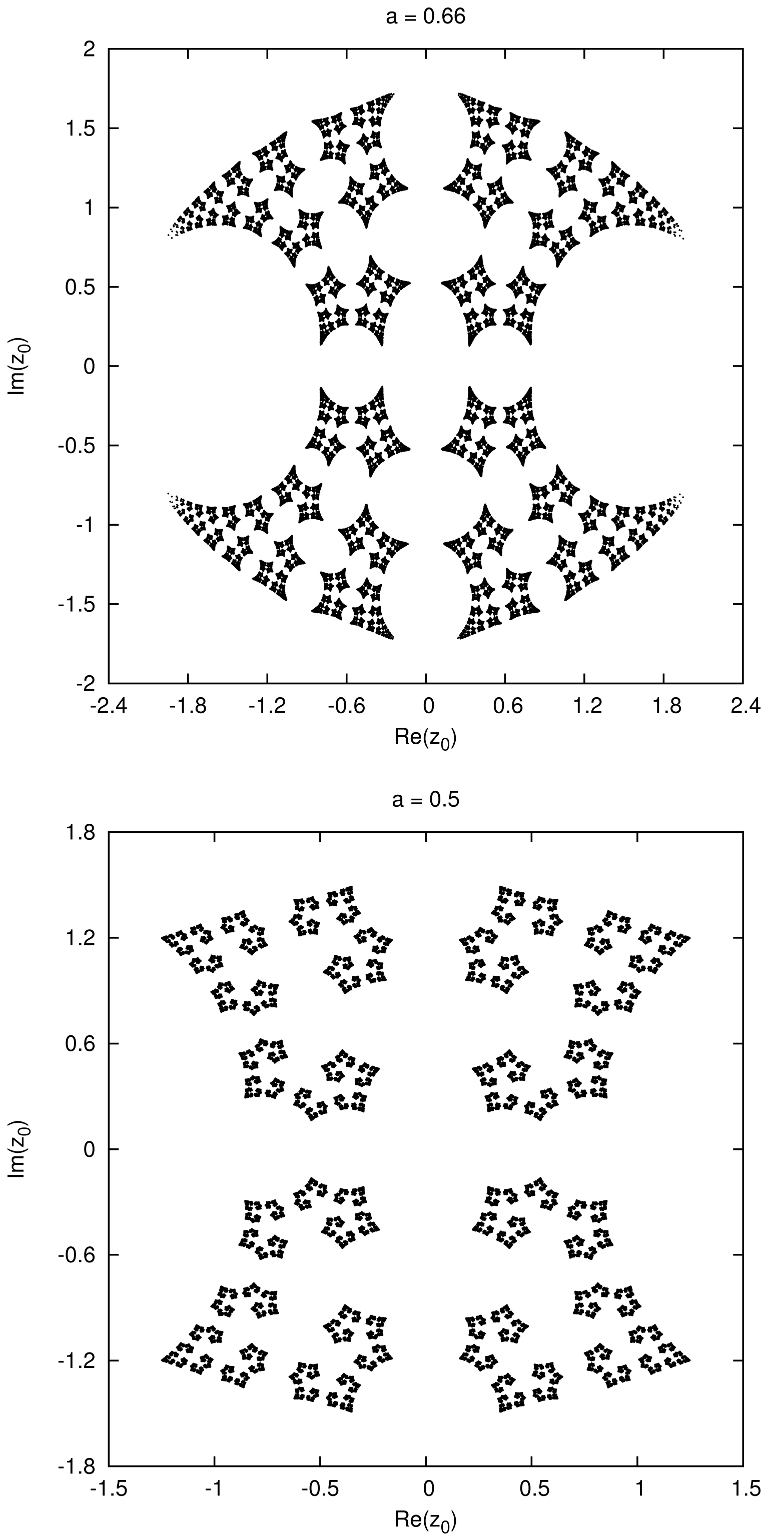

Figure 3.4: Totally disconnected Julia sets calculated for 21 backward steps (3.13) - dynamical systems are chaotic here (2.4.14) and $\mathcal{F}_{a,0,1}$ are expanding here (2.4.16)

.

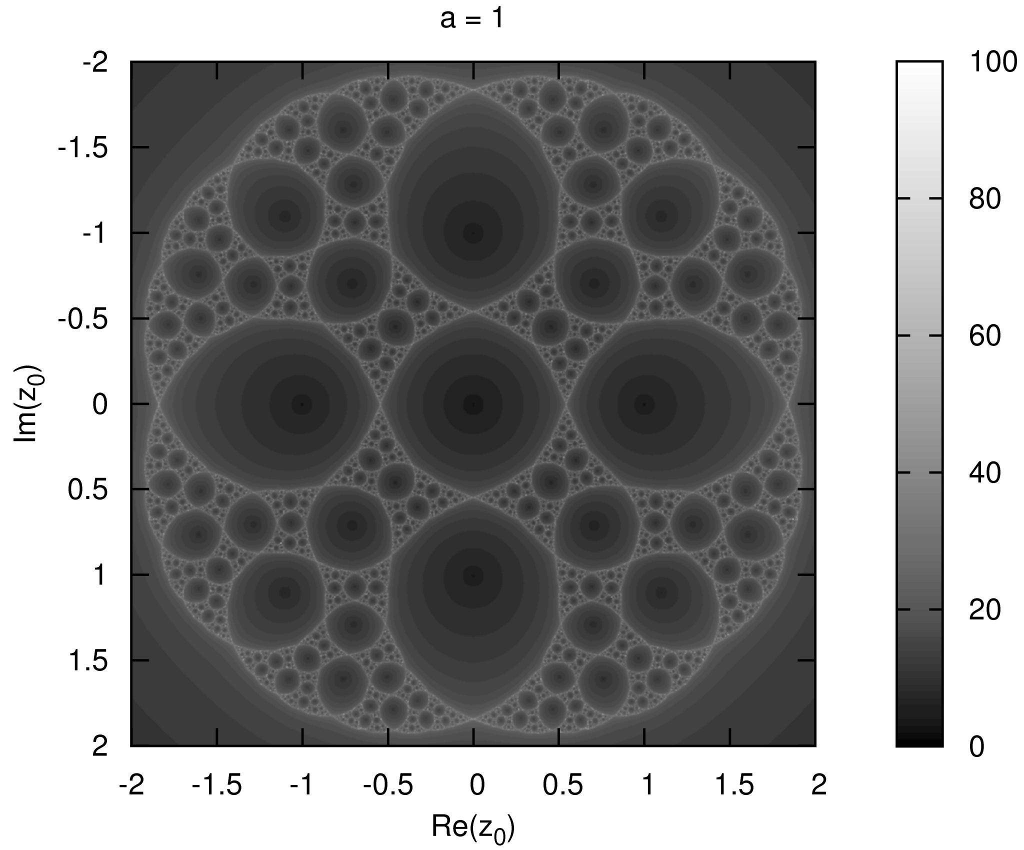

Figure 3.5: Speed of convergence to superattracting cycle $(-1, \infty)$ for $\mathcal{F}_{1,0,1}$ (3.11) in at most 100 purification steps. The precision of convergence is set on 10^{-4}.

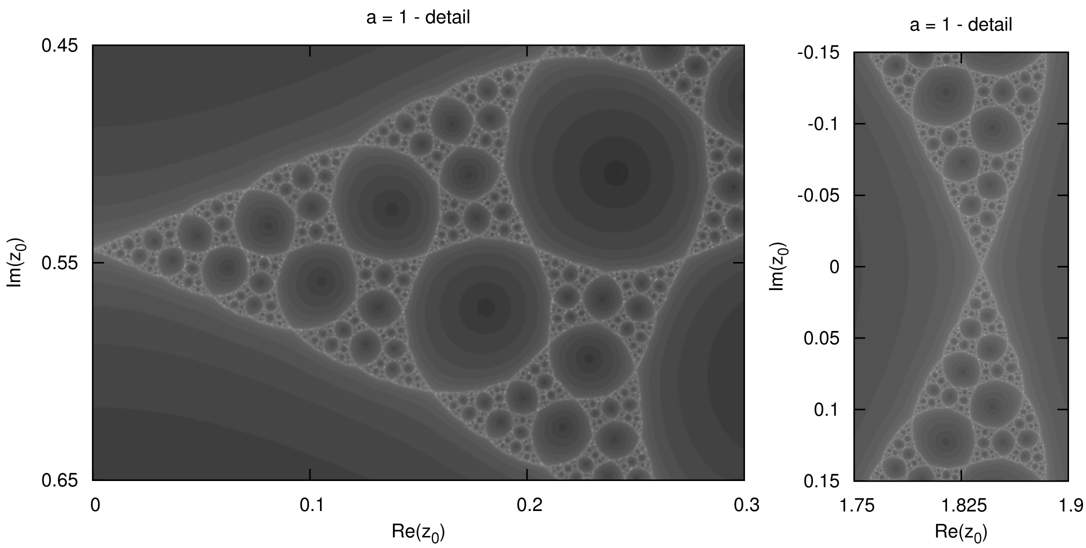

Figure 3.6: Details of speed of convergence to superattracting cycle $(-1, \infty)$ for $\mathcal{F}_{1,0,1}$.

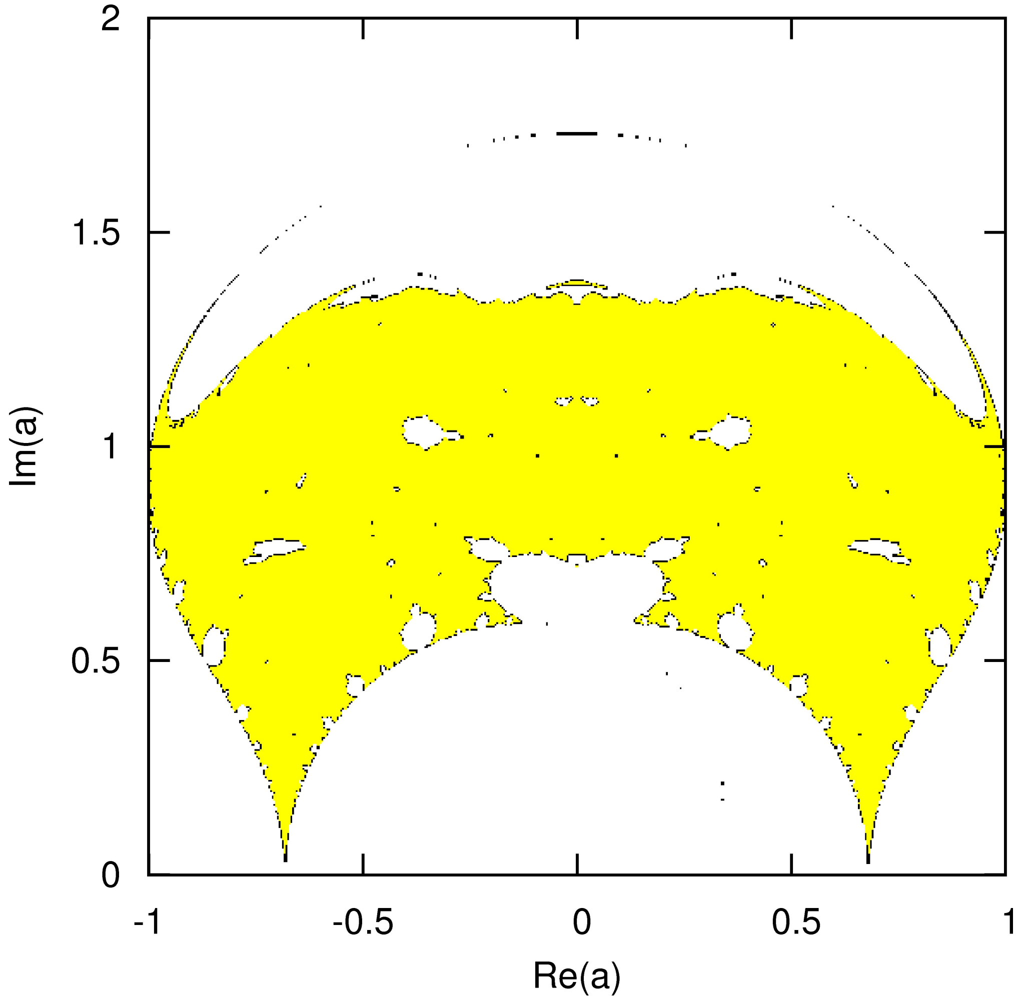

Figure 3.7: The figure represents the sensitivity of purifications $\mathcal{F}_{a,0,1}$ (3.11) to evolve the initial critical state with $z_0 = 0$. Black color marks the evolution which leads to superattracting cycle containing the point ∞. White color represents the evolution which leads to the attracting cycle without the point ∞. Yellow color represents the evolution without an attracting cycle. According to the theorem (2.4.17), black color areas identify $\mathcal{F}_{a,0,1}$ being hyperbolic and therefore expanding (2.4.16) on its Julia set.
The existence of the cycles, of the length at most 500, is searched in the first 10^4 iterations of the protocol. The cycle is recognized with the precision at most 10^{-5}, its stability (2.4.8) is calculated according to the chain rule (2.19).

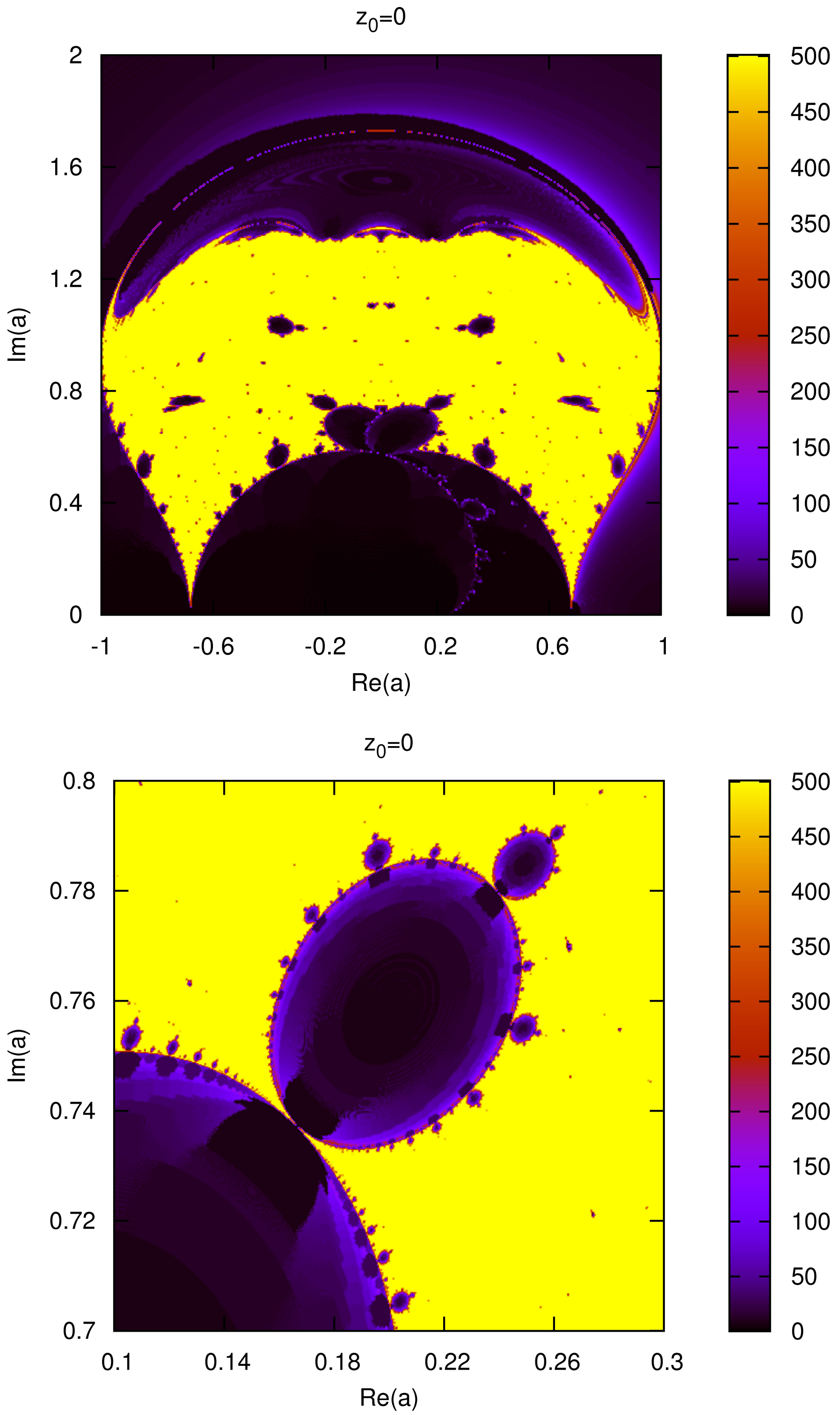

Figure 3.8: The figure represents the lengths of the attracting cycles for various parameters of $\mathcal{F}_{a,0,1}$ (3.11), yellow color means the absence of attracting cycle during the evolution of $z_0 = 0$.

Purification with the projections $P_{t_i} = |1\rangle\langle 1|$

Let us now complete the analysis of the dynamics of one-qubit pure state protocols, which uses an additional unitary of SU (2) gate. The analysis of the dynamics of the purification, represented by the map $\mathcal{F}_{a,p=1,N}$ (3.11) has following properties:

- purification filters out the pure states $|0\rangle$ and $|1\rangle$ and consequently purification stops, this corresponds to the states with $z = \{0, \infty\}$.

- if the number of the target systems $N = 1$, then protocol behaves like the trivial map
$$\mathcal{F}_{a,1,1}(z) = \frac{1+a}{1-a^*} = C_a, \;\; z \neq \{0, \infty\}, \;\; a \neq \pm 1.$$
The initial state $|\psi(C_a)\rangle$ is a superattracting fixed point and $\mathcal{F}_{a,1,1}$ purifies to $|\psi(C_a)\rangle$. For $a \in \{\pm 1\}$ no fixed point exists and $\mathcal{F}^{\circ 2}{}_{\pm 1,1,1}$ behaves as a filter of pure states (mixed states are not annihilated in general).

- for $N = 2$ the map $\mathcal{F}_{a,1,2}$ is rational of degree 1
$$\mathcal{F}_{a,1,2}(z) = \frac{1+az}{z-a^*}.$$
The map has two fixed points $z_{1,2} = Re\, a \pm \sqrt{1 + Re\,(a)^2}$, both are indifferent.

  - If $Im\,(a) = 0$ then the action of the map is simple
  $$\mathcal{F}_{a,1,2}{}^{\circ 2}(z) = z$$
  for each $z \in \hat{\mathbb{C}} \setminus \{-1/a, 0, a, \infty\}$ (because there exist the only orbits $-1/a \mapsto 0$ and $a \mapsto \infty$ which contain the points $\{0, \infty\}$). Then the Fatou set of the map is $\hat{\mathbb{C}}$.

  - For general complex value of a, the presence of chaos has not been observed. For example, if $a = \imath$, then the action of the map is also simple
  $$\mathcal{F}_{\imath,1,2}{}^{\circ 4}(z) = z$$
  for each $z \in \hat{\mathbb{C}} \setminus \{\imath, 0, \imath, \infty\}$ (because there exist the only orbits $\imath \mapsto 0$ and $-\imath \mapsto \infty$ which contain the points $\{0, \infty\}$). Then the Fatou set of the map is again $\hat{\mathbb{C}}$.

- For $N \geq 3$ the map $\mathcal{F}_{a,1,N}$ is a rational map with order at least 2. In agreement with (2.4.14) the Julia set of the map is not empty and the map is chaotic on the Julia set. There is a subset of the initial setting $Re\, a = 0$, so that

$$\mathcal{F}_{a,1,N}(z) = \mathcal{F}_{-1/a^*,0,N-2}(z)$$

and the dynamics $\mathcal{F}_{a,1,N}$ may be recursively compared to $\mathcal{F}_{-1/a^*,0,N-2}$. Especially, we observe $\mathcal{F}_{-1,1,3}(z) = \mathcal{F}_{1,0,1}(z)$ so the Julia set of $J(\mathcal{F}_{-1,1,3})$ is already known (3.1,3.2).

3.4.3 Purification using the Hadamard gate

Now, let us study the dynamics of the purification using the additional unitary gate of Hadamard (2.2). Still keeping in mind, that the extension of this purification protocol, for multi-qubit states, has been identified, in the paper [8], as effective deterministic protocol for purification of Werner states to the general Bell state. The analysis of the dynamics will be provided in similar way as already done for the protocols using additional unitary gates of SU (2), presented in section (3.4.2).

Purification of the interest may be uniquely represented by the map $\mathcal{F}_{p,N}$ in the form

$$\begin{aligned}\mathcal{F}_{p=0,N}(z) &= \frac{z^{N+1}+1}{z^{N+1}-1}\\ \mathcal{F}_{p=1,N}(z) &= \frac{z^{N-1}+1}{1-z^{N-1}}.\end{aligned} \tag{3.14}$$

Consequently the Jacobian $\mathcal{F}'_{p,N}(z)$ is equal to

$$\begin{aligned}\mathcal{F}'_{p=0,N}(z) &= -\frac{2(N+1)z^{N}}{\left(z^{N+1}-1\right)^2}\\ \mathcal{F}'_{p=1,N}(z) &= \frac{2(N-1)z^{N-2}}{\left(z^{N-1}-1\right)^2}.\end{aligned} \tag{3.15}$$

Let us analyze the dynamical regimes of the two main cases of the purifications.

Purification with the projections $P_{t_i} = |0\rangle\langle 0|$

The map $\mathcal{F}_{0,N}$ is the rational function of degree at least two. Then in agreement with (2.4.14), the Julia set of the map is not empty and the map is chaotic there. From the relations (3.14,3.11) we receive

$$\mathcal{F}_{0,N}(z) = -\mathcal{F}_{1,0,N}(z).$$

Consequently, the dynamics of $\mathcal{F}_{0,N}$ may be recursively comparable from already studied dynamics of $\mathcal{F}_{1,0,N}$. Especially, for odd N we receive ${\mathcal{F}_{0,N}}^{\circ n}(z) = -\mathcal{F}_{1,0,N}^{\circ n}(z)$ so the evolutions for both the maps are mutually symmetric under the center point 0.

Purification with the projections $P_{t_i} = |1\rangle\langle 1|$

From the relations (3.14,3.11) we receive

$$\mathcal{F}_{1,N}(z) = \mathcal{F}_{1,0,N-2}(z)$$

where $z \neq \{0, \infty\}$ (because the states $|1\rangle, |0\rangle$ are filtered out by the nonlinear part of the protocol). For different purifications defined by the various number of target systems N we receive following dynamics:

- for $N = 1$ the map $\mathcal{F}_{1,1}$ behaves as $\mathcal{F}_{1,1} : z \mapsto \infty$. It means that two steps of the purification behaves as the filter for all the pure states (after the first step the purification filters out only the states $|0\rangle, |1\rangle$).

- For $N = 2$, the dynamics of $\mathcal{F}_{1,2}$ is fully regular

  $${\mathcal{F}_{1,2}}^{\circ 4}(z) = z,$$

  the Fatou set of the map is all $\hat{\mathbb{C}}$ and there is no chaotic regime. The map has two indifferent fixed points $\{\pm\imath\}$ which represent the states $\frac{1}{\sqrt{2}}(\imath|0\rangle \pm |1\rangle)$.

- For the protocol with $N \geq 3$, the map $\mathcal{F}_{1,N} = \mathcal{F}_{1,0,N-2}$ was already studied (3.11). Just to repeat basic information, such a map is rational function of order at least 2 with chaotic dynamics on its nonempty Julia set.

3.4.4 Summary

One can conclude that the dynamics of the protocol (2.16) for one-qubit pure state is complicated, except the cases when the number of iterations the protocol behaves like a filter. For the protocols with or without the additional unitary transformation $U = U_1 \otimes U_2$, where $U_{1,2} \in \mathrm{SU}(2)$ or $U_{1,2} =$ Hadamard gate, a chaotic regime exists on the nonempty Julia set for every protocol with

- the number of the target systems $N \geq 1$ and with the target state projection $P_t = |0\rangle\langle 0|$,
- the number of the target systems $N \geq 3$.

For the simplest protocols, without additional unitary gate, we proved, using the framework (2.4), the existence of chaos for the purification on its Julia set and we also directly calculated positive speed of divergency of the close trajectories in the Julia set - maximal Liapunov characteristics exponent. Then we focused on the study of more complex protocols. We again proved the existence of chaotic dynamics on the Julia set. For this protocols, we also simulated the Julia set and we demonstrated its complicated (fractal) structure for the several purifications. Especially, we proved the Julia set sensitivity to change its topology from connected to disconnected set, depending on the setup of the additional unitary gate.

We also searched for the maximal length of the attractive cycle in the evolution of the critical point during purification. We investigated the fine structure and self similarities, especially for the appearance of the supper attracting cycles containing both the critical points $\{0, \infty\}$. By this analysis we also find the set of the protocols which, for the given simulation setup, exhibits irregular motion in the evolution of the critical point.

Finally, let us point out that an analysis was possible in such an easy way because we represented the purification protocol by the rational (or polynomial) map in one complex variable.

3.5 Dynamics for two-qubit separable pure states

It is clear, from chapters (3.1.1) and (3.1.2), that the step of the protocol maps a separable pure state onto a separable pure state. Each two-qubit separable pure state is described by the density matrix

$$\sigma = \sigma_1 \otimes \sigma_2$$

where the density matrices $\sigma^{1,2} \in \mathcal{B}\left(\mathcal{H}_{1,2}\left(2\right)\right)$ represent each qubit and $\sigma^{1,2} = |\psi^{1,2}\rangle\langle\psi^{1,2}|$ where

$$|\psi^{1,2}\rangle = \alpha_0^{1,2}|0\rangle_{1,2} + \alpha_1^{1,2}|1\rangle_{1,2}. \tag{3.16}$$

The dynamics of two-qubit separable pure states is composed from the dynamics of each qubit. Similarly to the one-qubit pure state parametrization (3.3), we introduce the parameters

$$z_{1,2} = \frac{\alpha_0^{1,2}}{\alpha_1^{1,2}} \in \hat{\mathbb{C}}.$$

The values $z_{1,2} \in \{0,\ \infty\}$ represent the states $\{|1\rangle,\ |0\rangle\}$ for the first and the second qubit.

3.5.1 Purification using $SU\left(2\right)$ gates

The protocol setting depends on the additional unitary transformation $U = U_1 \otimes U_2$, now let me suppose $U_{1,2} \in \mathrm{SU}\left(2\right)$ as defined by (2.1). The action of the complete protocol step (2.16) can be represented, depending on the target systems projections $P_{t_i} = |\mathbf{p}\rangle\langle\mathbf{p}|$ with $\mathbf{p} = p_1 \circ p_2 \in \{00, \ldots, 11\}$, by the pair of maps (3.4.2) $\mathcal{F}_{a,p_{1,2},N}$ onto $\hat{\mathbb{C}}$

$$\begin{aligned}
\mathcal{F}_{a,p_{1,2}=0,N}\left(z_{1,2}\right) &= \frac{{z_{1,2}}^{N+1} + a_{1,2}}{1 - {a_{1,2}}^*\ {z_{1,2}}^{N+1}} \\
\mathcal{F}_{a,p_1=0,N}\left(z_1\right) &= \frac{{z_1}^{N+1} + a_1}{1 - {a_1}^* {z_1}^{N+1}},\ \mathcal{F}_{a,p_2=1,N}\left(z_2\right) = \frac{1 + a_2\ {z_2}^{N-1}}{{z_2}^{N-1} - {a_2}^*} \\
\mathcal{F}_{a,p_1=1,N}\left(z_1\right) &= \frac{1 + a_1\ {z_1}^{N-1}}{{z_1}^{N-1} - a_1^*},\ \mathcal{F}_{a,p_2=0,N}\left(z_2\right) = \frac{{z_2}^{N+1} + a_2}{1 - {a_2}^*\ {z_2}^{N+1}} \\
\mathcal{F}_{a,p_{1,2}=1,N}\left(z_{1,2}\right) &= \frac{1 + a_{1,2}\ {z_{1,2}}^{N-1}}{{z_{1,2}}^{N-1} - {a_{1,2}}^*}
\end{aligned}$$

where $a_{1,2} = \tan\phi_{1,2} e^{\imath\psi_{1,2}} \neq 0$.

The dynamics for each qubit was already studied in details for one-qubit pure states. Let us point out important regimes:

- the maps with the projections $P_t = |00\rangle\langle 00|$ are represented by the rational map of degree at least two, then the dynamical system for each $i - th$ qubit is chaotic on nonempty Julia sets.
- the nonlinear map (3.4.2) with the partial projections $|1\rangle\langle 1|$ onto the first or the second qubit of the target system filters out every two-qubit separable pure state where i-th qubit is in state $|0\rangle$ or $|1\rangle$ - those are represent by $z_i = \{0, \infty\}$.
  - If the number of the target systems $N = 1$, then dynamics is trivial, the protocol behaves like the constant map or like a filter (in the case of the unitary parameter $a_i \in \{\pm 1\}$).
  - For $N \geq 2$ the protocol exhibits complicated dynamics, with either regular dynamics with empty Julia set or chaotic dynamics on nonempty Julia set.

3.5.2 Purification using the Hadamard gate

uses unitary transformation $U = H \otimes H$, where H is a Hadamard gate (2.2). The action of the complete protocol step (2.16) represented by the pair of the maps $\mathcal{F}_{p_{1,2},N} : \hat{\mathbb{C}} \mapsto \hat{\mathbb{C}}$ follows. In the same notation as before, one can study the dynamics for each of the qubit by the maps (3.4.3) $\mathcal{F}_{p_{1,2},N}$ with the actions:

$$
\begin{aligned}
\mathcal{F}_{p_{1,2}=0,N}(z_{1,2}) &= \frac{{z_{1,2}}^{N+1} + 1}{{z_{1,2}}^{N+1} - 1} \\
\mathcal{F}_{p_1=0,N}(z_1) &= \frac{{z_1}^{N+1} + 1}{{z_1}^{N+1} - 1}, \quad \mathcal{F}_{p_2=1,N}(z_2) = \frac{{z_2}^{N-1} + 1}{1 - {z_2}^{N-1}} \\
\mathcal{F}_{p_1=1,N}(z_1) &= \frac{{z_1}^{N-1} + 1}{1 - {z_1}^{N-1}}, \quad \mathcal{F}_{p_2=0,N}(z_2) = \frac{{z_2}^{N+1} + 1}{{z_2}^{N+1} + 1} \\
\mathcal{F}_{p_{1,2}=1,N}(z_{1,2}) &= \frac{{z_{1,2}}^{N-1} + 1}{1 - {z_{1,2}}^{N-1}}
\end{aligned}
$$

The dynamics of the protocol is characterized by this points:

- For the partial projection $|0\rangle\langle 0|$ onto the i-th qubit of the target system, $i \in \{1,2\}$ and for general N the map $\mathcal{F}_{0,N}$ is the rational function of degree at least 2, then the dynamics is chaotic on an nonempty Julia set.
- For the partial projection $|1\rangle\langle 1|$ and for $N \leq 3$ the dynamics of the map $\mathcal{F}_{\mathbf{p}_{1,2}=1,N}$ is completely regular.
- For $N \geq 3$, the map $\mathcal{F}_{1,N}$ is a rational map of the order at least 2 (and the map $\mathcal{F}_{0,N}$ has degree at least 4). Then, independent of the chose partial projections, the dynamical system generated by the purification protocol is chaotic on the Julia set.

3.5.3 Summary

One can conclude that the dynamics of the protocol (2.16) for two-qubit separable states is composed from the completely separated dynamics of the one-qubit systems (3.4.2,3.4.3), except the cases when after the certain iterations the protocol behaves like a filter. For the protocol with the additional unitary transformation $U = U_1 \otimes U_2$, where $U_{1,2} \in \{\mathrm{SU}(2), H\}$ (2.1,2.2), chaotic regime exists for each particle for every protocol with

- the number of the target systems $N \geq 1$ and for the projections $P_{t_i} = |0\rangle\langle 0|$, $i \in \{1,2\}$.
- the number of the target systems $N \geq 3$.

There exist various dynamics for the purifications of two-qubit separable states. For example, for the cases $N = 1$, $P_{t_1} = |01\rangle\langle 01|$ and for $U_{1,2} \in \mathrm{SU}(2)$ there exists chaotic regime for the first qubit of the control system, but the dynamics of the second qubit of the control system is fully regular and the protocol may even behave like a filter for the initial states $|\psi\rangle_1 \otimes |0\rangle$ resp. $|\psi\rangle_1 \otimes |1\rangle$ or the protocol may completely filter out all the separable pure states. For the same configuration of the purification except for $U_{1,2} =$ Hadamard gate latest after the second step of the purification all the separable pure states are filtered out.

3.6 Dynamics for two-qubit pure states close to separable pure states

So far, we studied the states with no entanglement. From chapters (3.1.1) and (3.1.2), we already know that the purifications map pure states onto pure states. Also, it is clear that the additional unitary gate $U = U_1 \otimes U_2$ (2.15) maps separable states onto separable states and that U preserves the norm of the input resp. distance between the states [20]. Finally, we can conclude that in a given step of purification it is the nonlinear part of the purification (2.14) which influences the entanglement of the output and the additional unitary gate U influences the input for next step of the purification. This forms generally complicated evolution and it is not easy to predict analytically the outcomes even for small perturbations of the initial states. However we can study the impact of one purification step on the perturbed separable states - we show, that the combination of certain perturbations together with the purification may lead to effective increase of entanglement.

Let be $|\psi_{\mathrm{Sep}}\rangle$ a two-qubit separable pure state of the form $|\psi_{\mathrm{Sep}}\rangle = |\psi^1\rangle \otimes |\psi^2\rangle$, where $|\psi^{1,2}\rangle$ is the state of individual qubit (3.16). Let $|\psi(\boldsymbol{\alpha})\rangle$ be a pure state close to $|\psi_{\mathrm{Sep}}\rangle$ of the form

$$|\psi(\boldsymbol{\alpha})\rangle = \alpha_{00}|00\rangle + \alpha_{01}|01\rangle + \alpha_{10}|10\rangle + \alpha_{11}|11\rangle$$

where $\boldsymbol{\alpha} = (\alpha_{00}, \ldots, \alpha_{11}) = \sqrt{\mathcal{N}}\,(\alpha_0^1\alpha_0^2 + \varepsilon_1, \alpha_0^1\alpha_2^2 + \varepsilon_2, \alpha_1^1\alpha_0^2 + \varepsilon_3, \alpha_1^1\alpha_1^2 + \varepsilon_4)$ and $\boldsymbol{\varepsilon} = (\varepsilon_1, \ldots, \varepsilon_4)$ represents an initial deviation of $|\psi(\boldsymbol{\alpha})\rangle$ from $|\psi_{\mathrm{Sep}}\rangle$.

The action of the nonlinear map (3.7) maps the pure state $|\psi(\boldsymbol{\alpha})\rangle$ onto the pure state $|\psi(\bar{\boldsymbol{\alpha}})\rangle$. The action depends on the number of the target states N and on the chosen target systems projections $P_{t_i} = |\mathbf{p}\rangle\langle\mathbf{p}|$, $\mathbf{p} \in \{00, \ldots, 11\}$:

$$\begin{aligned}
\mathbf{p} = 00: \quad & \boldsymbol{\alpha} \mapsto \bar{\boldsymbol{\alpha}} = \sqrt{\mathcal{N}}\left(\alpha_{00}^{N+1}, \alpha_{01}^{N+1}, \alpha_{10}^{N+1}, \alpha_{11}^{N+1}\right), \\
\mathbf{p} = 01: \quad & \boldsymbol{\alpha} \mapsto \bar{\boldsymbol{\alpha}} = \sqrt{\mathcal{N}}\left(\alpha_{00}\alpha_{01}^{N}, \alpha_{01}\alpha_{00}^{N}, \alpha_{10}\alpha_{11}^{N}, \alpha_{11}\alpha_{10}^{N}\right), \\
\mathbf{p} = 10: \quad & \boldsymbol{\alpha} \mapsto \bar{\boldsymbol{\alpha}} = \sqrt{\mathcal{N}}\left(\alpha_{00}{\alpha_{10}}^{N}, \alpha_{01}\alpha_{11}^{N}, \alpha_{10}{\alpha_{00}}^{N}, \alpha_{11}{\alpha_{01}}^{N}\right), \\
\mathbf{p} = 11: \quad & \boldsymbol{\alpha} \mapsto \bar{\boldsymbol{\alpha}} = \sqrt{\mathcal{N}}\left(\alpha_{00}{\alpha_{11}}^{N}, \alpha_{01}\alpha_{10}^{N}, \alpha_{10}{\alpha_{01}}^{N}, \alpha_{11}{\alpha_{00}}^{N}\right).
\end{aligned} \tag{3.17}$$

Let us focus on study of the purification step with projections $P_{t_i} = |00\rangle\langle 00|$. It is easy to verify that for finite N and small deviations $\boldsymbol{\varepsilon} \to 0$ the $|\psi(\bar{\boldsymbol{\alpha}})\rangle$ remains close to the output of purification of $|\psi_{\text{Sep}}\rangle = |\psi^1\rangle \otimes |\psi^2\rangle$ i.e. close to the separable state.

If the purification protocol uses huge number of target systems $N \gg 1$, then the nonlinear part simply factors out the nondominant coordinates (in absolute value) of $|\psi(\boldsymbol{\alpha})\rangle$ i.e. the output $|\psi(\bar{\boldsymbol{\alpha}})\rangle$ has nonzero coordinates only on positions of dominant coordinates of $|\psi(\boldsymbol{\alpha})\rangle$. One can verify, that any two-qubit separable pure state $|\psi_{\text{Sep}}\rangle$ may have one, two or four dominant coordinates, depending if

$$|\alpha_i^1| < |\alpha_j^1| \ \wedge \ |\alpha_i^2| < |\alpha_j^2|$$

or in the case of

$$|\alpha_i^1| = |\alpha_j^1| \ \wedge \ |\alpha_i^2| < |\alpha_j^2| \text{ (or vice versa)}$$

or when

$$|\alpha_i^{1,2}| = |\alpha_j^{1,2}|$$

for $i, j \in \{0, 1\}$. If the deviation keeps the dominant coordinates of $|\psi(\bar{\boldsymbol{\alpha}})\rangle$ in one of these combinations i.e. either there is the only one dominant coordinate α_{ij} or two dominant coordinates α_{ij},α_{ik} resp. α_{ij},α_{ik} or all the coordinates are dominant, then the output state $|\psi(\bar{\boldsymbol{\alpha}})\rangle$ remains separable. It is mainly true when $\boldsymbol{\varepsilon} \to 0$. On the other hand, if there is a significant deviation, and α_{00}, α_{11} (or α_{01}, α_{10}) become to dominant, then $|\psi(\bar{\boldsymbol{\alpha}})\rangle$ becomes strongly entangled (the index of correlation is close to the maximal value $I_c = 2\ln 2$ (2.11)) - especially if $\alpha_{00} = \alpha_{11}$ ($\alpha_{01} = \alpha_{10}$) then $|\psi(\bar{\boldsymbol{\alpha}})\rangle$ is close to the Bell state $|\psi_{00}\rangle$ ($|\psi_{01}\rangle$) (2.6). Hence we can expect that the combination of significant deviation and a large number of target systems significantly increase the entanglement of the output state.

Let us demonstrate the loss of separability on an example. Let us suppose purification with $P_{t_i} = |00\rangle\langle 00|$, $N \gg 1$ and let $|\psi_{\text{Sep}}\rangle = |00\rangle$. Let $|\psi(\boldsymbol{\alpha})\rangle$ be a perturbed state with

$$\alpha_{00} = 1 + \varepsilon_1, \ \ \alpha_{10} = \varepsilon_2, \ \ \alpha_{01} = \varepsilon_3, \ \ \alpha_{11} = \varepsilon_4.$$

If $|1+\varepsilon_1| > \max\{|\varepsilon_2|,\ldots,|\varepsilon_4|\}$ then $|\psi(\bar{\boldsymbol{\alpha}})\rangle$ stays close to the separable state $|00\rangle$. If $|1+\varepsilon_1| = |\varepsilon_2| = \max\{|\varepsilon_3|,|\varepsilon_4|\}$ then $|\psi(\bar{\boldsymbol{\alpha}})\rangle$ stays close to the separable orbit

$$\frac{1}{\sqrt{2}}\left(e^{\imath(N+1)\eta}|00\rangle + e^{\imath(N+1)\theta}|01\rangle\right)$$

where η, θ are the phases of $1+\varepsilon_1$, ε_2. If $|1+\varepsilon_1| = |\varepsilon_4| = \max\{|\varepsilon_2|,|\varepsilon_3|\}$ then $|\psi(\bar{\boldsymbol{\alpha}})\rangle$ stays close to the maximally entangled orbit

$$\frac{1}{\sqrt{2}}\left(e^{\imath(N+1)\eta}|00\rangle + e^{\imath(N+1)\vartheta}|11\rangle\right)$$

where η, ϑ are the phases of $1+\varepsilon_1$, ε_4. For the cases, when the nonlinear part of the purification maps the initial state $|\psi(\boldsymbol{\alpha})\rangle$ close to separable state, the action of the additional unitary gate does not affect the separability of the output $|\psi(\bar{\boldsymbol{\alpha}})\rangle$. For the cases when the nonlinear part maps $|\psi(\boldsymbol{\alpha})\rangle$ close to the entangled state the system may stay entangled - we can demonstrate it on the example of purification with the unitary gate $U = H \otimes H$ where H is the Hadamard gate (2.2). Let us suppose $|\psi(\bar{\boldsymbol{\alpha}})\rangle$ is of the form

$$|\psi(\bar{\boldsymbol{\alpha}})\rangle = \frac{1}{\sqrt{2}}\left(\bar{\alpha}_{00}|00\rangle + \bar{\alpha}_{11}|11\rangle\right),$$

and $|\bar{\alpha}_{00}| = |\bar{\alpha}_{11}| = 1$, then

$$U|\psi(\bar{\boldsymbol{\alpha}})\rangle = \frac{1}{2}\left(\left(\bar{\alpha}_{00}+\bar{\alpha}_{11}\right)|00\rangle + \left(\bar{\alpha}_{00}-\bar{\alpha}_{11}\right)|01\rangle + \left(\bar{\alpha}_{00}-\bar{\alpha}_{11}\right)|10\rangle + \left(\bar{\alpha}_{00}+\bar{\alpha}_{11}\right)|11\rangle\right).$$

One can see that the system is separable only if $\left(\bar{\alpha}_{00}+\bar{\alpha}_{11}\right)^2 = \left(\bar{\alpha}_{00}-\bar{\alpha}_{11}\right)^2$ i.e. $\bar{\alpha}_{00} = 0$ or $\bar{\alpha}_{11} = 0$, which can not happen for the studied case. One can verify that in this case the purification keeps the system in the completely entangled state.

Finally, let us investigate the purifications with the other purifications i.e. with the target system projections $P_{t_i} = |\mathbf{p}\rangle\langle\mathbf{p}| \neq |00\rangle\langle 00|$. Except the regimes already observed for the purification with $P_{t_i} \neq |00\rangle\langle 00|$ the possibility to annihilate the initial states appear. In other words the purification (3.17) stops. It happens whenever at least two different coordinates of $\boldsymbol{\alpha}$ satisfy

$$\alpha_{\mathbf{k}} = \alpha_{\mathbf{l}} = 0 \ \wedge \ \mathbf{k} \ominus \mathbf{l} \neq \mathbf{0}.$$

Except the annihilation, "mixing" of the components during purification (3.17) may be responsible for a significant increase/decrease of the entanglement of purified states.

3.7 Dynamics for two-qubit nonseparable pure states

Let us study now the dynamics of purification for two-qubit nonseparable pure states $|\psi\rangle \in \mathcal{H}_1(2) \otimes \mathcal{H}_2(2)$. The input state is given by

$$|\psi(\boldsymbol{\alpha})\rangle = \alpha_{00}|00\rangle + \alpha_{01}|01\rangle + \alpha_{10}|10\rangle + \alpha_{11}|11\rangle.$$

The action of the nonlinear map (3.7) maps the pure state $|\psi(\boldsymbol{\alpha})\rangle$ onto the pure state $|\psi(\bar{\boldsymbol{\alpha}})\rangle$. The action depends on the number of the target states N and on the chosen target systems projections $P_{t_i} = |\mathbf{p}\rangle\langle\mathbf{p}|$, $\mathbf{p} \in \{00, \ldots, 11\}$ (3.17). The general analysis of the purification protocols is very difficult. The mathematical framework do not seem to be fully developed. To prove the existence of chaos it is easier and sufficient to find a special example. Therefore, let us focus on the one complex parameter subdynamics and let us prove the existence of chaos in the entanglement. For this reason let us study the protocol [8] with the additional unitary transformation $U = H \otimes H$, composed from the Hadamard gates (2.2), and let us study the subdynamics for the ensemble of initial states

$$|\psi(r)\rangle = \mathcal{N}(r)\left(r|00\rangle + |11\rangle\right), \ \mathcal{N}(r) = \left(1 + |r|^2\right)^{-1/2}, \ r \in \hat{\mathbb{C}}. \tag{3.18}$$

Clearly, $|\psi(1)\rangle = |\psi_{00}\rangle$ represents Bell state (2.6) and therefore $\{|\psi(r)\rangle\}$ represent one parametric set of perturbed Bell state $|\psi_{00}\rangle$.

Depending on the setting of the projection P onto target states, the various actions of the nonlinear part of the protocol step appear:

- if $P_{t_i} \in \{|01\rangle\langle 01|, \ |10\rangle\langle 10|\}$ then the nonlinear part behaves as a filter for every $|\psi(r)\rangle$ and the protocol stops,
- if $P_{t_i} = |00\rangle\langle 00|$ then the nonlinear part maps $|\psi(r)\rangle \mapsto |\psi\left(r^{N+1}\right)\rangle$ i.e. the form of the output state is preserved,
- finally, if $P_{t_i} = |11\rangle\langle 11|$ then the nonlinear part maps $|\psi(r)\rangle \mapsto |\psi\left(r^{1-N}\right)\rangle$, $r \neq \{0, \infty\}$ (the form of the output state is also preserved) and for $r = 0$ or $r = \infty$ protocol stops.

Therefore the nontrivial subdynamics exist for the purifications with the projection $P_{t_i} \in \{|00\rangle\langle 00|,\ |11\rangle\langle 11|\}$. Two steps of complete purification maps initial state $|\psi(r)\rangle$ (3.18) as

$$|\psi(r)\rangle \mapsto |\phi(s)\rangle = \mathcal{N}\left(|00\rangle + s|01\rangle + s|10\rangle + |11\rangle\right) \mapsto |\psi(t)\rangle,$$

where $\mathcal{N} = 2\left(1+|s|^2\right)^{-1/2}$ and the values $s,t \in \hat{\mathbb{C}}$ depend on the projections P_{t_i}. Especially, for $P_{t_i} = |00\rangle\langle 00|$:

$$\begin{aligned} s &= \frac{r^{N+1}-1}{r^{N+1}+1} \\ t &= \frac{\left(r^{N+1}+1\right)\left(r^{N+1}+1\right)^N + \left(r^{N+1}-1\right)\left(r^{N+1}-1\right)^N}{\left(r^{N+1}+1\right)\left(r^{N+1}+1\right)^N - \left(r^{N+1}-1\right)\left(r^{N+1}-1\right)^N} \end{aligned} \tag{3.19}$$

and for $P_{t_i} = |11\rangle\langle 11|$:

$$\begin{aligned} s &= -\frac{r^{N-1}-1}{r^{N-1}+1} \\ t &= \frac{\left(r^{N-1}+1\right)\left(r^{N-1}+1\right)^N - \left(r^{N-1}-1\right)\left(1-r^{N-1}\right)^N}{\left(r^{N-1}+1\right)\left(r^{N-1}+1\right)^N + \left(r^{N-1}-1\right)\left(1-r^{N-1}\right)^N}. \end{aligned} \tag{3.20}$$

Regarding the fixed points, maximally entangled Bell state (2.6) $|\psi_{00}\rangle = |\psi(1)\rangle \mapsto |\phi(0)\rangle = |\psi_{00}\rangle$ is the fixed point for both the purifications. Especially, for the purification (3.19) $|\psi(\infty)\rangle \mapsto |\phi(1)\rangle \mapsto |\psi(\infty)\rangle$, this forms a cycle C of separable states (2.7)

$$C = \left(|00\rangle,\ \frac{1}{2}\left(|0\rangle + |1\rangle\right) \otimes \left(|0\rangle + |1\rangle\right)\right). \tag{3.21}$$

Now let us continue with the analysis for the purification, using $N = 1$ target systems and with the projections $P_{t_i} = |00\rangle\langle 00|$. Such a purification exhibits nontrivial dynamics in contrast to the purification with the projection $P_{t_i} = |11\rangle\langle 11|$ when $|\psi(r)\rangle \mapsto |\phi(0)\rangle = |\psi_{00}\rangle$, $r \neq \{0,\infty\}$. Purification with $P_{t_i} = |00\rangle\langle 00|$ and $N = 1$ has following evolution

$$|\psi(r)\rangle \mapsto |\phi(f(r))\rangle \mapsto |\psi(g(r))\rangle$$

where

$$f(r) = \frac{1-r^2}{1+r^2},\ \ g(r) = \frac{1+r^4}{2r^2}\ \text{ i.e. }\ g = \frac{1}{f} \circ \frac{1}{f},\ \ r \in \hat{\mathbb{C}}.$$

We can study one dimensional subdynamics of the purification in even $(2l)$ resp. odd $(2l+1)$ steps of the purification. The initial state $|\psi(r)\rangle$ is mapped:

- after $2l$ steps onto the state $|\psi\left(g^{\circ l}\left(r\right)\right)\rangle$,

- after $2l+1$ steps onto the state $|\phi\left(f\circ g^{\circ l}\left(r\right)\right)\rangle$. Because $f\circ g=-f^{\circ 3}$ and $f(-x)=f(x)$ we can use the induction to prove $f\circ g^{\circ l}=-f^{\circ 2l+1}$.

Finally, we can conclude that the dynamics of the purification in even resp. odd steps is generated by the maps $\mathcal{G}\equiv g$ resp. $\mathcal{F}\equiv -f^{\circ 2}$

$$\mathcal{G}\left(r\right)=\frac{1+r^4}{2r^2},\ \ \mathcal{F}\left(s\right)=\frac{1}{\mathcal{G}(s)} \tag{3.22}$$

with the closed evolutions of the states in even ($2l$) resp. odd ($2l+1$) steps

$$|\psi\left(r_0\right)\rangle\mapsto|\phi\left(s_0\right)\rangle\mapsto\ldots\mapsto|\psi\left(\mathcal{G}^{\circ l}\left(r_0\right)\right)\rangle\mapsto|\phi\left(\mathcal{F}^{\circ l}\left(s_0\right)\right)\rangle\ \ s_0=f\left(r_0\right). \tag{3.23}$$

By calculating stability 2.4.8) of the maps $\mathcal{G}$ resp. $\mathcal{F}$ for the points $r\in\{1,\infty\}$ resp. $s\in\{0,1\}$ one can verify that a fixed point $|\psi_{00}\rangle$ (2.6) and the cycle C (3.21) are superattracting for the purification. Functions $\mathcal{F}$, $\mathcal{G}$ are the rational functions of order four i.e. they belong to *Rat* (2.4.5). Consequently, according to the theorems (2.4.11,2.4.14), their Julia sets $J\left(\mathcal{F}\right)$, $J\left(\mathcal{G}\right)$ are nonempty and generated subdynamics are chaotic on the Julia sets. Figures (3.9) represent the numerical calculations of $J\left(\mathcal{G}\right)$, $J\left(\mathcal{F}\right)$ as the backward orbits of repelling periodic points $r_0=1.83928676$, $s_0=-0.77184451+1.11514251\imath$ (2.4.6). For the calculations we used the expressions of backward orbits $r^{-1,\mathcal{G}}_{1,\ldots,4}$ and $s^{-1,\mathcal{F}}_{1,\ldots,4}$ of the points r in $J\left(\mathcal{G}\right)$ resp. s in $J\left(\mathcal{F}\right)$ of the form

$$r^{-1,\mathcal{G}}_{1,\ldots,4}=\pm\sqrt{r\pm\sqrt{r^2-1}},\ \ s^{-1,\mathcal{F}}_{1,\ldots,4}=\pm\sqrt{\frac{1\pm\sqrt{1-s^2}}{s}} \tag{3.24}$$

i.e. $r^{-1,\mathcal{G}}_{1,\ldots,4}\left(1/x\right)=s^{-1,\mathcal{F}}_{1,\ldots,4}\left(x\right)$. From the relations $\mathcal{F}\equiv 1/\mathcal{G}$ and $\mathcal{G}(x)=\mathcal{G}(1/x)$ one can prove the equivalency in the evolution $\mathcal{F}^{\circ n}\left(x_0\right)=1/\mathcal{G}^{\circ n}\left(x_0\right)$ which induces similar dynamics of $\mathcal{F}$, $\mathcal{G}$ and the equivalence of their Julia sets. The Julia sets also correspond to the structure of the Julia set (3.1) generated by the map $\mathcal{F}_{1,0,1}$ (3.11), $\mathcal{G}^{\circ n}\left(x_0\right)=-\mathcal{F}^{\circ 2n}_{1,0,1}\left(x_0\right)$.

Let us turn our attention to the existence of chaos in entanglement. Instead of calculation of von Neuman index correlation I_c (2.11) during purification, we can numerically prove the existence of chaos in entanglement by study of the entanglement of the limit states being purified for various initial states. For numerical calculation let us use the Fano representation (2.17) for two-qubit states, as an numerically effective method using only 15 real (not complex) variables, which make the calculation easier and faster. The action of studied purification for general two-qubit state may be represented by the rational map $\mathcal{F}_{\text{Fano}}: \ \mathbb{R}^{15} \mapsto \mathbb{R}^{15}$ with the net effect

$$\begin{aligned}
c_{\mathcal{I}\mathcal{X}} &\mapsto 2\mathcal{N}\left(c_{\mathcal{I}\mathcal{Z}} + c_{\mathcal{Z}\mathcal{I}}c_{\mathcal{Z}\mathcal{Z}}\right), \\
c_{\mathcal{I}\mathcal{Y}} &\mapsto -2\mathcal{N}\left(c_{\mathcal{I}\mathcal{X}}c_{\mathcal{I}\mathcal{Y}} + c_{\mathcal{Z}\mathcal{X}}c_{\mathcal{Z}\mathcal{Y}}\right), \\
c_{\mathcal{I}\mathcal{Z}} &\mapsto \mathcal{N}\left(c_{\mathcal{I}\mathcal{X}}^2 - c_{\mathcal{I}\mathcal{Y}}^2 + c_{\mathcal{Z}\mathcal{X}}^2 - c_{\mathcal{Z}\mathcal{Y}}^2\right), \\
c_{\mathcal{X}\mathcal{I}} &\mapsto 2\mathcal{N}\left(c_{\mathcal{Z}\mathcal{I}} + c_{\mathcal{I}\mathcal{Z}}c_{\mathcal{Z}\mathcal{Z}}\right), \\
c_{\mathcal{X}\mathcal{X}} &\mapsto 2\mathcal{N}\left(c_{\mathcal{I}\mathcal{Z}}c_{\mathcal{Z}\mathcal{I}} + c_{\mathcal{Z}\mathcal{Z}}\right), \\
c_{\mathcal{X}\mathcal{Y}} &\mapsto -2\mathcal{N}\left(c_{\mathcal{I}\mathcal{Y}}c_{\mathcal{Z}\mathcal{X}} + c_{\mathcal{I}\mathcal{X}}c_{\mathcal{Z}\mathcal{Y}}\right), \\
c_{\mathcal{X}\mathcal{Z}} &\mapsto 2\mathcal{N}\left(c_{\mathcal{I}\mathcal{X}}c_{\mathcal{Z}\mathcal{X}} - 2c_{\mathcal{I}\mathcal{Y}}c_{\mathcal{Z}\mathcal{Y}}\right), \\
c_{\mathcal{Y}\mathcal{I}} &\mapsto -2\mathcal{N}\left(c_{\mathcal{X}\mathcal{I}}c_{\mathcal{Y}\mathcal{I}} + c_{\mathcal{X}\mathcal{Z}}c_{\mathcal{Y}\mathcal{Z}}\right), \\
c_{\mathcal{Y}\mathcal{X}} &\mapsto -2\mathcal{N}\left(c_{\mathcal{X}\mathcal{Z}}c_{\mathcal{Y}\mathcal{I}} + c_{\mathcal{X}\mathcal{I}}c_{\mathcal{Y}\mathcal{Z}}\right), \\
c_{\mathcal{Y}\mathcal{Y}} &\mapsto 2\mathcal{N}\left(c_{\mathcal{X}\mathcal{Y}}c_{\mathcal{Y}\mathcal{X}} + c_{\mathcal{X}\mathcal{X}}c_{\mathcal{Y}\mathcal{Y}}\right), \\
c_{\mathcal{Y}\mathcal{Z}} &\mapsto -2\mathcal{N}\left(c_{\mathcal{X}\mathcal{X}}c_{\mathcal{Y}\mathcal{X}} - c_{\mathcal{X}\mathcal{Y}}c_{\mathcal{Y}\mathcal{Y}}\right), \\
c_{\mathcal{Z}\mathcal{I}} &\mapsto \mathcal{N}\left(c_{\mathcal{X}\mathcal{I}}^2 + c_{\mathcal{X}\mathcal{Z}}^2 - c_{\mathcal{Y}\mathcal{I}}^2 - c_{\mathcal{Y}\mathcal{Z}}^2\right), \\
c_{\mathcal{Z}\mathcal{X}} &\mapsto 2\mathcal{N}\left(c_{\mathcal{X}\mathcal{I}}c_{\mathcal{X}\mathcal{Z}} - c_{\mathcal{Y}\mathcal{I}}c_{\mathcal{Y}\mathcal{Z}}\right), \\
c_{\mathcal{Z}\mathcal{Y}} &\mapsto -2\mathcal{N}\left(c_{\mathcal{X}\mathcal{X}}c_{\mathcal{X}\mathcal{Y}} - c_{\mathcal{Y}\mathcal{X}}c_{\mathcal{Y}\mathcal{Y}}\right), \\
c_{\mathcal{Z}\mathcal{Z}} &\mapsto \mathcal{N}\left(c_{\mathcal{X}\mathcal{X}}^2 - c_{\mathcal{X}\mathcal{Y}}^2 - c_{\mathcal{Y}\mathcal{X}}^2 + c_{\mathcal{Y}\mathcal{Y}}^2\right).
\end{aligned} \tag{3.25}$$

where

$$\mathcal{N} = \left(1 + c_{\mathcal{I}\mathcal{Z}}^2 + c_{\mathcal{Z}\mathcal{I}}^2 + c_{\mathcal{Z}\mathcal{Z}}^2\right)^{-1}.$$

According to the definition (2.4.23), by evaluating the eigenvalues of the Jacobian matrix

$$\mathcal{F}^{'}_{\text{Fano}}\left(c_{\mathcal{I}\mathcal{X}}, \ldots, c_{\mathcal{Z}\mathcal{Z}}\right) = \frac{\partial}{\partial c_{\alpha\beta}} F_{\text{Fano}}\left(c_{\mathcal{I}\mathcal{X}}, \ldots, c_{\mathcal{Z}\mathcal{Z}}\right), \ \ \alpha, \beta \in \mathcal{I}, \mathcal{X}, \mathcal{Y}, \mathcal{Z} \ \ \wedge \ \ c_{\alpha\beta} \neq c_{\mathcal{I}\mathcal{I}}, \tag{3.26}$$

one can reconfirm that the fixed point $|\psi_{00}\rangle$ (2.6) and the cycle C (3.21) are both attracting (2.4.23) for the studied purification. Now, let us calculate the coordinates of the Bloch vector $\mathbf{b}_{\rho(r)}$ (2.18) for the initial state $|\psi\left(r\right)\rangle$ (3.18)

$$\begin{aligned}
&c_{\mathcal{IX}} = c_{\mathcal{IY}} = c_{\mathcal{XI}} = c_{\mathcal{XZ}} = c_{\mathcal{YI}} = c_{\mathcal{YZ}} = c_{\mathcal{ZX}} = c_{\mathcal{ZY}} = c_{\mathcal{ZY}} = 0,\\
&c_{\mathcal{IZ}} = c_{\mathcal{ZI}} = \frac{|r|^2 - 1}{1 + |r|^2},\\
&c_{\mathcal{XX}} = -c_{\mathcal{YY}} = 2\frac{Re\left(r\right)}{1 + |r|^2},\\
&c_{\mathcal{XY}} = c_{\mathcal{YX}} = -2\frac{Im\left(r\right)}{1 + |r|^2},\\
&c_{\mathcal{ZZ}} = 1.
\end{aligned}$$

Finally, let us purify various initial states. Then the figure (3.10) clearly demonstrates strong resistance as well as significant sensitivity of purification to converge the initial state $|\psi\left(r\right)\rangle$ (3.18) either to maximally entangled Bell state ψ_{00} (2.6) - blue area - or to the separable cycle C (3.21) - green area. Blue and green areas represent existence of regular dynamics. Chaos in entanglement appears on the border of both areas.

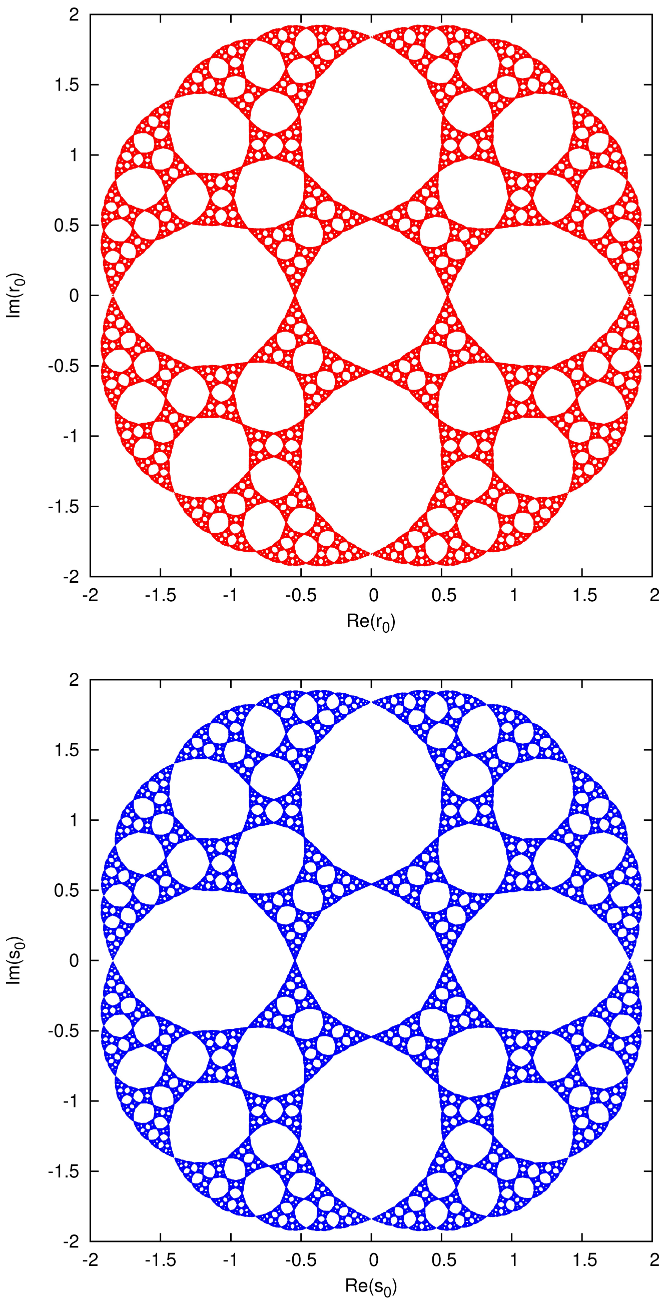

Figure 3.9: The Julia sets for one complex parameter subdynamics generated by the maps $\mathcal{G}$ (red color), $\mathcal{F}$ (blue color) (3.22) - calculated for 10 backward steps (3.24). Structures of the Julia sets correspond to similar dynamics generated by the maps $\mathcal{G}$, $\mathcal{F}$ as $\mathcal{F}^{\circ n}(x_0) = 1/\mathcal{G}^{\circ n}(x_0)$. The Julia sets also correspond to the structure of the Julia set (3.1) generated by the map $\mathcal{F}_{1,0,1}$ (3.11), $\mathcal{G}^{\circ n}(x_0) = -\mathcal{F}^{\circ 2n}_{1,0,1}(x_0)$.

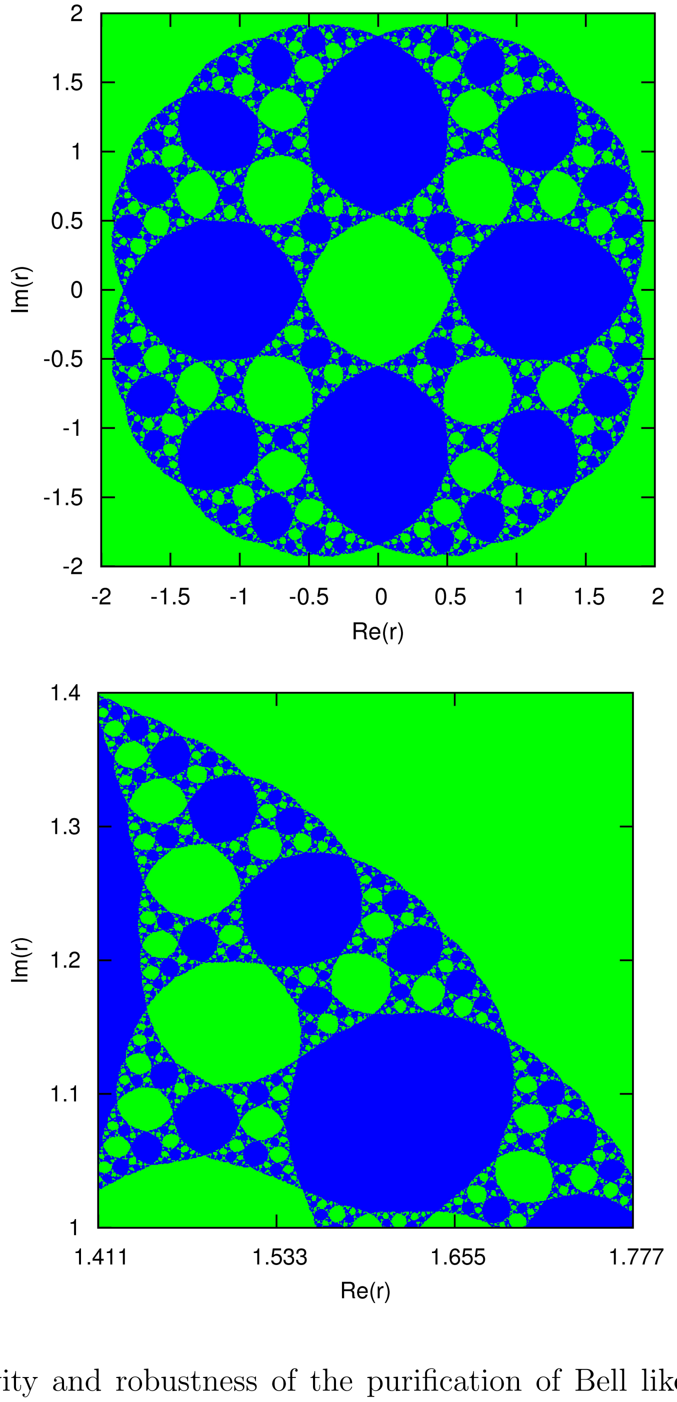

Figure 3.10: Sensitivity and robustness of the purification of Bell like states (3.18) either to the attracting maximally entangled Bell state $|\psi_{00}\rangle$ (2.6) - blue color, or to attracting separable cycle C (3.21) - green color. Purification was simulated for 200 steps, precision of convergence was 10^{-4}.

3.8 Dynamics of the two-qubit mixed states

For the general mixed state, one can nicely prove the existence of chaotic dynamics by numerical simulation, using the Fano representation (3.25) as we applied successfully for the simulation of two-qubit pure state dynamics. Let us focus now for the simulation of the purification of the perturbed Werner like states

$$\rho(\lambda, r) = \lambda|\psi(r)\rangle\langle\psi(r)| + \frac{1-\lambda}{4}\mathcal{I}, \;\; 0 \leq \lambda \leq 1, \;\; \lambda \in \hat{\mathbb{C}}. \tag{3.27}$$

One can see that for $\lambda = 1$ we received the set of the pure states, already studied (3.18), so we are going to analyze an extension of previously studied pure states to observe the sensitivity of the purification, when the initial system loose the purity.

The initially perturbed Werner state (3.27), in Fano representation (2.17), is represented by the Bloch vector $\mathbf{b}_{\rho(\lambda,r)}$ (2.18) with the coordinates

$$\begin{aligned}
&c_{\mathcal{IX}} = c_{\mathcal{IY}} = c_{\mathcal{XI}} = c_{\mathcal{XZ}} = c_{\mathcal{YI}} = c_{\mathcal{YZ}} = c_{\mathcal{ZX}} = c_{\mathcal{ZY}} = c_{\mathcal{ZY}} = 0,\\
&c_{\mathcal{IZ}} = c_{\mathcal{ZI}} = \lambda\frac{|r|^2 - 1}{1 + |r|^2},\\
&c_{\mathcal{XX}} = -c_{\mathcal{YY}} = 2\lambda\frac{Re\,(r)}{1 + |r|^2},\\
&c_{\mathcal{XY}} = c_{\mathcal{YX}} = -2\lambda\frac{Im\,(r)}{1 + |r|^2},\\
&c_{\mathcal{ZZ}} = \lambda.
\end{aligned}$$

The figures (3.11,3.12) illustrate the convergence of purification for various initial states (3.27) to three attracting periodic points: maximally entangled Bell state $|\psi_{00}\rangle$ (2.6), separable pure states cycle C (3.21) (these were already introduced for (3.10)) and finally separable mixed state cycle $\tilde{C}$

$$\tilde{C} = \left(\frac{1}{2}\left(|00\rangle\langle 00| + |11\rangle\langle 11|\right), \; \frac{1}{4}\left(|00\rangle\langle 00| + |11\rangle\langle 11| + \left(|01\rangle + |10\rangle\right)\left(\langle 01| + \langle 10|\right)\right)\right) \tag{3.28}$$

The convergence to the third, completely mixed state $\tilde{C}$ is in coincidence with our expectation that initial mixed state (3.27) may converge also to the mixed state. The areas of convergence to the three attracting states are islands of regular dynamics, border between the areas represent sensitivity of purification to the initial conditions - chaos in entanglement.

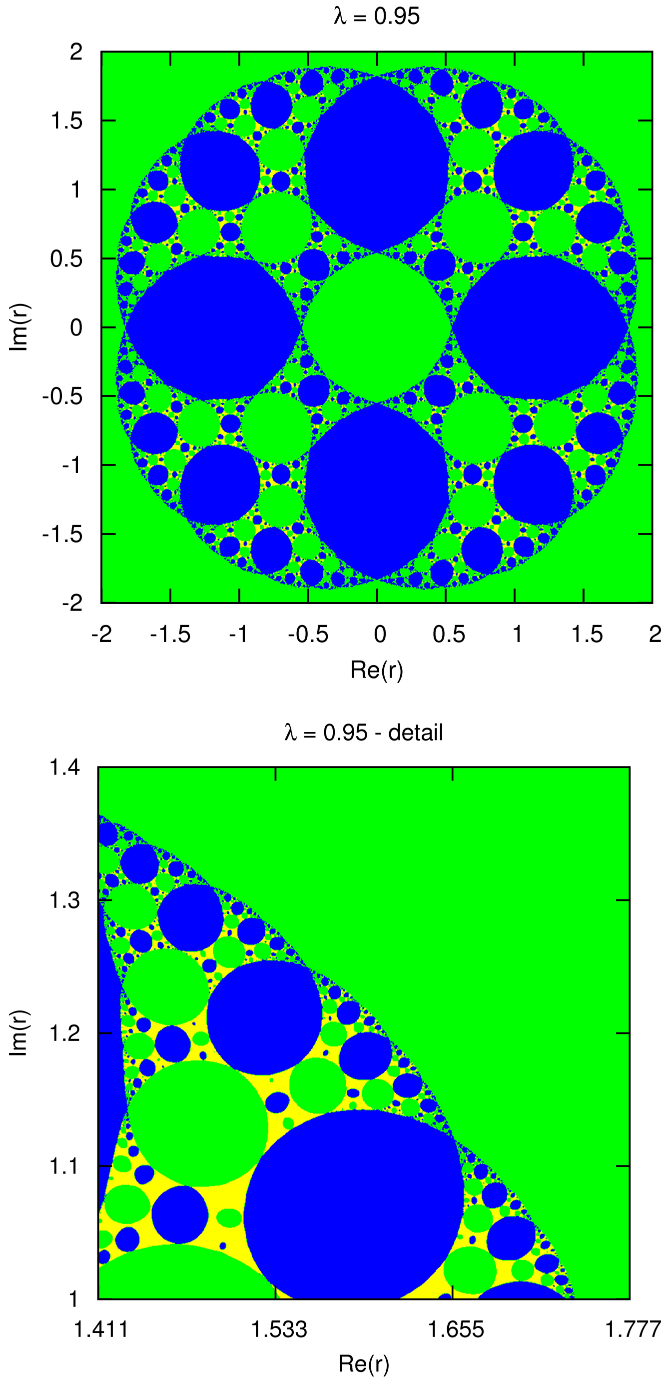

Figure 3.11: Sensitivity and robustness of the purification of Werner like states $\rho(\lambda, r)$ (3.27) either to maximally entangled Bell state $|\psi_{00}\rangle$ (2.6) - blue color - or to separable pure cycle C (3.21) - green color - or to separable mixed cycle $\tilde{C}$ (3.28) - yellow color. Purification was simulated for 200 steps, precision of convergence was 10^{-4}.

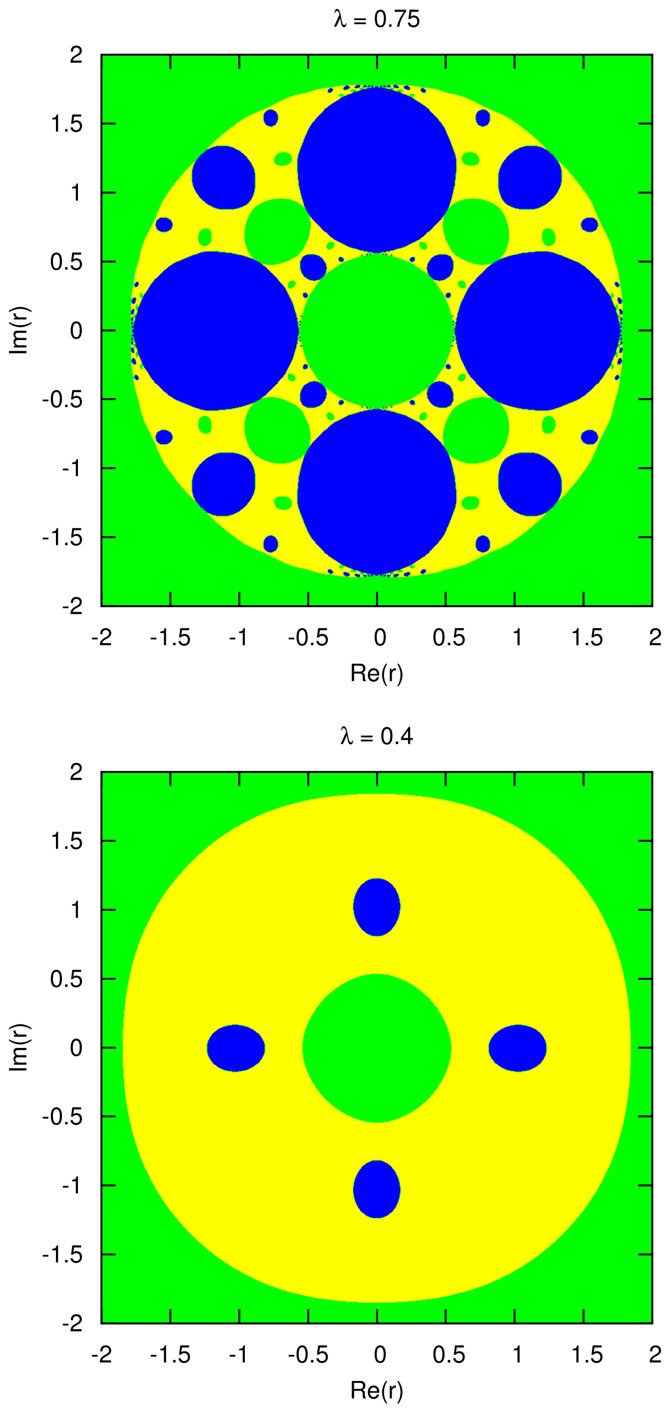

Figure 3.12: More the initial Werner like states $\rho(\lambda, r)$ (3.27) looses purity by decreasing λ, more the purification converge to separable mixed cycle $\tilde{C}$ (3.28) - yellow color. On contrary, the size of the areas of convergence to maximally entangled Bell state $|\psi_{00}\rangle$ (2.6) - blue color - and to separable pure cycle C (3.21) - green color - are decreasing.

3.9 Example of holomorphic dynamics

As mentioned in section (3.2.2), two-qubit pure state dynamics can be generally described by three complex variables. For the purpose of the thesis, we introduced necessary mathematical framework for study of dynamics of multidimensional holomorphic maps (2.4.2) which we applied for calculation of chaos in entanglement (3.7,3.8). We also mentioned (2.4.2), that the theory of dynamical systems for multidimensional maps is far more complicated than for one dimensional maps [13; 14]. An interesting example of the different dynamics for one and multidimensional holomorphic maps provides the analysis of motion for the states in the basis of attraction. While for one dimensional map the motion can be linearized, for two complex variable map there exist nonlinear regimes (Lattés theorem (3.9.1) [13]). Let us prove, that the motion for three complex variables map is even more complicated than a behavior of the map of two complex variables. Now, let us present the theorem of Lattés [13].

Theorem 3.9.1 (Lattés - the $\mathbb{C}^2$ map behavior close to the attracting fixed point - see [13])**.** *Let $\mathcal{F}$ be an invertible holomorphic map with an attracting fixed point $a \in \mathbb{C}^2$. Suppose that the eigenvalues λ, μ of the Jacobian $\mathcal{F}'(\mathbf{a})$ satisfy the condition $0 < |\mu| \leq |\lambda| < 1$. Let us define the holomorphic maps from $\mathbb{C}^2$ to $\mathbb{C}^2$*

$$\begin{aligned} L_{\lambda,\mu}: \ & (x,y) \mapsto (\lambda x, \mu y)\,, \ \ (\lambda, \ \ \mu \neq 0)\,, \\ E_{\lambda,k}: \ & (x,y) \mapsto \left(\lambda x, \lambda^k \left(y + x^k\right)\right)\,, \ \ (\lambda \neq 0, \ \ k = 1, 2, \ldots)\,. \end{aligned}$$

Following claims are valid:

1. *if $\lambda^k \neq \mu$ for any positive integer k, then $\mathcal{F}$ is conjugate by $L_{\lambda,\mu}$,*

2. *if $\lambda^k = \mu$ for some positive integer k, then $\mathcal{F}$ is conjugate either to $L_{\lambda,\mu}$ or to $E_{\lambda,\mu}$.*

Let us present, in main steps, the prove of the similar claims to Lattés theorem (3.9.1) for the map of three complex variables.

Theorem 3.9.2. *Let $\mathcal{F}$ be an invertible, holomorphic map with attracting fixed point $\mathbf{a} \in \mathbb{C}^3$. Suppose that the eigenvalues λ, μ, ν of Jacobian $\mathcal{F}'(\mathbf{a})$ satisfy the condition* $0 < |\mu| \leq |\nu| \leq$

$|\lambda| < 1$. *Then the map $\mathcal{F}$ in iteration limit converges uniformly in the neighborhood of* $\mathbf{a}$ *to the map $\mathcal{I}$ where*

$$\mathcal{I}: \ (x, y, z) \mapsto (\lambda x, \mu y + g(x, z), \nu z + h(x, y)),$$

g, h are holomorphic. Let us define

$$\begin{aligned} \mathcal{I}_{\lambda,\mu,\nu}: &\ (x, y, z) \mapsto (\lambda x, \mu y, \nu z) \\ \mathcal{I}_{\lambda,k,\nu}: &\ (x, y, z) \mapsto \left(\lambda x, \lambda^k \left(y + x^k\right), \nu z\right). \end{aligned}$$

If $g(x, z) \equiv g(x)$ and $h(x, y) \equiv h(x)$ then:

1. *if $\lambda^k \neq \mu$ and $\lambda^l \neq \nu$ for every k, l, then $\mathcal{I} = \mathcal{I}_{\lambda,\mu,\nu}$,*

2. *if there exists k such that $\lambda^k = \mu$ and if $\lambda^l \neq \nu$ for every l, then $\mathcal{I} = \mathcal{I}_{\lambda,k,\nu}$.*

Proof. Firstly, it can be seen that the behavior of $\mathcal{F}$ in iteration limit converges on a sufficiently small neighborhood U of $\mathbf{a}$ to the map

$$(x, y, z) \mapsto (\lambda x, \ \ g(x, y, z), \ \ h(x, y, z)),$$

where g, h are holomorphic. Moreover, $\mathcal{F}$ can be reduced to

$$(x, y, z) \mapsto \left(\lambda x, \ \ \mu y + \bar{g}(x, z), \ \ \nu z + \bar{h}(x, y)\right),$$

where $\bar{g}$, $\bar{h}$ are holomorphic.

Let $\mathcal{F} \equiv (f, g, h)$. Let us deal with the sequence

$$\left\{\frac{1}{\lambda^n} f^{\circ n}(\mathbf{p})\right\}, \ \ \mathbf{p} \in U.$$

where $f^{\circ n}(\mathbf{p})$ represents x-th coordinate of $\mathcal{F}^{\circ n}(\mathbf{p})$ (n-th iterate of $\mathcal{F}$). One can prove that

$$\left\{\frac{1}{\lambda^n} f^{\circ n}(\mathbf{p})\right\} \overset{U}{\rightrightarrows} \varphi(\mathbf{p}).$$

Because $f(\mathcal{F}^{\circ n}) = f^{\circ n+1}(z)$ then both sides of the equation

$$\left\{\frac{1}{\lambda^n} f^{\circ n}(\mathcal{F}(\mathbf{p}))\right\} = \lambda \left\{\frac{1}{\lambda^{n+1}} f^{\circ n+1}(\mathbf{p})\right\}$$

converge uniformly to

$$\varphi(\mathcal{F}(\mathbf{p})) = \lambda\varphi(\mathbf{p}).$$

Thus, by regarding $(\varphi(x), y, z)$ as local coordinates, the map $\mathcal{F}$ is reduced to the form

$$\mathcal{F}: \ (x, y, z) \mapsto (\lambda x, g(x, y, z), h(x, y, z)).$$

Secondly, $\mathcal{F}$ can be expanded into Taylor series in each coordinate and in iteration limit $\mathcal{F}$ behaves as

$$(x, y, z) \mapsto (\lambda x, \mu y + \ldots, \nu z + \ldots).$$

One can prove that

$$\left\{\frac{1}{\mu^n}\frac{\partial}{\partial y}g^{\circ n}(\mathbf{p})\right\} \overset{U}{\rightrightarrows} \chi(\mathbf{p}) \ \text{ and } \ \left\{\frac{1}{\nu^n}\frac{\partial}{\partial z}h^{\circ n}(\mathbf{p})\right\} \overset{U}{\rightrightarrows} \psi(\mathbf{p})$$

where $\chi(\mathbf{a}) = \psi(\mathbf{a}) = 1$, consequently

$$\mathcal{F}: \ (x, y, z) \mapsto \left(\lambda x, \mu y + \bar{g}(x, z), \nu z + \bar{h}(x, y)\right).$$

To prove the final tuning of $\mathcal{F}$, one need to find out the coordinates where $\mathcal{F}$ behaves as $\mathcal{I}_{\lambda,\mu,\nu}$ or $\mathcal{I}_{\lambda,k,\nu}$. For the two complex variables case it was proved in [13] that the final tuning depends on the value of the power of λ with respect to the remaining eigenvalues. For our $\mathcal{F}$ the situation is more complicated: $\bar{g}$ and $\bar{h}$ mix the values of coordinates. One can study less complicated cases in the sense of [13] and tune $\mathcal{F}$ when $\bar{g}(x, z) \equiv \bar{g}(x)$ and $\bar{h}(x, z) \equiv \bar{h}(x)$. One can find out local coordinates η_1, η_2 in the forms $\eta_1(p) \equiv (x, q_1(x), z)$ and $\eta_2(p) \equiv (x, y, q_2(x))$ such that $\mathcal{F}$ has desired form in the new coordinates $\eta_1 \circ \eta_2$. $\square$

According to the theorem a general invertible, holomorphic map $\mathcal{F}$ in the iteration limit behaves as linear in the direction corresponding to the basis vector associated with the largest eigenvalue. In the remaining directions, in general, the behavior is different. For special cases when the map depends in these directions only on two specific variables, we have linear or exponential behavior in these directions as well.

Chapter 4

Conclusion and outlook

This thesis has been dedicated to the study of dynamics for the discrete dynamical system generated by the purification protocol [8]. The results clearly proved the existence of true chaos for conditional dynamics of the purification protocol on the set of the qubits.

The results are unique for several reasons. Firstly we proved the existence of true chaos for the truly quantum dynamical system, without any classical analogue. Also, our results pointed out that the purification protocols, designed for purification of wide set of the initial states [8], may exhibit strong sensitivity in the initial setting. To achieve both analytical and numerical results, it was necessary to combine the mathematical results from several branches. Mainly, we used the recently developed mathematical framework for the study of discrete dynamical system, generated by rational and polynomial maps in one complex variable [11; 13].

Before we started to study the dynamics of the purification, we summarized the general properties of the purification protocols. Namely the property to map pure resp. separable states onto pure resp. separable states. Then we proved the possibility to represent purification dynamics of qubit by the rational(or polynomial) map in one complex variable. To achieve this, we used the knowledge about the conformal maps of qubit state space onto the Riemann variet of $\hat{\mathbb{C}}$. Empowered with this knowledge, we started to analyze the dynamics of the purification.

Firstly, we studied the one parametric class of the one-qubit pure state protocols, parametrized by the various additional unitary transformations of $SU(2)$ gates. We also studied the purification for the protocol using the additional unitary of Hadamard gate (general protocol recommended by [8] for the purification of the Werner states (2.13)). We observed strong sensitivity of the protocol dynamics either for the setting of the initial state, represented by the complicated structure of the Julia set for the purification map. We also observed strong sensitivity of the purification for the internal setting of additional unitary gate. This we proved by the possible change of the Julia set topology, from connected to disconnected and vice versa. Also, we observed the complicated structure of the patterns, describing the length of attracting cycles during the purification of the critical point state and consequently we could identify the set of the protocols, so the evolution of the critical point was irregular.

Then we studied the two-qubit purification. Firstly, we focused on the study of subdynamics for the purification of the perturbed Bell states $|\psi(r)\rangle$ (3.18) and namely for the protocol using one target system and for the target state projections $P_{t_i} = |00\rangle\langle 00|$ (for the other projections the dynamics was trivial). Such a simple subdynamics allowed us to describe the purification by rational map in one complex variable and to prove the existence of chaotic dynamics on its Julia set. Using Fano representation (2.17) of the purified states, it was possible to prepare efficient numerical simulations and to prove strong sensitivity of the process to purify either to completely separable cycle or to maximally entangled Bell state $|\psi_{00}\rangle$.

On the example of the perturbed Werner states $\rho(\lambda, r)$ (3.27), we proved the strong sensitivity of the purification protocol also for the mixed states. We studied the same protocol setting, as for the perturbed Bell states, and using the Fano reperesentation we proved the protocol sensitivity to evolve the states either to the pure, separable or maximally entangled states or to the completely mixed, separable state. We also observed a lost of fine structure in the purification patterns as we increased the mixture of the initial state.

As already mentioned, the complete analysis of the multi-qubit dynamics is limited by the lack of the mathematical framework. Nevertheless, with the existing knowledge, it is still possible to explore many subdynamcs of the purification protocols, similarly as done in the thesis. From this point of view the field of future research is still open, namely for the qudits purifications.

In the end, I would like to point out, that the physical realization of the purification protocol faces certain difficulties as we need huge (exponentially large) sets of qubits to follow the chaotic dynamics. However at least to prove rudiments we can limit ourselves to moderate numbers.

Appendix A

Numerical framework

The verification of mathematical relations necessary for the analysis of various problems discussed in thesis, were using Mathematica 6.0 program from Wolfram Research, Inc. All the numerical simulations have been programmed in C language, using the GNU GCC compiler (Mingw 32-gcc.exe) integrated inside the developer environment of Code::Blocks. Certain calculations in C using complex numbers operations are stored in the files complex.c, complex.h, the correctness of the implemented functions were reviewed by the author of the thesis. For the creation of the figures in EPS format from the txt data files the open-source software of GNU Plot 4.4. has been used. For the transformation EPS figures into JPG format the open source-source software of GIMP 2.6.8 has been used. All the simulations and calculations are stored in the attached DVD disc under the path: "Thesis_SV\Calculations" and may be run on a personal computer with the operational system of Windows of 32bit from Microsoft Inc.

A.1 List of Mathematica notebooks

Mathematica notebooks are stored on the attached DVD disc under the path:
"Thesis_SV\Calculations\Mathematica". There are following notebooks:

OneQubitPurifCalc.nb - calculates repelling fixed points and verifies regular dynamics for one qubit pure states purifications - used for results of section (3.4).

JuliaPropertiesSU2.nb - dynamical plot of the Julia sets for various one-qubit pure state purifications with unitary gate of SU (2) - connected/disconnected Julia sets properties of figures (3.1-3.4)

TwoQubitsPurifCalc.nb - calculates the equation for one parametric subdynamics for two-qubit Bell like states purification, also calculates repelling fixed points - used for results of section (3.7,3.8).

FanoCalc.nb - calculates equations of two-qubit purification in Fano representation and Bloch vector coordinates for various two-qubit states - used for results of section (3.7,3.8).

A.2 List of C programs

C programs are stored on the attached DVD disc under the path: "Thesis_SV\Calculations\C" Following programs are available:

LogisticsMap : calculates the evolutions of the system under logistics maps with the output for the figure (1.1).

EvolutionAbsZ : calculates the evolutions of one-qubit pure state under various purifications with the output for the figure (1.2).

JuliaSetBackward1Q : calculates the Julia set of the dynamical system for one-qubit pure state purification. Calculations are used to generate the figures (3.1-3.4).

JuliaSetClosure : calculates the speed of purification to super attracting cycle for various initial one-qubit pure states. Calculations are used to generate the figures (3.5,3.6).

AttrCycleCommon : evolves one of the critical points for various one-qubit pure state purifications and calculates if there exist attractive cycle during the evolution, especially if the evolution contains also the second critical point. The calculation is used to determine the purifications with disconnected Julia set and to generate the figure (3.7).

AttrCycleLength : evolves one of the critical points for various one-qubit pure state purifications and calculates the length of attractive cycle during the evolution. The calculation is used to to generate the figures (3.8).

JuliaSetBackward2Q : calculates the Julia set of the subdynamics for two-qubit pure state purification. The calculations are used to generate the figure (3.9).

FanoCalc : calculates the final states of the purification of two-qubit states in Fano representation. The calculations are used to generate the figures (3.10-3.12).

References

List of author's publications

[I] Kiss T., Jex I., Alber G., Vymětal S. *Phys. Rev. A* **74**, 040301 (2006)

[II] Kiss T., Jex I., Alber G., Vymětal S. *Acta Phys. Hung. B* **26**, 229 (2006)

[III] Vymětal S., Kiss T., Jex I., Alber G., Gábris A., Langrová T. *AIP Conference Proceedings* **1076**, 255 (2008)

[IV] Vymětal S., Kiss T., Jex I., Alber G., Gábris A., Langrová T. *Poster for conference: Let's face chaos through nonlinear dynamics* (University of Maribor, Slovenia) (2008)

External sources

[1] Einstein, A. and Podolsky, B. and Rosen, N. *Phys. Rev.* **47**, 777 (1935)

[2] Zeilinger A. *Physica Scripta* **76**, 203 (1998)

[3] Horodecki M., Horodecki P. *Quant. Inf. and Comp.* **1**, 1 (2001)

[4] Bennett Ch. H., Brassard G., Popescu S., Schumacher B., Smolin J. A., Wootters W. K. *Phys. Rev. Lett.* **76**, 722 (1996)

[5] Horodecki M., Horodecki P. *Phys. Rev. A* **59**, 4206 (1999)

[6] Deutsch D., Ekert A., Jozsa R., Macchiavello Ch., Popescu S., Sanpera A. *Phys. Rev. Lett.* **77**, 2818 (1996)

[7] Bechmann-Pasquinucci H., Huttner B., Gisin N. *Phys. Lett. A* **242**, 198 (1998)

[8] Alber G., Delgado A., Gisin N., Jex I. *J. Phys. A: M*ath. Gen. **34**, 8821 (2001)

[9] Cvitanović P., Artuso R., Mainieri R., Tanner G., Vattay, G. *Chaos: Classical and Quantum* (Niels Bohr Institute, Copenhagen) (2009)

[10] Lichtenberg A. J., Lieberman M. A. *Regular and chaotic dynamics* (Springer - Verlag New York Inc.) (2001)

[11] Milnor J. W. *Dynamics in One Complex Variable* (Vieweg) (2000)

[12] Milnor J. W. *(*Experimental Math.) **2**, 37 (1993)

[13] Morosawa S., Nishimura Y., Taniguchi M., Ueda T. *Holomorphic dynamics* (Cambridge University Press) (2000)

[14] Fornæs J. E. *Dynamics in several complex variables* (Amer. Math. Soc.) (1994)

[15] Chueshov I. D. *Introduction to the Theory of Infinite Dimensional Dissipative Systems* (*Acta Scientific Publishing House*) (1999)

[16] Stockmann H.-J. *Quantum chaos: an introduction* (Cambridge University Press) (2000)

[17] Habib S., Bhattacharya T., Greenbaum B., Jacobs K., Shizume K., Sundaram B. *Annals of the New York Academy of Sciences* **1045**, 308 (2005)

[18] Deutsch D. *Proc. of the Royal Soc. of London. Series A, Math. and Phys. Sciences* **425**, 73 (1989)

[19] Cerf N. J., Adami C., Kwiat P. G. *Phys. Rev. A* **57**, 1477 (1998)

[20] Blank J., Exner P., Havlíček M. *Lineární operátory v kvantové fyzice* (Univerzita Karlova) (1993)

[21] Hayashi M. *Quantum Information An Introduction* (Springer - Verlag Berlin Heidelberg) (2006)

[22] Barnett S. M., Phoenix S. *Phys. Rev. A* **44**, 535 (2000)

[23] Pittenger A. O., Rubin M. H. *Optics Comm.* **179**, 447 (2000)

[24] Benenti G., Strini G. *Phys. Rev. A* **80**, 022318 (2009)

[25] Fano U. *Rev. Mod. Phys.* **29**, 74 (1957)

[26] Temam R. *Infinite-Dimensional Dynamic Systems in Mechanics and Physics* (Cambridge University Press) (1988)

[27] Lee J., Kim Ch. H., Lee E. K., Kim, J., Lee S. *Quant. Inf. Proc.* **1**, 129 (2002)